GIS-BASED LANDSLIDE SUSCEPTIBILITY MAPPING IN DEVREK (ZONGULDAK – TURKEY)

A THESIS SUBMITTED TO
THE GRADUATE SCHOOL OF NATURAL AND APPLIED SCIENCES
OF
MIDDLE EAST TECHNICAL UNIVERSITY

BY

ÇAĞATAY YILMAZ

IN PARTIAL FULFILLMENT OF THE REQUIREMENTS
FOR
THE DEGREE OF MASTER OF SCIENCE
IN
GEOLOGICAL ENGINEERING

SEPTEMBER 2007

GIS-BASED LANDSLIDE SUSCEPTIBILITY MAPPING IN DEVREK (ZONGULDAK – TURKEY)

submitted by **ÇAĞATAY YILMAZ** in partial fulfillment of the requirements for the degree of **Master of Science in Geological Engineering Department, Middle East Technical University** by,

Prof. Dr. Canan Özgen _____
Dean, Graduate School of **Natural and Applied Sciences**

Prof. Dr. Vedat Doyuran _____
Head of Department, **Geological Engineering**

Prof. Dr. Tamer Topal _____
Supervisor, **Geological Engineering Dept., METU**

Assoc. Prof. Dr. M. Lütfi Süzen _____
Co-Supervisor, **Geological Engineering Dept., METU**

Examining Committee Members:

Prof. Dr. Vedat Doyuran _____
Geological Engineering Dept., METU

Prof. Dr. Tamer Topal _____
Geological Engineering Dept., METU

Prof. Dr. Vedat Toprak _____
Geological Engineering Dept., METU

Assoc. Prof. Dr. M. Lütfi Süzen _____
Geological Engineering Dept., METU

Assoc. Prof. Dr. Murat Ercanoğlu _____
Geological Engineering Dept., Hacettepe University

Date: 14/09/2007

I hereby declare that all information in this document has been obtained and presented in accordance with academic rules and ethical conduct. I also declare that, as required by these rules and conduct, I have fully cited and referenced all material and results that are not original to this work.

Name, Last Name: ÇAĞATAY YILMAZ

Signature :

ABSTRACT

GIS-BASED LANDSLIDE SUSCEPTIBILITY MAPPING
IN DEVREK (ZONGULDAK – TURKEY)

Yılmaz, Çağatay
M.Sc., Department of Geological Engineering
Supervisor: Prof. Dr. Tamer Topal
Co-supervisor: Assoc. Prof. Dr. M. Lütfi Süzen

September 2007, 105 pages

The purpose of this study is to evaluate and to compare the results of bivariate statistical analysis conducted with three different data sets in Geographical Information Systems (GIS) based landslide susceptibility mapping applied to the Devrek region. The data sets are created from the seed cells of crowns and flanks, only crowns, and only flanks of the landslides by using 10 different parameters of the study area. To increase the data dependency of the analysis, all parameter maps are classified into equal frequency classes based directly on the percentile divisions of each seed cells data set. The resultant maps of the landslide susceptibility analysis indicate that all data sets produce acceptable results. In each seed cell data set analysis, elevation, lithology, slope, aspect and drainage density parameters are found to be the most contributing factors in landslide occurrences. The results of the three data sets are compared by Seed Cell Area Index (SCAI). This comparison shows that the crowns data set produces the most accurate and successful landslide susceptibility map of the study area.

Keywords: Devrek, Geographical Information Systems, Landslide Susceptibility Mapping

ÖZ

DEVREK YÖRESİ İÇİN COĞRAFİ BİLGİ SİSTEMLERİ TABANLI HEYELAN DUYARLILIK HARİTALAMASI

Yılmaz, Çağatay
Yüksek Lisans, Jeoloji Mühendisliği Bölümü
Tez Yöneticisi: Prof. Dr. Tamer Topal
Ortak Tez Yöneticisi: Doç. Dr. M. Lütfi Süzen

Eylül 2007, 105 sayfa

Bu çalışmanın amacı, Coğrafi Bilgi Sistemleri (CBS) tabanlı heyelan duyarlılık haritalaması içinde, Devrek yöresine üç ayrı veri setiyle uygulanan iki değişkenli istatistiksel analiz sonunda bulunan sonuçları değerlendirmek ve bunları kendi aralarında karşılaştırmaktır. Veri setleri, çalışma alanının 10 değişik parametresini kullanarak, taçlar ve kanatlar, sadece taçlar ve sadece kanatlar kısımlarını içeren kök hücrelerinden yaratılmıştır. Analizin veriye bağımlılığını arttırmak için parametre haritaları, her bir kök hücre veri setinin yüzdelik değerlerine göre eşit ağırlıklı bölümlere ayrılmıştır. Analiz sonucunda bütün veri setlerinin geçerli sonuçlar ürettiği görülmüştür. Bütün kök hücre veri seti analizlerinde, çalışma alanındaki heyelan oluşumlarına en fazla katkıyı sağlayan parametrelerin, yükseklik, litoloji, eğim, bakı ve drenaj yoğunluğu olduğu bulunmuştur. Sonuçlar, Kök Hücre Alan Endeksi (KHAE) kullanılarak karşılaştırılmış ve taçlardan üretilen kök hücre setinin, çalışma alanının en doğru ve en başarılı heyelan duyarlılık haritasını ürettiği tespit edilmiştir.

Anahtar Kelimeler: Devrek, Coğrafi Bilgi Sistemleri, Heyelan Duyarlılık Haritalaması

In Loving Memory of My Father

ACKNOWLEDGEMENTS

I would like to express my special thanks and gratitude to my supervisor Prof. Dr. Tamer Topal for his guidance, comments, encourage, trust and support at every point of this study.

I would like to express my special thanks and appreciation to my co-supervisor Assoc. Prof. Dr. M. Lütfi Süzen for his valuable contributions, comments, suggestions and unbelievable patience by sparing his time out of his busy schedule.

I would like to thank to Müge Akın for her valuable help in the data gathering processes.

I would also like to thank to my friends Başak Şener, Çağıl Kolat, Alper Fulat, Nesrin Tüfekçi, Deniz Gerçek and Pınar Ertepınar for their help and continuous support.

Finally, I would like to thank to my family and Aslı Gücüyener for their patience, encourage and support throughout the study. I would like to express my deepest gratitude to my father. Without you I couldn't have accomplished all this. Wish you were here, and share my pride and happiness. Rest in peace.

TABLE OF CONTENTS

LIST OF TABLES

TABLES

LIST OF FIGURES

FIGURES

CHAPTER 1

INTRODUCTION

1.1. Purpose and Scope

Throughout the history of the world, natural hazards, such as landslides, earthquakes and floods have caused great numbers of casualties and huge economic losses to mankind. They affect countries large and small, rich and poor. The consequences of such hazards are more devastating in developing countries, where hazard mitigation programs cannot be introduced mainly due to financial and administrative weaknesses.

Among natural hazards, landslides occur in virtually every country in the world almost on a daily basis. They result from a variety of factors including heavy precipitation, melting snow or ice, earthquakes, volcanic activity and human activities. Landslides damage residential and industrial buildings, structures, agricultural and forest lands, and transportation networks. In addition, erosion caused by landslides can lead to water quality problems in nearby streams and reservoirs.

Landslide activity has an increasing trend worldwide, especially in developing countries. Unplanned urbanization and development in unstable hillside areas under the pressures of increasing populations, deforestation, and increased precipitation by changing climates are the main reasons for this increasing trend. Landslide susceptibility maps provide valuable information to planners, developers and engineers who implement land use strategies. These maps are very useful in hazard mitigation studies.

Black Sea Region, which comprises the northern part of Turkey, has the most number of landslides recorded every year (SSGM, 2007). Steep topography and high precipitation sometimes make the region very prone to landslides. Devrek lies in the western part of the Black Sea Region, established in a valley formed by the Devrek Stream. Increasing population causes to urbanize in the hillside areas around Devrek.

The purpose of this thesis is to generate a landslide susceptibility map for the Devrek area. Three susceptibility maps will be produced from three different data sets by using bivariate statistical technique utilizing Geographical Information Systems (GIS). The most accurate and the most successful one will be introduced after applying comparison methods. The susceptibility map may serve as useful information to determine the landslide-free areas for future growth and urbanization of the town.

In the first chapter, general characteristics of the study area, and the methodology of the study are summarized. Chapter 2 covers background information on GIS-based landslide susceptibility mapping. Data production processes and creation of input parameter maps and databases for the analysis are explained in Chapter 3. The analysis for creating the susceptibility maps and their results are given in Chapter 4. Finally, the results are discussed in Chapter 5, and conclusions and recommendations are given in Chapter 6.

1.2. Location and Accessibility of the Study Area

Devrek is a district of Zonguldak and located in the western part of the Black Sea Region of Turkey; approximately 30 kilometers south of Zonguldak. The study area is accessible by asphalt paved D750 highway connected to Zonguldak in north and to the Trans European Motorway (TEM) in south (Figure 1.1).

The study area is bounded by the coordinates 4565400 N and 410700 E in the northwestern edge, and 4561500 N and 418300 E in the southeastern edge in Universal Transverse Mercator (UTM) projection with 36 North zone in European

1950 Mean Datum (Figure 1.2). The study area covers approximately 54 square kilometers. A general panoramic view of Devrek in the S-N direction is presented in Figure 1.3.

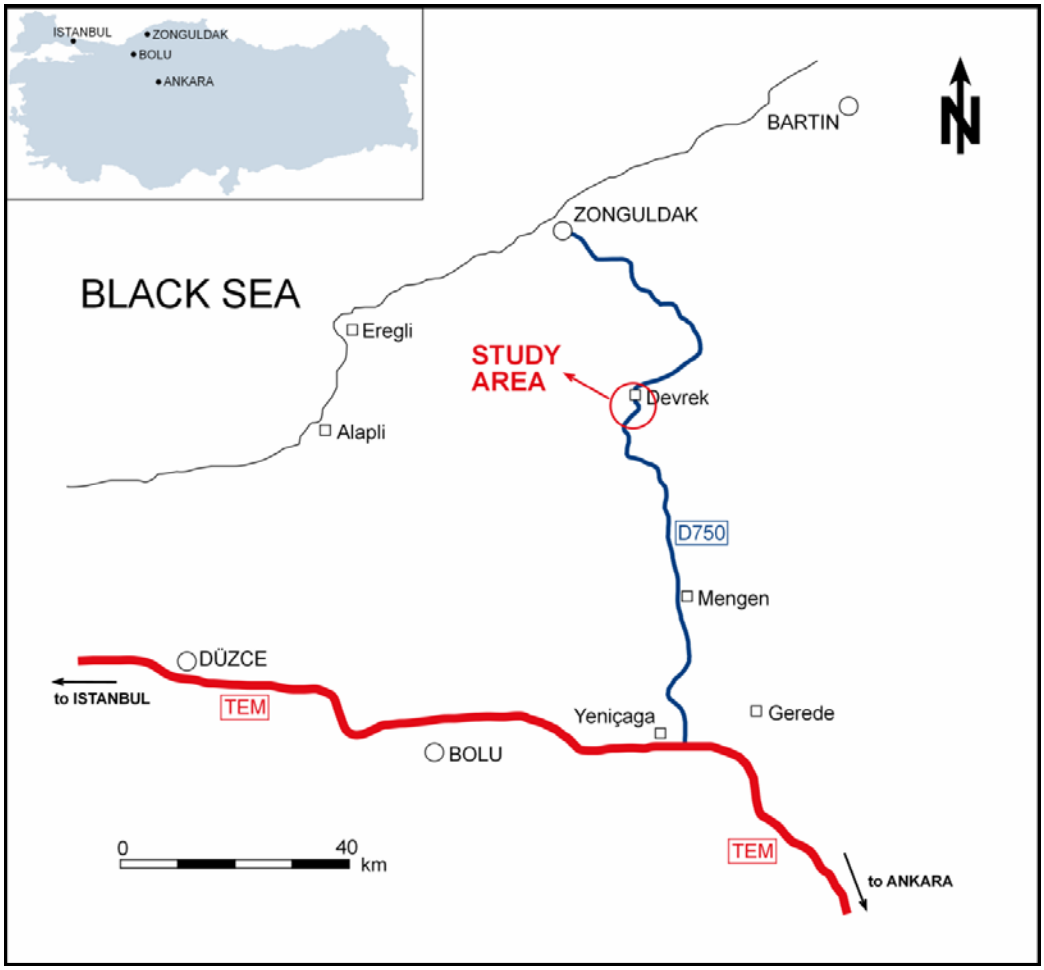

Figure 1.1. Location map of the study area.

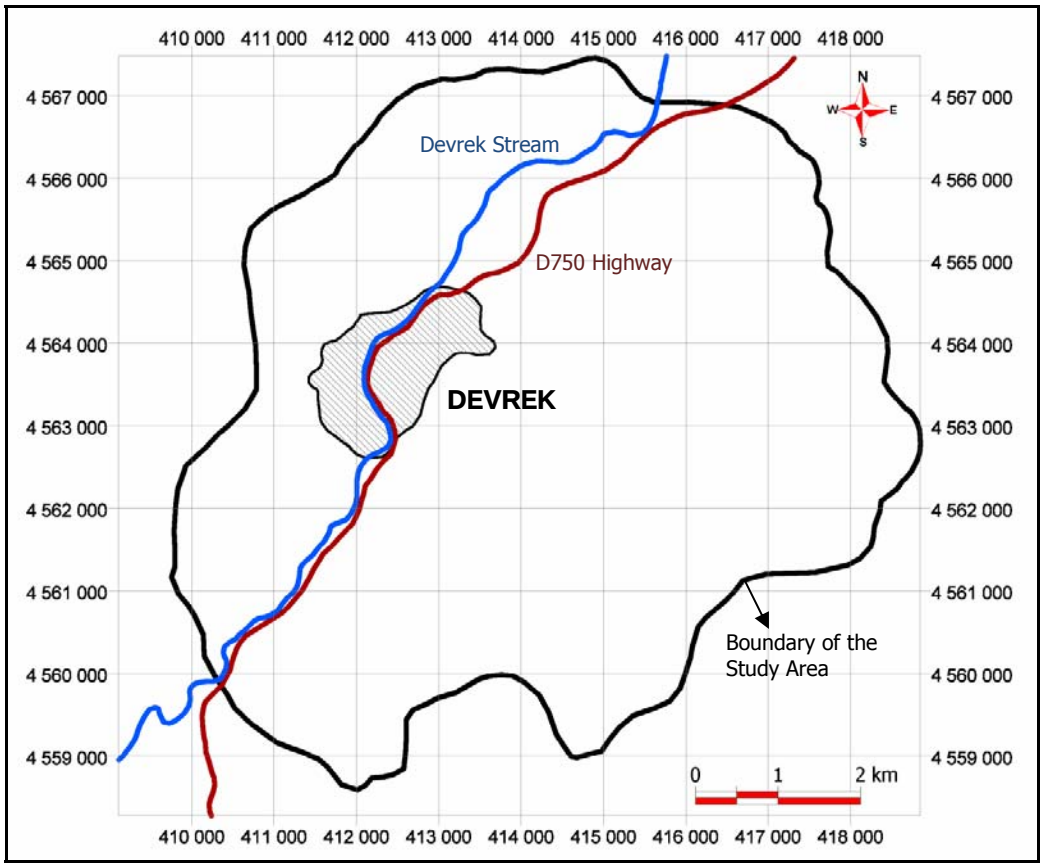

Figure 1.2. Outline of the study area.

1.3. Climate and Vegetation

The climate in Devrek region has the characteristics peculiar to the Black Sea type of climate. The summers are chilly, and the winters are temperate but cold with rain and snow in higher areas. Precipitation occurs in all four seasons. The annual average precipitation is approximately 170 kg/m^2 throughout the region. The average temperature is highest in July with 22.1°C, whereas it is the coldest in January with 4.2°C through the year. The average value of humidity is 71% (DMİ, 2007).

The eastern hillside parts of the study area are partly vegetated (Figure 1.4). The forests here are mainly composed of pine and oak trees.

Figure 1.3. General panoramic view of Devrek in S-N direction.

Figure 1.4. Eastern hillside areas partly covered with pine trees.

1.4. Geology

Based on the studies by Yergök et al. (1987), five lithological units are identified in the study area, which are presented in Figure 1.5. Early Cretaceous is characterized by Kazpınar Formation, overlaid by the Late Cretaceous Alaplı Formation. The Tertiary period is represented by the sequence of Paleocene aged Yahyalar and Eocene aged Çaycuma formations. Finally, Quaternary alluvial deposits partially overlie the whole sequence in the study area. The generalized columnar section of the area is presented in Figure 1.6. There are no mappable geologic structures (faults, folds, lineaments) in the study area.

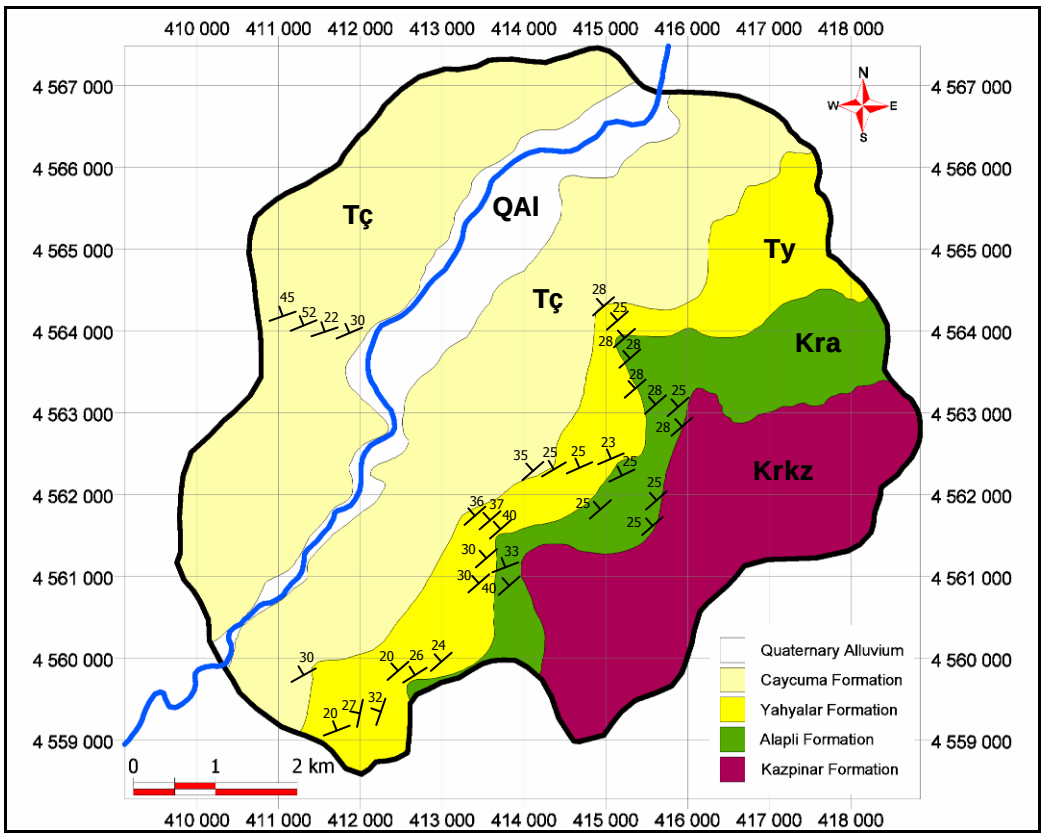

Figure 1.5. Geological map of the study area (modified from Yergök et al., 1987).

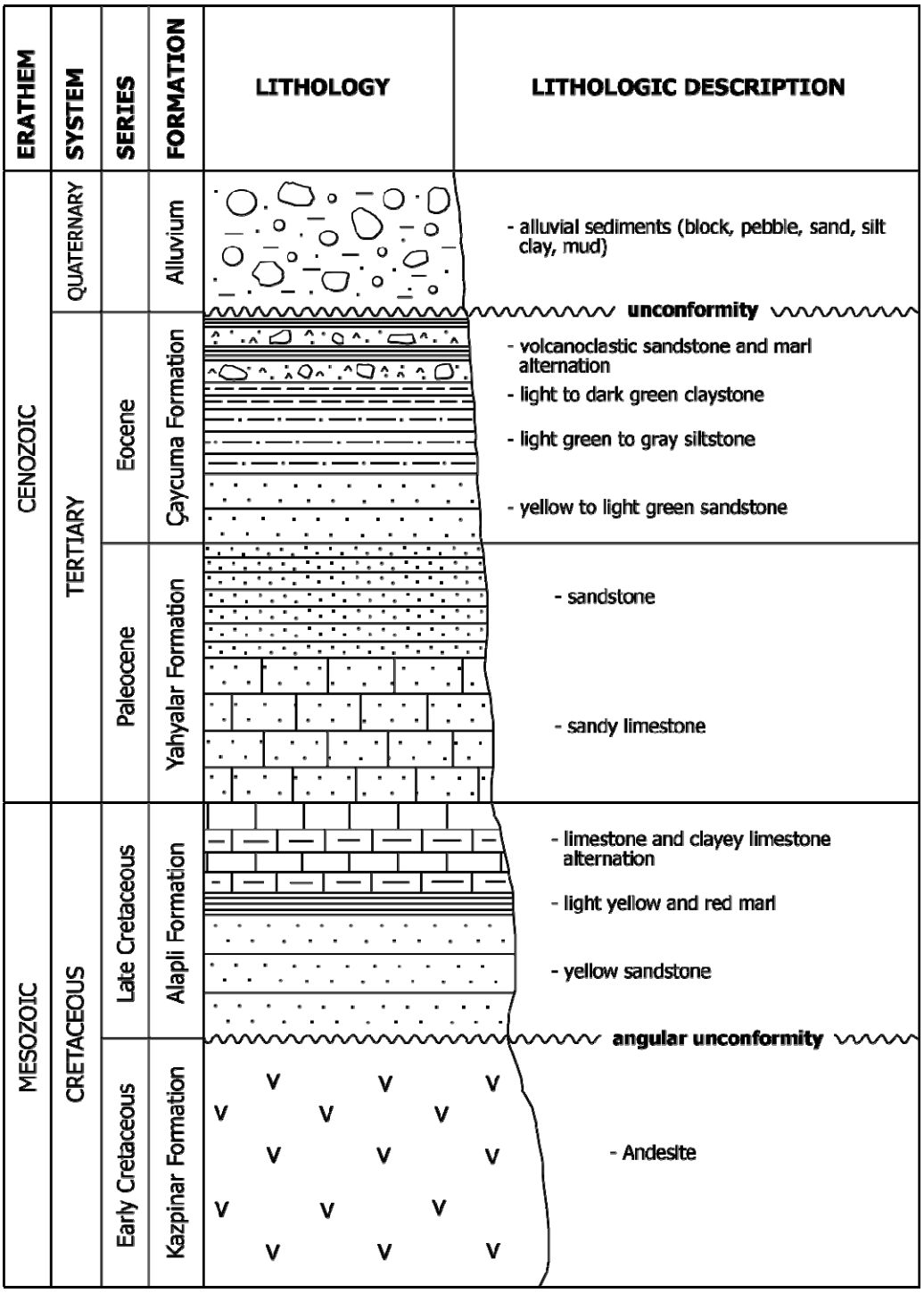

Figure 1.6. Generalized columnar section of the study area (not to scale) (modified from Yergök et al., 1987).

Kazpınar Formation (Krkz)

The volcanic and volcanoclastic Kazpınar Formation is the oldest geologic unit in the study area. It crops out in the southeastern parts of the study area. The formation has a pink, partly green to gray andesite with small amounts of tuff and marl. Andesite dominantly consists of plagioclase crystals with small amounts of hornblende and biotite. The age of the Kazpınar Formation is Early Creataceous.

Alaplı Formation (Kra)

Alaplı Formation overlies the Kazpınar Formation by an angular unconformity. The formation consists of an alternating sequence of sandstone, marl and limestone (Figure 1.7). The sequence starts with yellow, thick to very thick bedded sandstone. Thin layers of light yellow and red marl overlie the sandstone bed. Above them, there are light yellow to green clayey limestone and limestone beds in moderate thickness. The beds are dipping towards northwest with an average amount of 25 degrees. The age of the formation is Late Cretaceous.

Figure 1.7. The alternating sequence in Alaplı Formation.

Yahyalar Formation (Ty)

Yahyalar Formation overlies the Alaplı Formation conformably. It consists of an alternating sequence of sandy limestone and sandstone (Figure 1.8). The sandy limestone is gray to white and thick bedded. The sandstone is gray and thin bedded. The beds are dipping towards northwest with an average amount of 30 degrees. The age of the Yahyalar Formation is Paleocene.

Figure 1.8. Sandy limestone beds in Yahyalar Formation.

Çaycuma Formation (Tç)

Çaycuma Formation overlies the Yahyalar Formation conformably. It consists of an alternating sequence of sandstone, siltstone, claystone and volcanoclastic sandstone (Figure 1.9). Sandstone is yellow to light green and has moderately thick beds. Siltstone is light green to gray and observed as thin layers. Claystone is light to dark green and has very thin layers. The volcanoclastic sandstone includes agglomerate and tuff. It is unconsolidated, thin layered and alternating with thin layers of marl. The beds are dipping towards northwest with an average amount of 35 degrees. The age of the formation is Eocene.

Figure 1.9. The alternating sequence in Çaycuma Formation.

Quaternary Alluvium (QAl)

Alluvial deposits crop out along the Devrek Stream in the study area. The alluvial fill covers a wide area where the city center of Devrek is located. The alluvium includes unsorted sediments from mud to block sizes. The coarse components are subangular to round in shape.

1.5. Seismicity of the Study Area

The study area lies approximately at 55 kilometers north of the North Anatolian Fault Zone (NAFZ) (Figure 1.10) (MTA, 2007). The earthquake activity of this region is directly controlled by the presence and activity of NAFZ, and its associated fault segments. The study area is located within the first degree earthquake zone of Turkey (Figure 1.11) (AİGM DAD, 2007). The epicenters of past and recent earthquakes are presented in Figure 1.12 (BÜ KRDAE, 2007). The study area and its vicinity are seismically not very active. Earthquakes may trigger landslides in the future. However, no information exists about the effect of past earthquakes on landsliding in the study area. Since the study area is small, the effect of seismicity is considered equal in all of the area. Thus, seismicity is not considered as a parameter in this study.

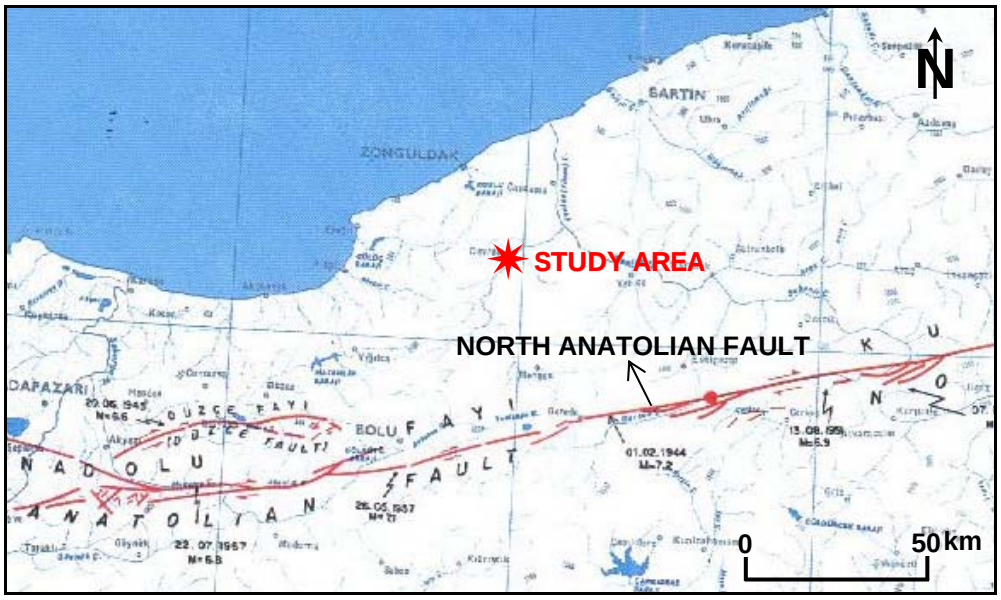

Figure 1.10. Map showing the active faults in the western part of Black Sea Region (modified from MTA, 2007).

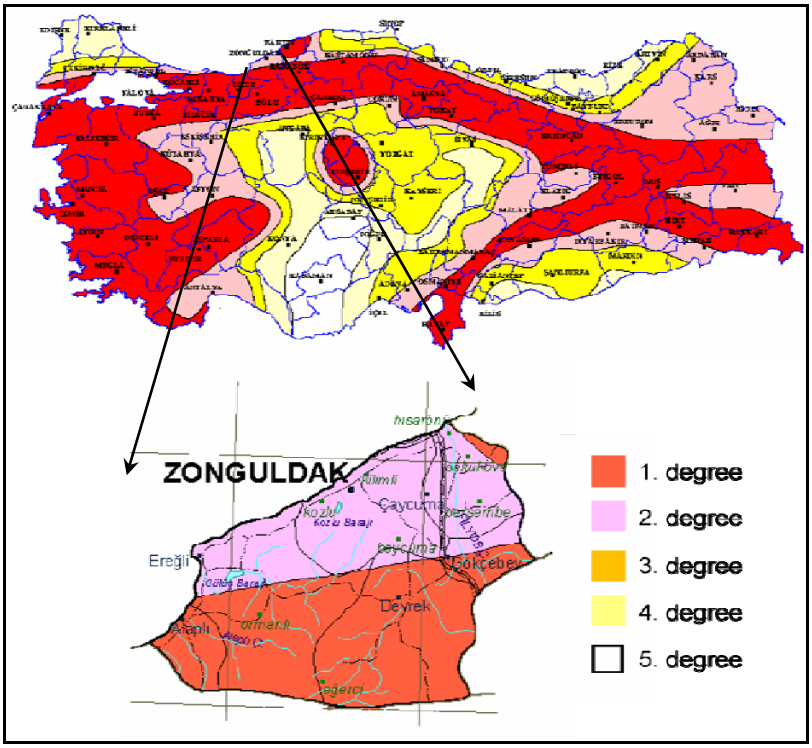

Figure 1.11. Earthquake zone map of Turkey and Zonguldak (AİGM DAD, 2007)

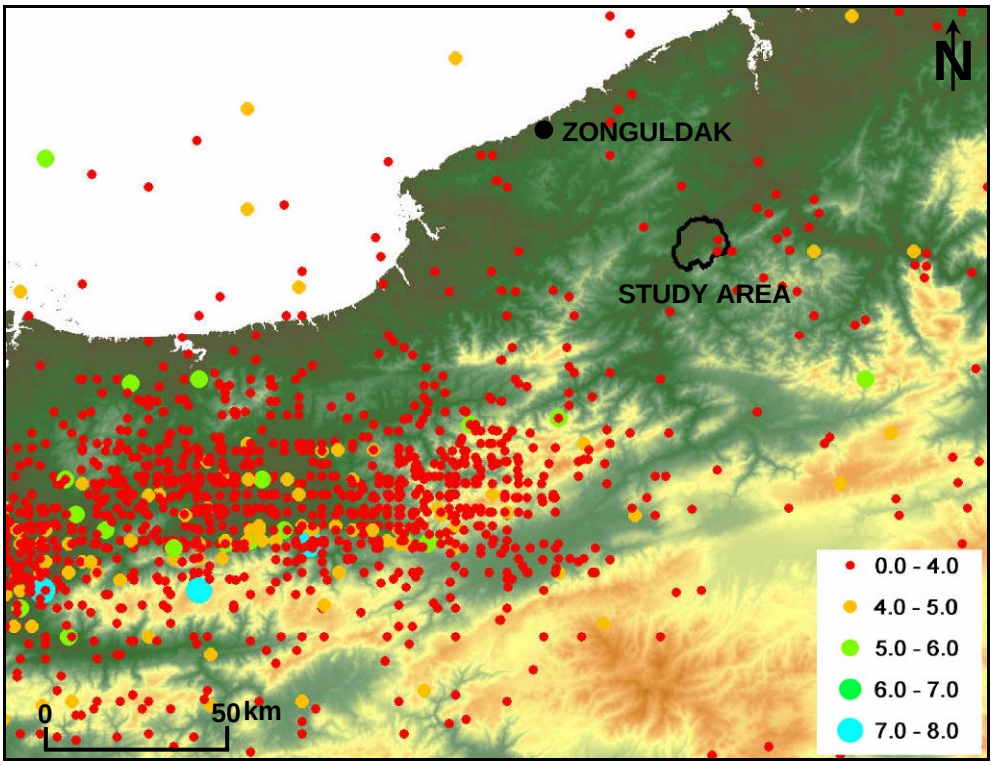

Figure 1.12. Epicenter locations of past and recent earthquakes (BÜ KRDAE, 2007).

1.6. Method of the Study

The studies are carried out in four main stages. Briefly, these stages are:

1. Data acquisition.
2. Data production.
3. Data manipulation, analysis and constructing the product maps.
4. Discussions and conclusions.

Before beginning the studies, a review of GIS-based landslide susceptibility mapping methods were carried out.

The data acquisition part of the study is based on literature review of geology of the study area, gathering geological and topographical maps, and conducting

fieldworks to visually inspect the lithologic units and map the landslides in the study area. The geology and geologic map of the study area were gathered from the previous works published by General Directorate of Mineral Research and Exploration. The topographical map was obtained from the General Command of Mapping of Turkish Army. Two field studies were conducted on October and December, 2006. In these field investigations, geological map from the literature was checked, the lithologic units were identified, photographs of lithological units and landslides were taken, and the landslides were mapped on the topographical map.

The data production stage consists of data entry, creating the parameter maps, and constructing the databases for the analyses for the next stage. A total of 10 parameter maps were created by utilizing TNT Mips software (Version 6.9, 2004).

The data of the parameter maps were exported and prepared for the statistical analyses. The preparation of the data was carried out by introducing two new concepts (Süzen and Doyuran, 2004a). These are seed cells for defining the decision rules of slope instabilities and percentile class divisions for transforming the continuous variables into categorical variables. Seed cells are considered as the best undisturbed morphological conditions before landslide occurs. They were extracted by adding a buffer zone to the crown and flanks of a landslide. In this study, three different sets of seed cell databases were prepared for the analysis as decision rule generators. These seed cells were extracted from the crowns and flanks, only from the crowns, and only from the flanks from the buffer zones added to the landslides in the study area. Then, the continuous data sets extracted from the parameter maps were classified into categories based on percentile divisions of seed cells. The percentile divisions and distributions of seed cells were calculated by using SPSS software (Version 12.0, 2003). The parameter maps were reclassified into percentile maps by using the percentile limits.

For creating the landslide susceptibility maps, bivariate statistical technique was used. Statistical methods were preferred because of their relative objectivities

and data dependencies. According to the landslide susceptibility analysis, landslide occurrences in each percentile class for each parameter map were calculated. Then, weighting values were calculated by comparing the landslide occurrences in each percentile class with the overall landslide occurrence in the parameter map of the study area. The weighting values gave the influence of each parameter map. To build the final product maps, the parameter maps were spatially summed up according to their weight values.

Lastly, the final product maps created by using three different seed cell data were compared. The results were discussed, and finally, conclusions and recommendations were given.

CHAPTER 2

BACKGROUND INFORMATION ON GIS-BASED LANDSLIDE SUSCEPTIBILITY MAPPING

2.1. Geographical Information Systems and Landslide Susceptibility Mapping

In recent years, the assessment of landslide hazard has become a major interest for scientists, planners and local administrations. In the literature, many methods have been proposed to deal with the prediction of landslide hazards. These methods may involve interpretation of aerial photographs, field surveys, rock property tests in laboratory, and spatial and statistical analyses. All these stages are time and labor consuming with significant costs. GIS is a powerful tool in manipulation and analysis of spatial and non-spatial data. Introducing GIS facilitates the application of the methods and production of output maps in a more efficient and cost-effective way.

The occurrence of slope failure depends generally on complex interactions among a large number of partially interrelated factors. Analysis of landslide susceptibility requires evaluation of the relationships between various terrain conditions and landslide occurrences. An experienced earth scientist has the capability to mentally assess the overall slope conditions and to extract the critical parameters. However, an objective procedure is often desired to quantitatively support the slope instability assessment. This procedure requires the evaluation of the spatially varying terrain conditions as well as the spatial representation of landslides. A GIS allows for the storage and manipulation of information concerning the different terrain factors as distinct data layers and

thus provides an excellent tool for slope stability susceptibility zonation (Soeters and van Westen, 1996).

The advantages of GIS for assessing landslide hazard include the followings:

- A much larger variety of hazard analysis techniques become attainable. Because of the speed of calculation, complex techniques requiring a large number of map overlays and table calculations become feasible.
- It is possible to improve models by evaluating their results and adjusting the input variables. Users can achieve maximum results by a process of trial and error, running the models several times, whereas it is difficult to use these models even once in the conventional manner. Therefore, more accurate results can be expected.

The disadvantages of GIS for assessing landslide hazard include the followings:

- A large amount of time is needed for data entry. Digitizing is especially time consuming.
- There is a danger in placing too much emphasis on data analysis as much as the expense of data collection and manipulation based on professional experience. A number of different techniques of analysis are theoretically possible, but often the necessary data are missing. In other words, the tools are available but cannot be used because of the lack or uncertainty of the data.

2.2. Phases of Landslide Susceptibility Mapping using GIS

A GIS-supported landslide susceptibility assessment project requires a number of unique phases, which are distinctly different from those required by a conventional landslide susceptibility assessment project (Soeters and van Westen, 1996). An overview of these phases is given in Table 2.1. Table 2.1 also indicates the estimations of relative amount of time spent on each phase at each of the three scale of analysis.

Table 2.1 Percentage of time spent on various phases of landslide susceptibility assessment projects at different scales using GIS and conventional methods (modified from Soeters and van Westen, 1996).

PHASES	Regional Scale		Medium Scale		Large Scale	
	Conventional Methods	GIS-based Methods	Conventional Methods	GIS-based Methods	Conventional Methods	GIS-based Methods
Choice of scale and methods	<5	<5	<5	<5	<1	<5
Collection of existing data	<5	<5	<5	<5	8	8
Image interpretation	50	50	30	30	10	20
Database design	0	<5	0	<5	0	<5
Fieldwork	<5	<5	7	7	10	20
Data entry	0	20	0	30	0	15
Data validation	0	<5	0	5	0	5
Data manipulation	0	<5	0	5	0	5
Data analysis	30	10	48	10	61	10
Error analysis	0	<5	0	<5	0	<5
Final map production	10	<5	10	<5	10	<5

Working with a GIS considerably increases the time needed for the pre-analysis phases, mainly because of the tedious job of hand-digitizing input maps. Time needed for data analysis, however, is not more than 10 percent in the GIS approach versus almost 50 percent using conventional techniques. Many of the analysis techniques are almost impossible to execute without GIS. Working with GIS considerably reduces the time needed to produce the final maps, which are no longer drawn by hand.

2.3. GIS-based Landslide Susceptibility Mapping Methods

Broadly speaking, methods of landslide susceptibility mapping may be qualitative or quantitative. A number of methods have been developed and these are summarized in Figure 2.1 (modified from Aleotti and Chowdhury, 1999). Overview of these methods can be found in Aleotti and Chowdhury

(1999), Ercanoğlu (2005a), Guzetti et al. (1999), and Soeters and van Westen (1996).

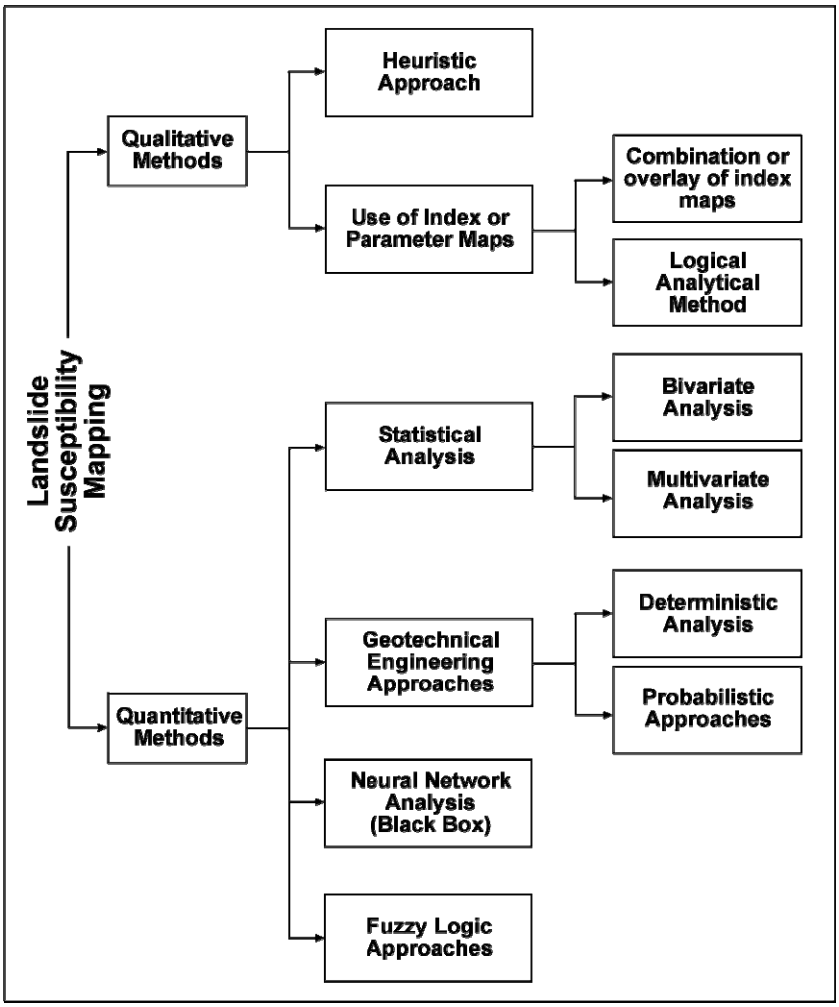

Figure 2.1. Classification of landslide susceptibility mapping methods (modified from Aleotti and Chowdhury, 1999).

2.3.1. Qualitative Methods

In general qualitative approaches are based entirely on the judgment of the person or persons carrying out the susceptibility assessment. The input data are usually derived from assessment during field visits, possibly supported by aerial photo interpretation. They can be divided into two types: heuristic approach and the combination or overlaying of index maps with or without weighting.

2.3.1.1. Heuristic Approach

This group is probably the simplest of the qualitative methods. The zonation is carried out directly in the field or by aerial photo or satellite image interpretation by the earth scientist, based on his/her experience in other similar situations, with no clear indication of any rules which have led to the zonation. In this case the stability maps are directly evolved from detailed geomorphological maps (van Westen et al., 2000). The main disadvantages of such approaches are (Leroi, 1996):

- The subjectivity in the selection of both the data and the rules that govern the stability of slopes. This fact makes it difficult to compare landslide susceptibility maps produced by different investigators or experts.
- Use of implicit rather than explicit rules hinders the critical analysis of results and makes it more difficult to update the assessment as new data become available.
- Lengthy field surveys are required.

GIS serves as an undeniable tool for manipulating the entered data and producing the zonation maps. This method can be applied at all scales in a relatively short period.

Examples of direct mapping of landslide hazards can be found in Barredo et al. (2000) and van Westen et al. (2000).

2.3.1.2. Use of Index or Parameter Maps

2.3.1.2.1. Combination or Overlay of Index or Parameter Maps

In this approach, the expert selects and maps the factors that affect slope stability and, based on personal experience, assigns to each a weighted value that is proportionate to its expected relative contribution in generating failure. The following operations should be carried out (Soeters and van Westen, 1996):

a) Subdivision of each parameter into a number of relevant classes.

b) Attribution of a weighted value to each class.

c) Attribution of weighted values to each of parameters.

d) Overlay mapping of the weighted maps.

e) Development of the final map showing susceptibility classes.

The advantages of such a methodological approach are that it considerably reduces the problem of the hidden rules and enables total automation of the operations listed above through appropriate use of GIS. Furthermore, it enables the standardization of data management techniques, from acquisition through to final analysis. This technique can be applied at any scale. The major disadvantage is the lengthy operations involved, especially where large areas are concerned. The problem of subjectivity in attributing weighted values to each parameter and to the different factors also remains, as well as the difficulty of extrapolating a model developed in a particular area to other sites or zones (Carrara, 1983).

Some examples of this method can be found in Abella and van Westen (2007), Ayanew and Barbieri (2005), Barredo et al. (2000), Mejia-Navarro and Wohl (1997), and Wachal and Hudak (2000)

2.3.1.2.2. Logical Analytical Method

The first stage of this method consists of a tentatively proposed relationship which links some experience-based weighted factors. Using the proposed relationship it is possible to predict the slope displacements of some landslides and, by comparing the results with the monitoring data, to define the degree of agreement. At this stage the established relationship can be calibrated by varying the weights of the elements. Once the degree of agreement is good, the relationship can be used to classify all the failures, even those for which subsurface instrumented data are not available (Aleotti and Chowdhury, 1999). A logical analytical model has been used in Bughi et al. (1996) to predict the slope displacement in geologically unstable areas crossed by gas pipelines.

2.3.2. Quantitative Methods

The approaches of this group of methods are more rigorous than qualitative methods. It is possible to distinguish these methods between statistical analysis, which can be subdivided into bivariate or multivariate, and deterministic methods that involve the analysis of specific sites or slopes based on geo-engineering models.

2.3.2.1. Statistical Analysis

The subjectivity in assigning the weighted values to numerous factors that govern slope stability is the main limitation in qualitative methods. The solution to this problem could be to adopt a statistical approach that compares the spatial distribution of landslides with the parameters that are being considered. Statistical approach is defined as a direct comparison technique based on the relationship between various fundamental maps with landslide distribution maps. The results could then be applied to areas currently free of landslides but where conditions may exist for susceptibility to future instability. The major difficulty consists in establishing the slope failure processes and in systematically identifying and assessing the different factors related to

landsliding (Carrara, 1988). One of the principal advantages is that the investigator can validate the importance of each factor and decide on the final input maps in an interactive manner. The use of GIS makes these operations much easier and to a large extent. From the beginning of the 80's, the enormous potential of GIS tools enables storage and processing of huge amounts of data through the use of complex statistical techniques. Because of their objectivity and flexibility, statistical techniques are widely preferred among scientists recently. The statistical analyses can be either bivariate or multivariate.

2.3.2.1.1. Bivariate Analysis

In bivariate techniques, the importance of each parameter or specific combinations of parameters can be analyzed individually. Several methods exist for calculating weighting values. Most are based on the relationship between the landslide densities per parameter class compared with the landslide density over the entire area. Each method has its specific rules for data integration required to produce the total hazard map.

GIS is very suitable for use with this method, especially with commands for repetitive calculations involving a large number of map combinations and manipulation of attribute data. The following GIS operations are used:

a) Selection and mapping of significant parameters and their categorization into a number of relevant classes,

b) Landslide mapping,

c) Overlay mapping of the landslide map with each parameter map,

d) Determination of density of landslides in each parameter class and definition of weighted values,

e) Assignment of weighting values to the various parameter maps, and

f) Final overlay mapping and calculation of the final hazard or susceptibility value of each identified land unit.

Although the bivariate statistical analysis is considered to be a quantitative approach to landslide susceptibility assessment, a certain degree of subjectivity exists, particularly in step (a) and (f) in categorization of parameters into classes and hazard classes in the final hazard map. In addition, it must be appreciated that in many situations, the analyzed factors are not independent and may show either high or low correlation (Leroi, 1996).

In bivariate statistical analysis numerous parameters may be taken into consideration such as; lithology, slope angle, slope height, land use, distance from major structures, drainage density, relief morphology, closeness of the facet to river, attitude of lithotypes (Aleotti and Chowdhury, 1999).

As the name implies there are two variables in bivariate statistical analyses (van Westen, 1993). Between these two variables the occurrence of mass movements are considered as dependent and parameters are independent variables. In bivariate statistical analysis each parameter map (as independent variable) is crossed with landslide distribution map and weighting values, which demonstrates the relative effect of each parameter or variable to instability, are calculated. Weight value for landslide susceptibility is calculated from the landslide density of each class of each parameter map. The landslide density of each class is calculated from following equation:

$$D_{area} = 1000 \frac{Npix(SX_i)}{Npix(X_i)}$$

where D_{area} is the areal density per mileage, $Npix(SX_i)$ is the number of pixels with mass movements within variable class X_i, and $Npix(X_i)$ is the number of pixels within variable class X_i.

The weight value of each control factor class for landslide is defined as the difference between the landslide density of each class and the average landslide density in the study area. The formula for the weight value is:

$$W_{area} = 1000\frac{Npix(SX_i)}{Npix(X_i)} - 1000\frac{\sum Npix(SX_i)}{\sum Npix(X_i)}$$

The calculated weight values are the equal to the degree of susceptibility to landslides of each parameter class. Landslide susceptibility analysis was used in Süzen and Doyuran (2004a and 2004b) with new approaches to increase data dependency. Guinau et al. (2005) suggested that using this method for developing countries would be very feasible because of its simplicity and comprehensiveness by non-specialized users.

Other bivariate statistical methods are the statistical (Wi) index method (van Westen, 1997), the weighting factor (Wf) method (Çevik and Topal, 2003), the information value method (Yin and Yan, 1988) and the weights of evidence modeling (Sabto, 1991). Çevik and Topal (2003), and Yalçın (2007) have found in their studies that the Wf method gives better results than the Wi method. Lin and Tung (2003) constructed a predictive model for the assessment of earthquake-triggered landslide potential by information value method. Examples for the weights of evidence modeling in landslide susceptibility assessment can be found in Lee et al. (2002), Neuhauser and Terhorst (2007), and Thiery et al. (2007).

2.3.2.1.2. Multivariate Analysis

The multivariate statistical analysis involves several preliminary steps that are undertaken in a test area. Once the results achieved have been verified they are extended to the entire area under examination. The following steps are required (Aleotti and Chowdhury, 1999):

a) Classification of the study area into land units. The land units can be square with sides of varying dimensions (usually 100 or 200 m), depending upon the extent of knowledge of the area.

b) Identification of significant factors and creation of input maps. The input variables include information concerning the landslides (type, degree of

activity, etc.) and geo-referencing. An important aspect is the conversion of various parameters from nominal to numeric, for example rock types or vegetation cover. Preferred method is ranking the classes based on the relative percentage of the area affected by landsliding.

c) Construction of a landslide map. In this phase the collection and storage of all information concerning landslides into databases.

d) Identification of the percentage of landslide-affected areas in every land unit and their classification into unstable and stable units.

e) Combination of the parameter maps with the land unit map and creation of an absence/presence matrix of a given class of a given parameter within each land unit.

f) Multivariate statistical analysis using GIS software programs. The statistical analyses most frequently used are discriminant analysis (based on discriminating the land units as stable or unstable) or regressive multiple analysis (to correlate factors related to instability and mass movements) which are often employed in parallel within the same project. It is preferable to apply discriminant analysis with continuous variables, while the regressive analysis can be used even with nominal variables.

g) Reclassification of land units based on the results achieved in the previous phase and their classification into susceptibility classes. In the discriminant analysis for example, the contribution of various parameters in causing slope instability can be quantified and, as a result, enables objective reclassification of the study area. By transforming the classification function scores into probabilities, the susceptibility map can then be converted into a hazard map.

Examples for discriminant analysis include Santacana et al. (2003), and Baeza and Corominas (2001). Studies carried out by logistic regression can be found in Atkinson et al. (1998), Dai et al. (2001), Dai and Lee (2001), Dai and Lee (2003), Lee and Min (2001), Süzen (2002), Süzen and Doyuran (2004b), Ayalew

and Yamagishi (2005), Yeşilnacar and Topal (2005), and Nefeslioğlu et al. (2007).

2.3.2.2. Geotechnical Engineering Approaches

2.3.2.2.1. Deterministic Analysis

The methods described far give no information on the stability of a slope as expressed in terms of its factor of safety. For such information, slope stability models are necessary. These models require input data on soil layer thickness, soil strength, depth below the terrain surface to the potential sliding surfaces, slope angle and pore pressure conditions to be expected on the slip surfaces. The following parameter maps must be available in order to use such models (Soeters and van Westen, 1996):

- A material map showing the distribution both at ground surface and in the vertical profile with accompanying data on soil characteristics,
- A groundwater level map based on a groundwater model or on field measurements, and
- A detailed slope-angle map derived from a very detailed Digital Elevation Model (DEM).

Several approaches allow for the application of GIS in deterministic modeling:

- The use of an infinite slope model, which calculates the safety factor for each pixel,
- Selection of a number of profiles from the DEM and the other parameter maps, which are exported to external slope stability models, and
- Sampling of data at predefined grid points and exportation of these data to a 3-D slope stability model.

The result is a map showing the average safety factor for a given magnitude of groundwater depth and seismic acceleration. The variability of the input data can be used to calculate the probability of failure in connection with the return

period of triggering events. This method is applicable at large scales and over small areas, since detailed input data is required for the analysis. Examples for this method are Fall et al. (2006), Sakellariou and Ferentinou (2001), Gökçeoğlu and Aksoy (1996), and Montgomery et al. (1998).

2.3.2.2.2. Probabilistic Approaches

For decades, geotechnical modeling and analysis within a deterministic framework has facilitated the quantification of safety or reliability. However, performance indicators such as factor of safety do not take into consideration the variability of geotechnical material parameters such as cohesion, angle of internal friction and the undrained shear strength, some of which may also vary in magnitude and time. The spatial and temporal variability of pore water pressures is again very important but is not reflected in the calculated values of conventional factor of safety (Aleotti and Chowdhury, 1999).

There is now increasing recognition of the importance of uncertainties in geotechnical engineering. Parameter variability is only one example; there are also systematic uncertainties which arise from the fact that:

- A soil mass can only be investigated at a finite number of points.
- The number of field and laboratory tests conducted to determine soil parameters is limited by financial and time constraints.
- The testing equipment and methods are not perfect.

In addition to real parameter variability and systematic errors, there are often significant uncertainties associated with geotechnical models. Finally, uncertainties are also associated with the mechanisms of failure, occurrence of failure and its impact.

The recognition of uncertainties has led to the development of methods of analysis within a probabilistic framework while maintaining the basic geotechnical models. The probability of failure is defined as the probability that the performance function has a value below the threshold value. In probabilistic

analysis, factor of safety is the performance function and the threshold value is 1.

Capolongo et al. (2002) used a GIS-based probabilistic analysis to assess earthquake-triggered landslide hazard.

2.3.2.3. Neural Network Analysis

The procedure of neural network analysis consists, firstly, of attributing the weights to the connections in a casual manner and of choosing the input parameters (Figure 2.2). The calculated output is compared to that expected and the error is determined. The procedure progresses in an iterative manner until convergence of the calculated and expected output is reached. This is the learning phase, in which the function of the neural network is created (Aleotti and Chowdhury, 1999).

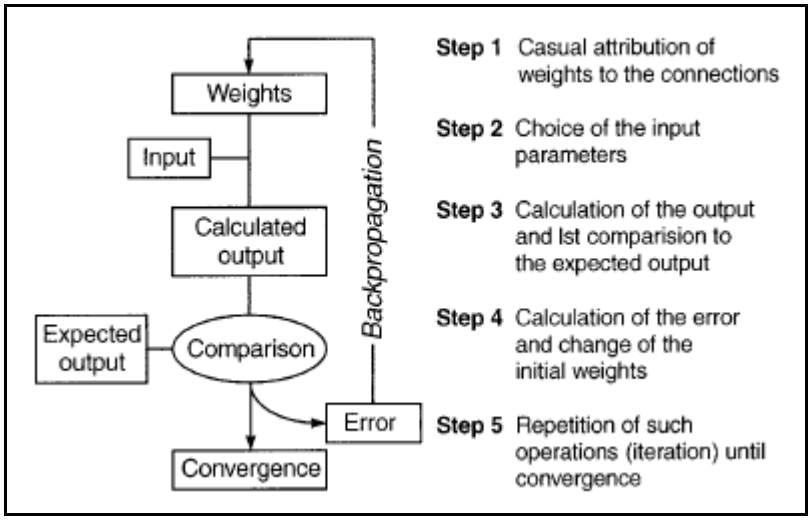

Figure 2.1. The procedure of neural network analysis (modified from Aleotti and Chowdury, 1999).

Some studies carried out by artificial neural network analysis in landslide susceptibility assessment are Lee et al. (2003a), Lee et al. (2004), Ercanoğlu (2005b), Ercanoğlu et al. (2006), Gomez and Kavzaoğlu (2005), and Yeşilnacar and Topal (2005).

2.3.2.4. Fuzzy Logic Approaches

Fuzzy logic is a powerful problem-solving methodology with a myriad of applications in embedded control and information processing. Fuzzy provides a remarkably simple way to draw definite conclusions from vague, ambiguous or imprecise information. In a sense, fuzzy logic resembles human decision making with its ability to work from approximate data and find precise solutions. Unlike classical logic which requires a deep understanding of a system, exact equations, and precise numeric values, Fuzzy logic incorporates an alternative way of thinking, which allows modeling complex systems using a higher level of abstraction originating from our knowledge and experience. Fuzzy Logic allows expressing this knowledge with subjective concepts such as very hot, bright red, and a long time which are mapped into exact numeric ranges.

Studies of landslide susceptibility assessment by fuzzy logic approaches include Abdolmasov and Obradovic (1997), Davis and Keller (1997), Chi et al. (2002), Ercanoğlu and Gökçeoğlu (2002), Ercanoğlu and Gökçeoğlu (2004), Ercanoğlu (2003), Ercanoğlu et al. (2006), Gorsevski et al. (2003), Lee et al. (2003b), Remondo et al. (2003), and Tangestani (2004).

CHAPTER 3

DATA PRODUCTION

This section presents the data production stage of this study. The sources of input data and production of parameter maps of all 10 parameters are explained. Also, the generation of databases for the statistical analysis is introduced in this chapter. The distributions of the data of all parameters used are analyzed and presented with histograms.

3.1. Production of Parameter Maps

3.1.1. Landslide Inventory

The landslide inventory map is compiled from the field surveys. It is presented in Figure 3.1. A total of 26 landslides were identified in the study area. These landslides are classified as slides according to Varnes (1978). The sliding mechanism of the landslides is rotational, and turns into translational when the sliding mass intersects with the bedding surface of the rock units. The depth of the landslides is generally shallow. They are generally observed at gentle slopes of Çaycuma Formation. Examples of some landslides in the study area are presented in Figures 3.2 and 3.3.

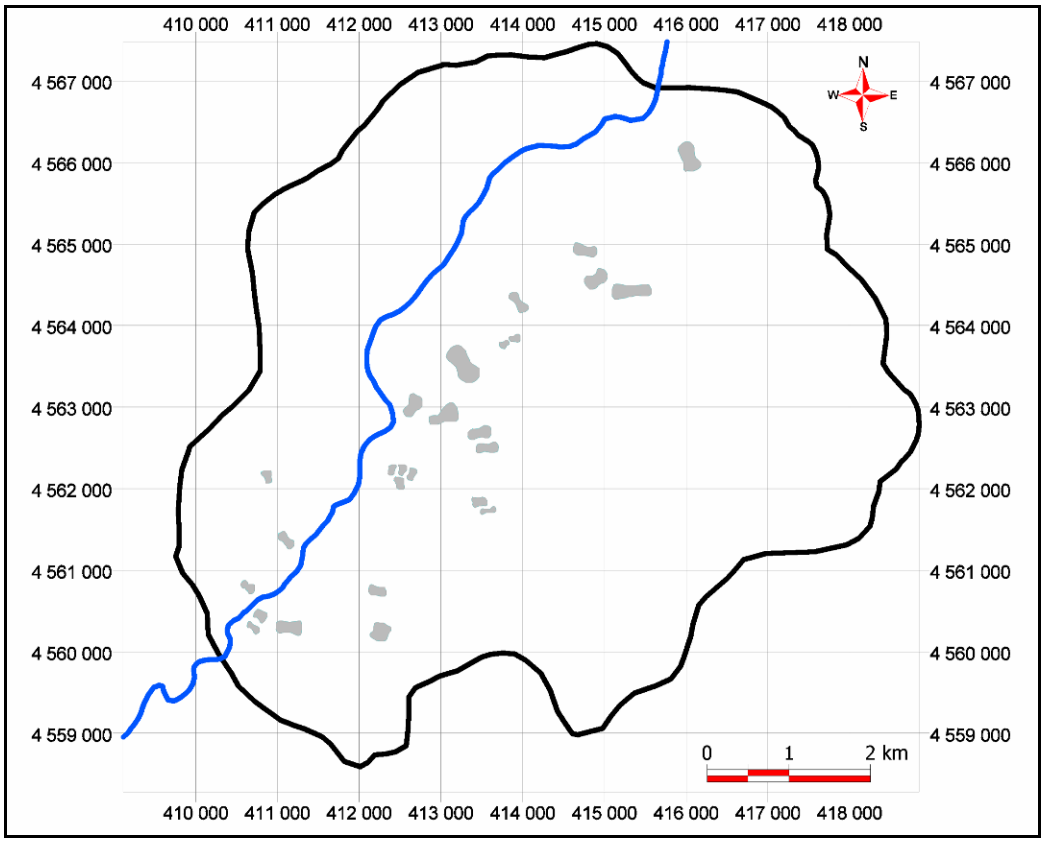

Figure 3.1. Landslide inventory map of the study area.

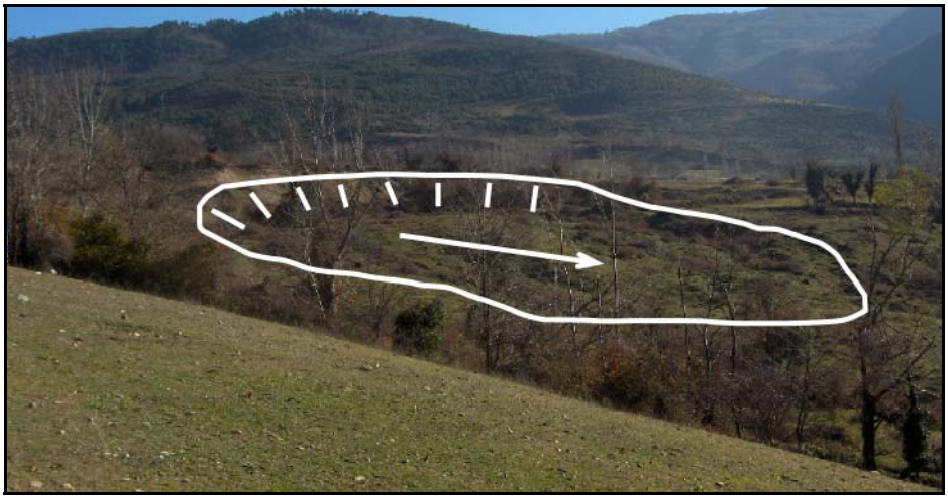

Figure 3.2. An example of landslides in the study area.

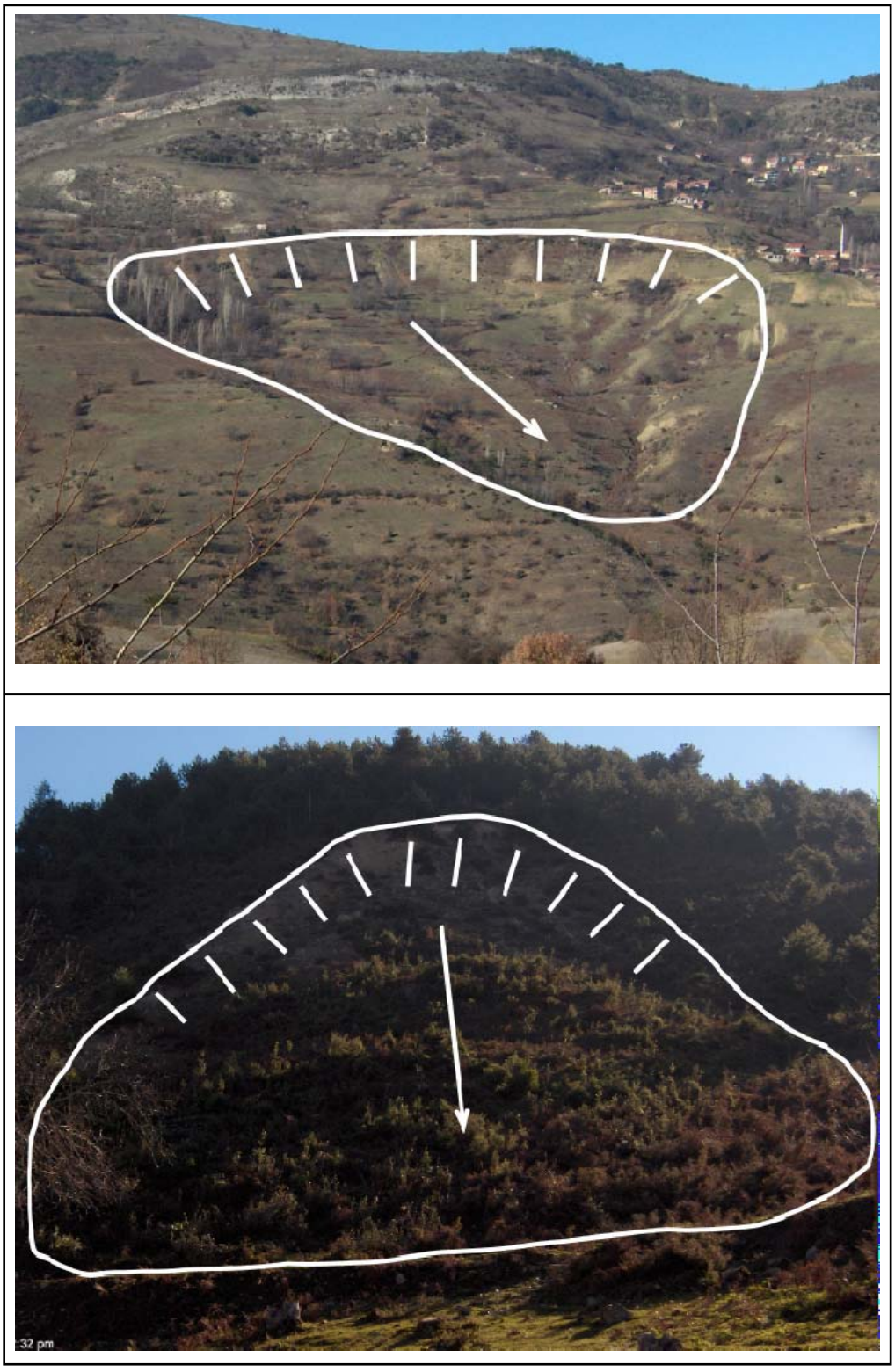

Figure 3.3. Some examples of landslides in the study area.

3.1.2. Digital Elevation Model (DEM) and its Derivatives

Digital Elevation Model (DEM) is a digital representation of ground surface topography. DEMs are often represented as raster, a regular grid of elevation values of the ground surface. The parameter maps including elevation, slope, aspect, curvature, distance to drainage lines, drainage density and distance to ridges are extracted from the DEM of the study area.

The DEM of the study area is constructed from 1:25000 scale topographical maps gathered from the General Command of Mapping (Turkish Army) as hard copies. The maps were revised by the General Command of Mapping in 1999. The hard copies were scanned and then, georeferenced on the computer with 4 control points having residual values of less than 1.5 meters. Then, the contour lines were manually digitized, and elevation values of the contour lines were assigned.

The contour data was converted to a raster map (DEM) by the minimum curvature surface fitting method in TNT Mips. This method was chosen as it provided the least Root Mean Square Error (RMSE) values than the other methods. The minimum curvature method applies a two-dimensional cubic spline function to fit a smooth surface to the set of input elevation values. The computation requires a number of iterations to adjust the surface so that the final result has a minimum amount of curvature (TNT Mips, 2000). The resolution of the DEM was chosen as 12.5 meters. All other parameter maps will have the same resolution value in this study.

3.1.2.1. Elevation

The DEM of the study area is presented in Figure 3.4. It will be used as the elevation input data in the analyses. Figure 3.5 presents the relief map of the study area with x3 vertical exaggeration generated from the DEM.

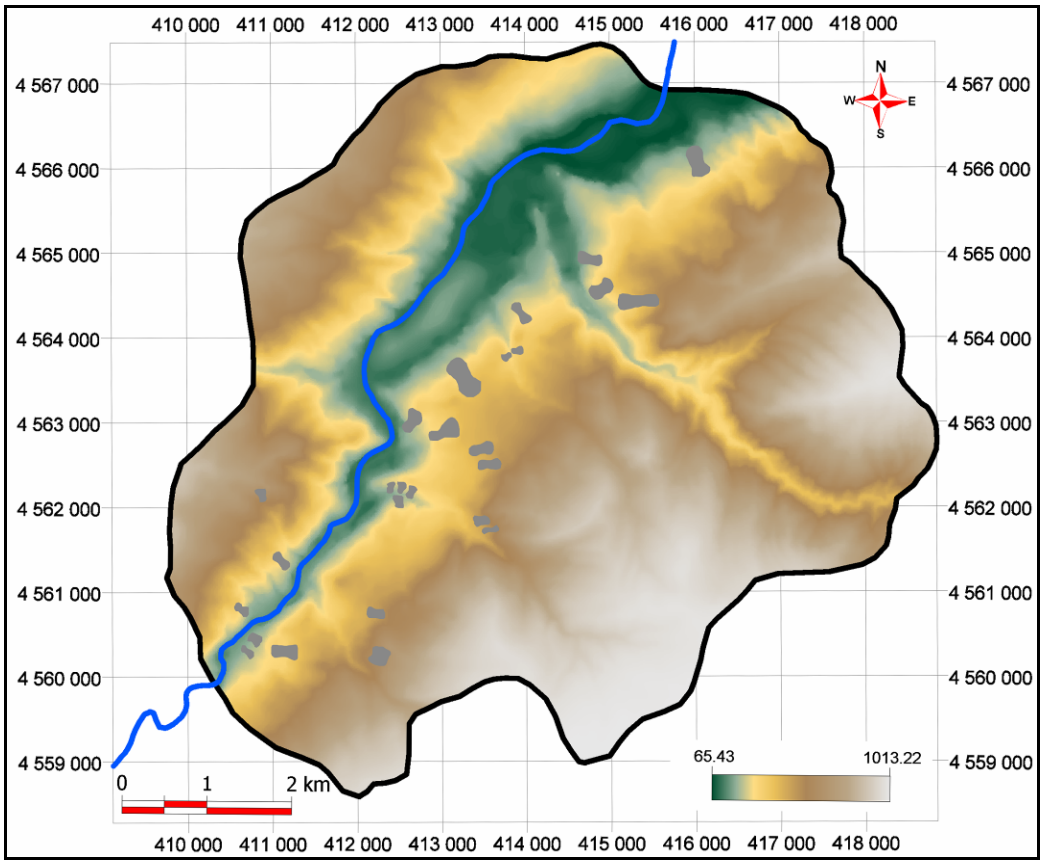

Figure 3.4. Digital Elevation Model (DEM) of the study area presented with landslides (gray polygons).

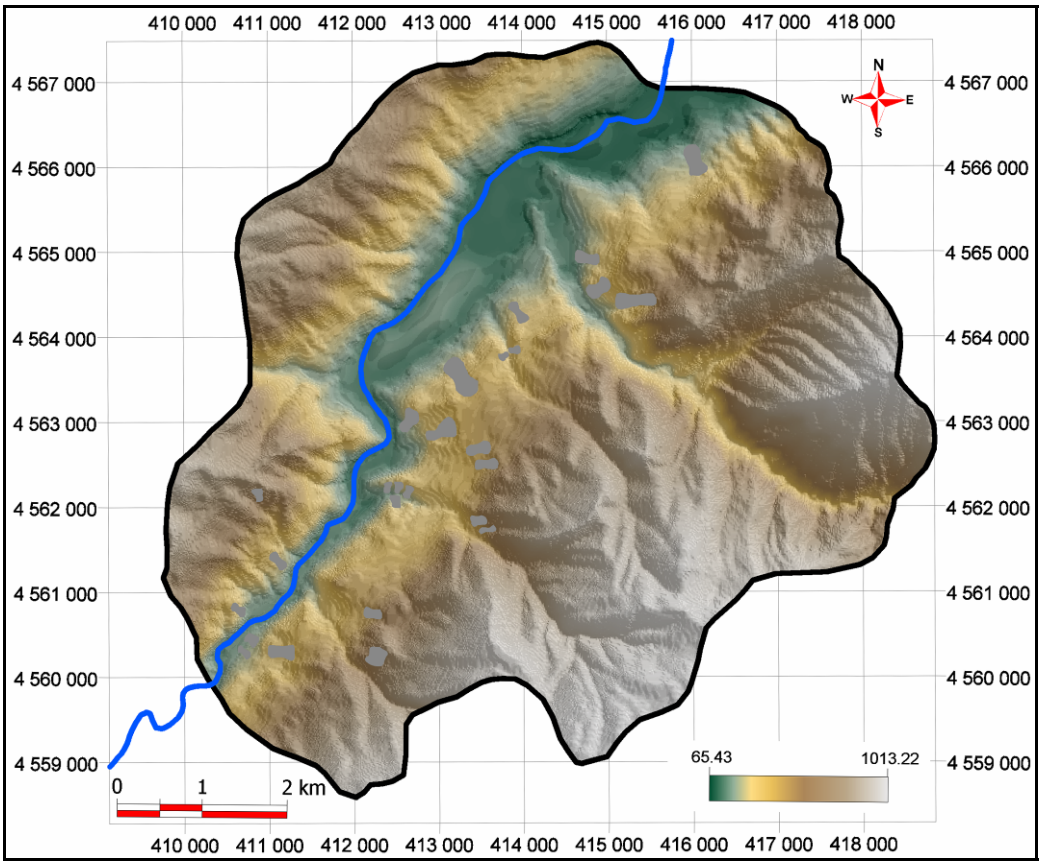

Figure 3.5. Relief map of the study area with x3 vertical exaggeration, presented with landslides (gray polygons).

3.1.2.2. Slope

Slope is the measure of surface steepness and measured in degrees. It has a range between 0 and 90 degrees, where 0 represents the flat and 90 represents the vertical areas. The slope values in the study area (Figure 3.6) range between 0 and 63 degrees. The mean value of the slope data is 17 and the standard deviation is 10.

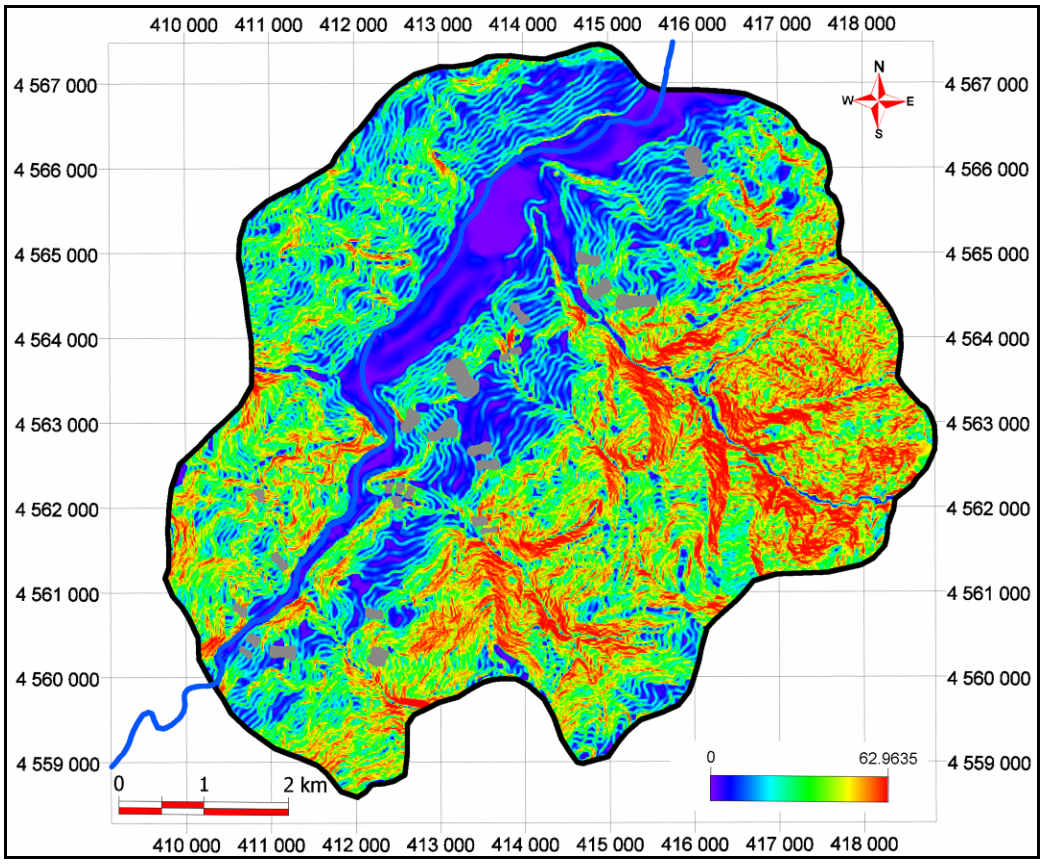

Figure 3.6. Slope map of the study area presented with landslides (gray polygons).

3.1.2.3. Aspect

Aspect is a measure of slope orientation and measured in degrees. Aspect tells you the direction that the slope faces. It is calculated as the compass direction of a slope. Aspect values of the area vary between -1 to 360 degrees where -1 represents the flat lying areas (Figure 3.7). The mean value of the aspect data is 200 and the standard deviation is 112.

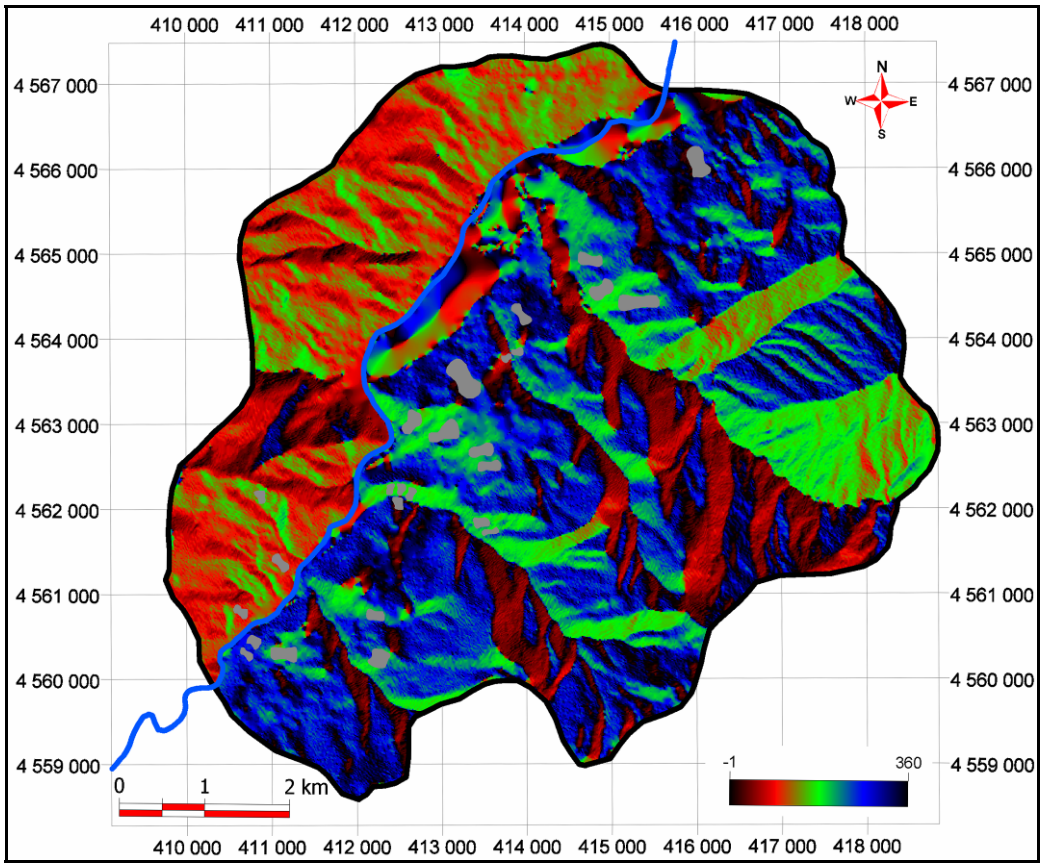

Figure 3.7. Aspect map of the study area presented with landslides (gray polygons).

3.1.2.4. Curvature

Surface curvature is the curvature of a line formed by intersecting a plane (in some chosen orientation) with the terrain surface. The curvature value is the reciprocal of the radius of curvature of the line, so a broad curve has a small curvature and a tight curve has a high curvature value (Figure 3.8). The curvature is measured in radians per meter.

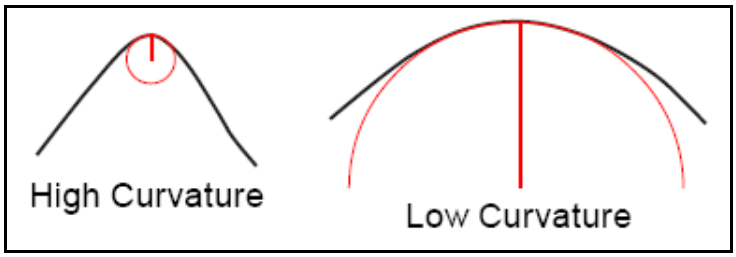

Figure 3.8. Types of surface curvature.

Profile curvature is the curvature in the vertical plane parallel to the slope direction. It measures the rate of change of slope and therefore influences the flow velocity of water draining the surface and thus erosion and the resulting downslope movement of sediment. Plan curvature (also called contour curvature) is the curvature of a contour line formed by intersecting a horizontal plane with the surface. Plan curvature influences the convergence or divergence of water during downhill flow (MicroImages, 2007).

Profile (vertical) curvature raster produced is presented in Figure 3.9. Positive values indicate convex upward surfaces. The values vary between -0.04 to 0.03. The mean value of the profile curvature data is 0 and the standard deviation is 0.003.

Plan (contour) curvature raster produced is presented in Figure 3.10. Positive values indicate convex outward surfaces. The values vary between -1.8 to 1.5. The mean value of the plan curvature data is 0 and the standard deviation is 0.02.

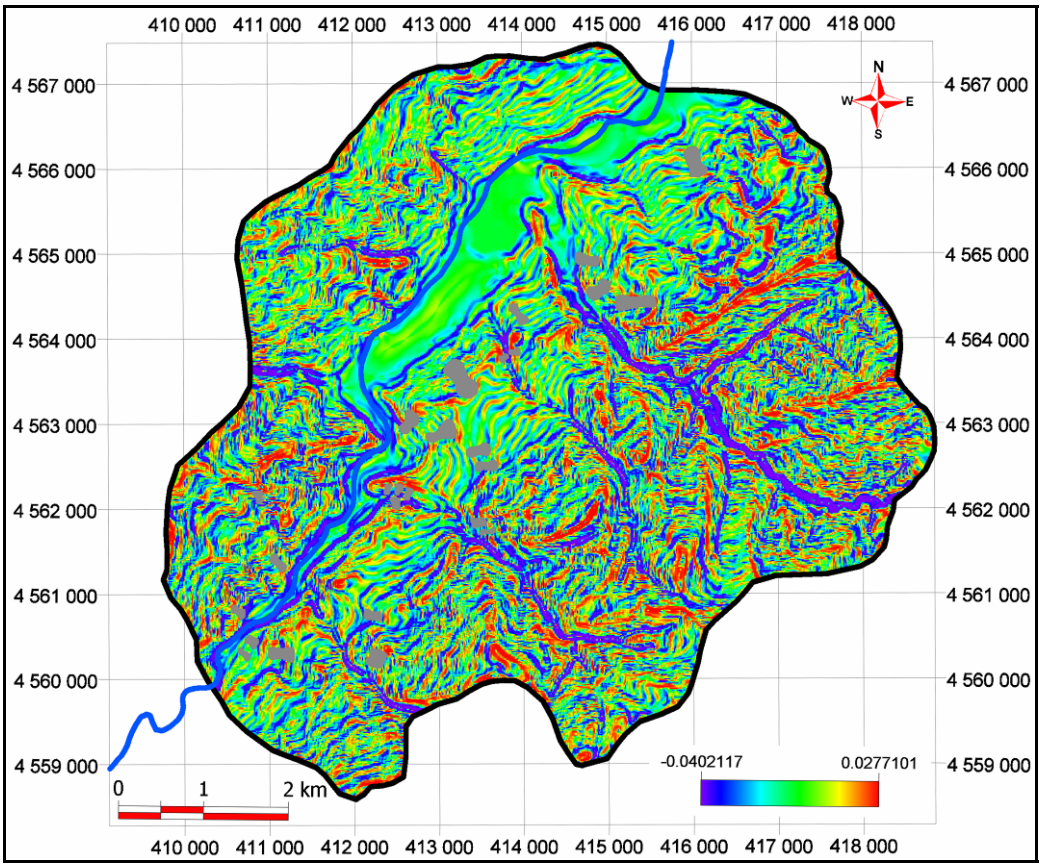

Figure 3.9. Profile curvature map of the study area presented with landslides (gray polygons).

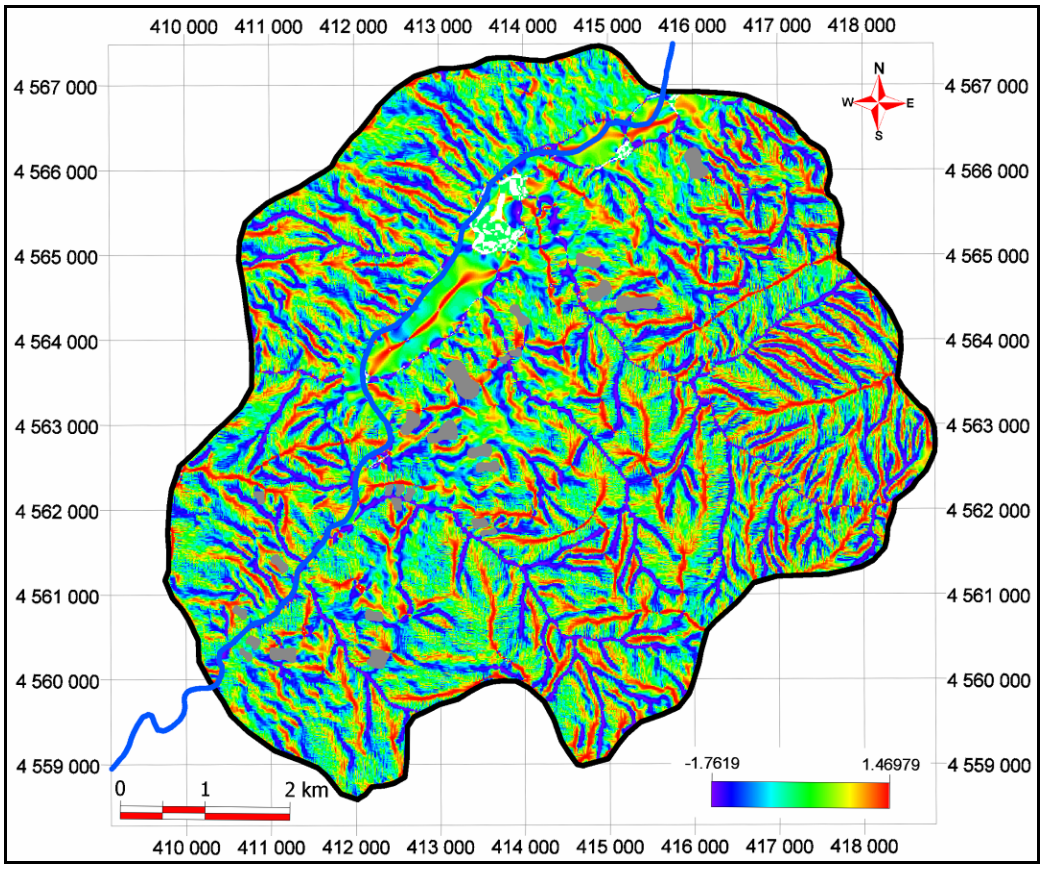

Figure 3.10. Plan curvature map of the study area presented with landslides (gray polygons).

3.1.2.5. Derivatives of Watershed Analysis

The watershed process provides comprehensive processing and evaluation of raster DEMs to define watersheds, flow paths, and basins (Figure 3.11). The process begins by evaluating the elevation raster for depressions and constructs watershed polygons based on the depressions recognized. Vector objects are generated comprised of polygon, line, and/or point elements that reveal the watershed, flow path, and pour point locations. The drainage network and ridgelines generated by the watershed analysis are used to produce the

parameter maps distance to drainage lines, drainage density and distance to ridges.

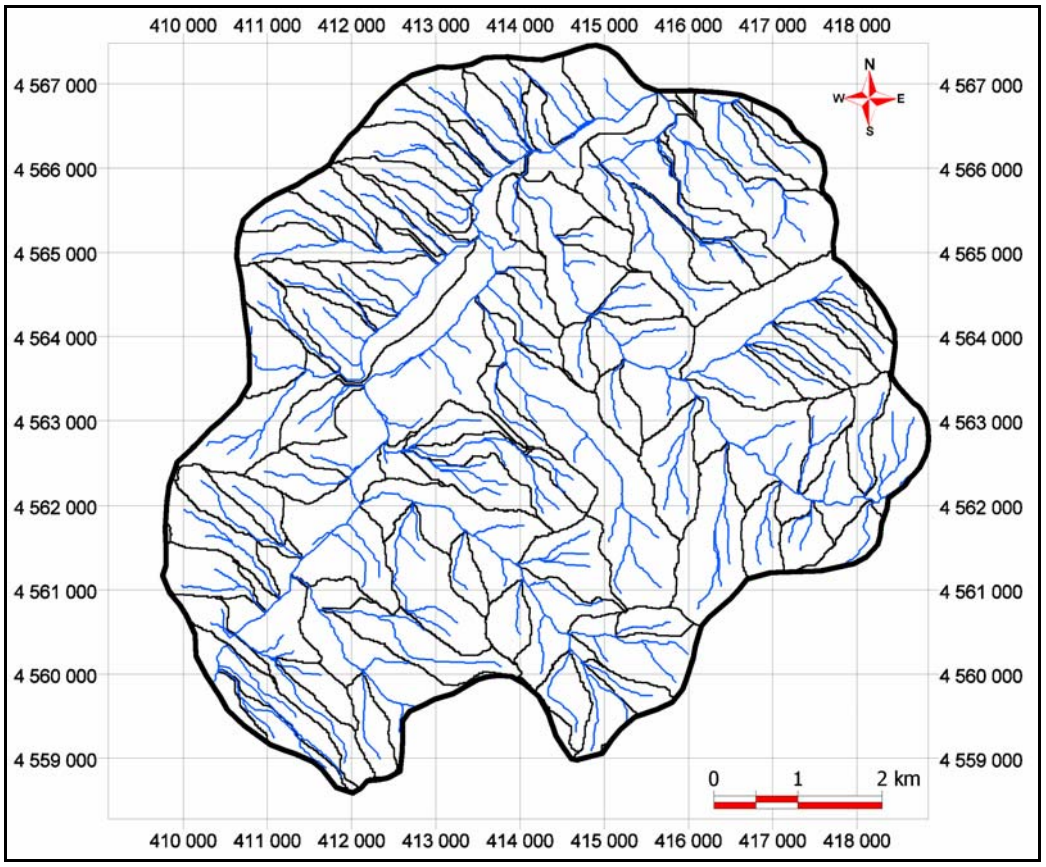

Figure 3.11. The drainage system of the study area including microcatchments, ridges and the drainage network.

The distances of every pixel regarding the drainage lines are calculated and presented in Figure 3.12. The minimum distance of pixels is 0 and the maximum is 545 meters. The mean value of the distance to drainage lines data is 107 and the standard deviation is 82.

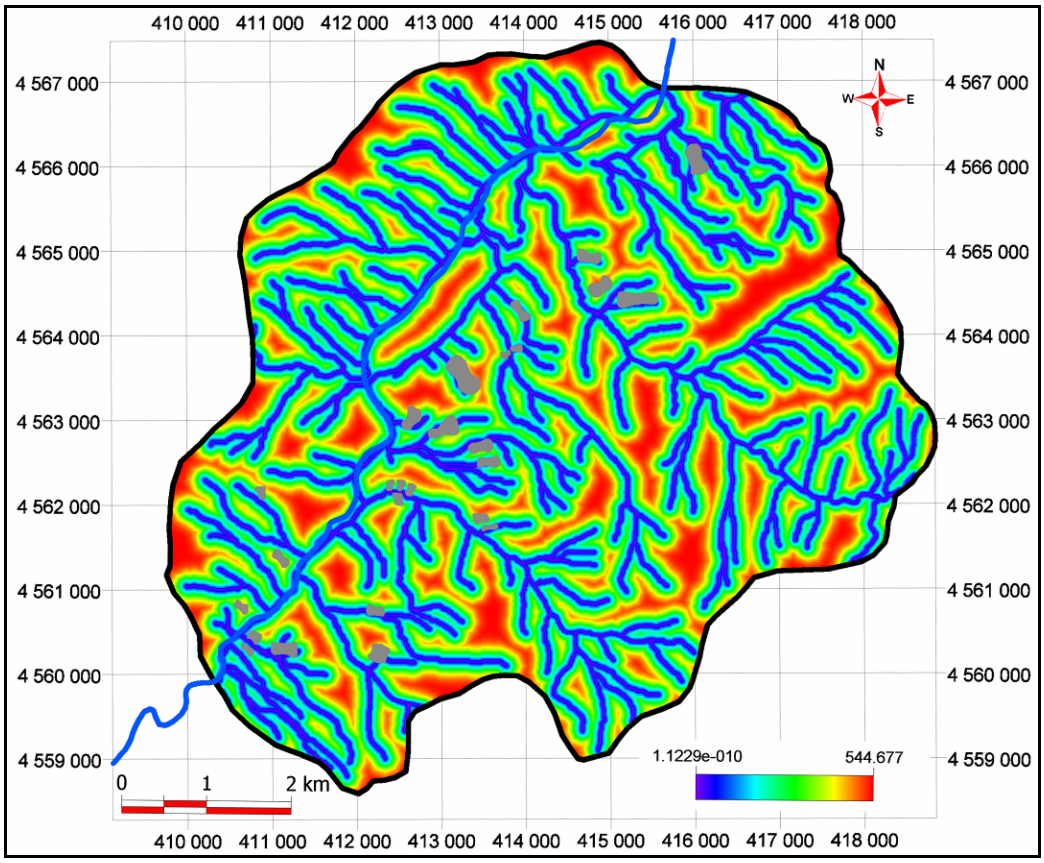

Figure 3.12. Distance to drainage lines map of the study area presented with landslides (gray polygons).

The drainage lines are also used to calculate the kilometer square density of drainage lines in the whole study area. To maintain the 1 square kilometer search distance 564 meter search radius is used (Figure 3.13). The vector of drainage lines are converted to point data with a distance of 12.5 meters and put into point density analysis. The drainage density values of the study area range from 19 to 638. The mean value of the drainage density data is 293 and the standard deviation is 99.

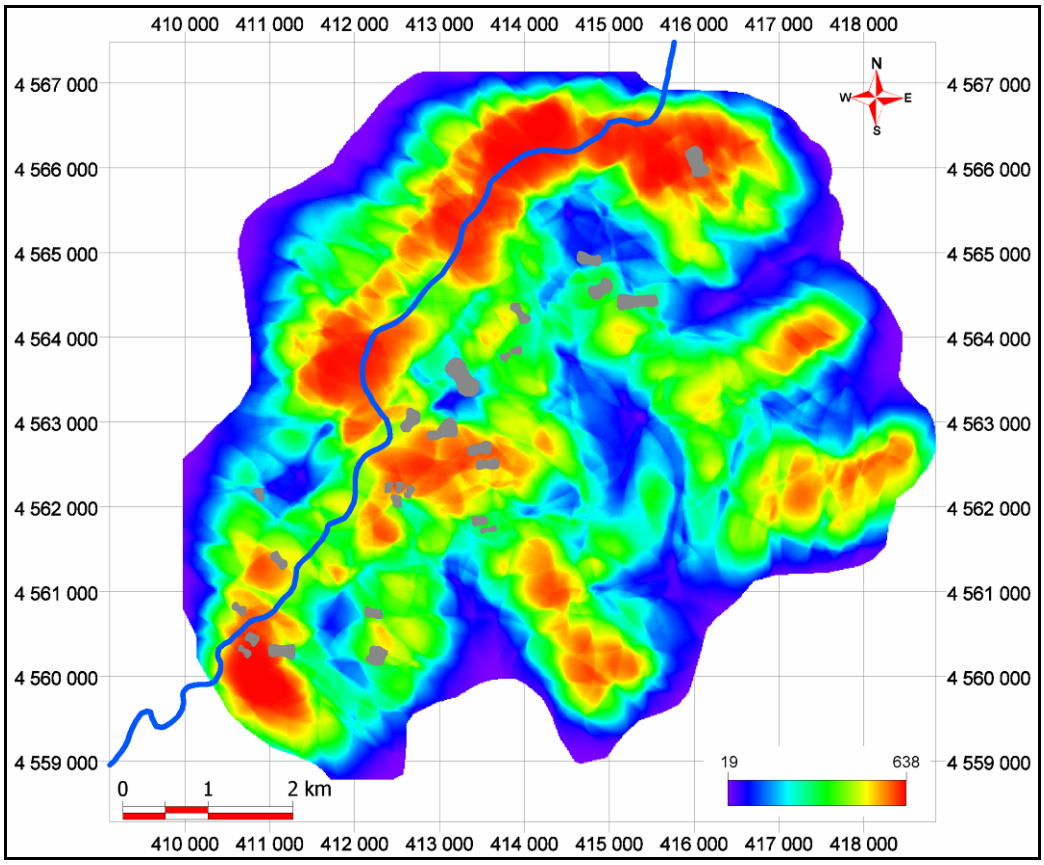

Figure 3.13. Drainage density map of the study area presented with landslides (gray polygons).

The ridgelines output of the watershed analysis is used to calculate the nearest distances to the ridges of each pixel (Figure 3.14). The minimum value for the distance to ridges is 6 meters and the maximum is 728 meters. The distribution has a mean of 168 meters with standard deviation of 110.

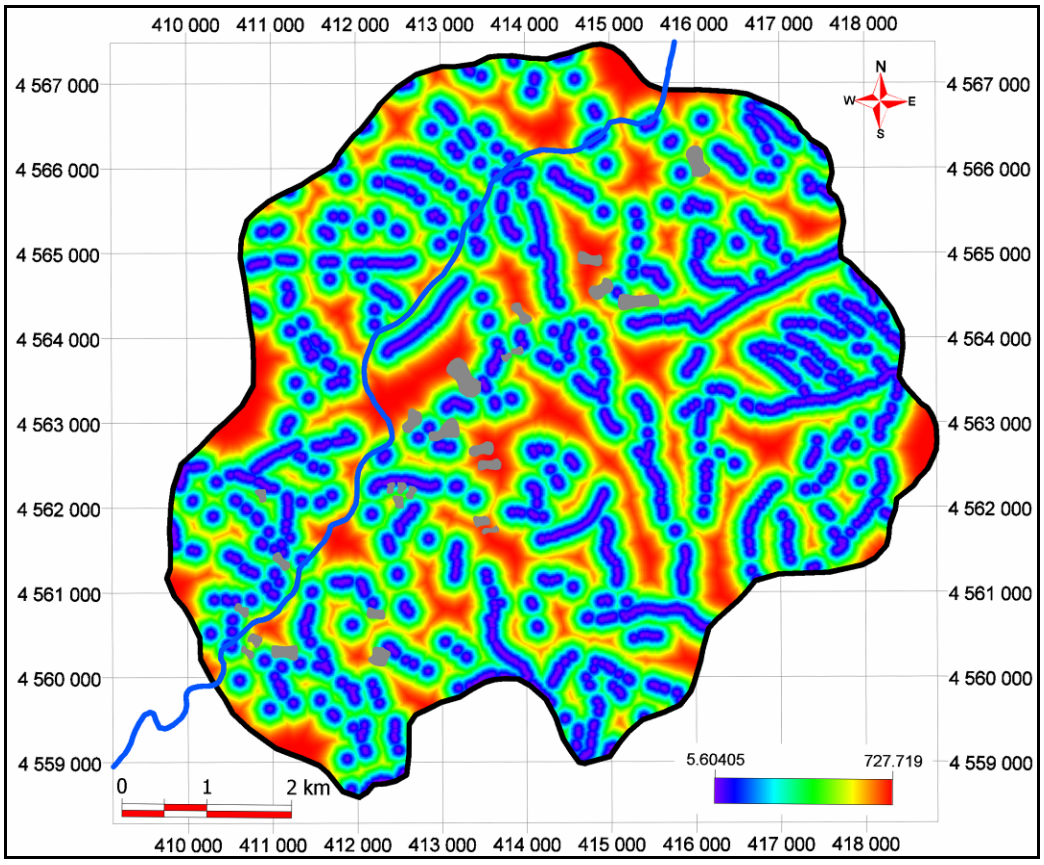

Figure 3.14. Distance to ridges map of the study area presented with landslides (gray polygons).

3.1.3. Distance to Road and Power Line Network

Building the infrastructure elements such as roads and power lines are considered as the man-made activities affecting slope instabilities. For the construction of power line poles, the forest under and in the vicinity of the pylon is cut, so land cover changes. For the road building both the cut slopes, the land cover change and the economical activity near the roads, due to highway tourism, attract people.

The roads and power lines in the study area are digitized from the topographical maps. The vector data of roads and power lines are merged together and the

distances of every pixel regarding the roads and power lines are calculated (Figure 3.15). The minimum distance of pixels is 0 and the maximum is 746 meters. The distribution has a mean of 100 with a standard deviation of 99.

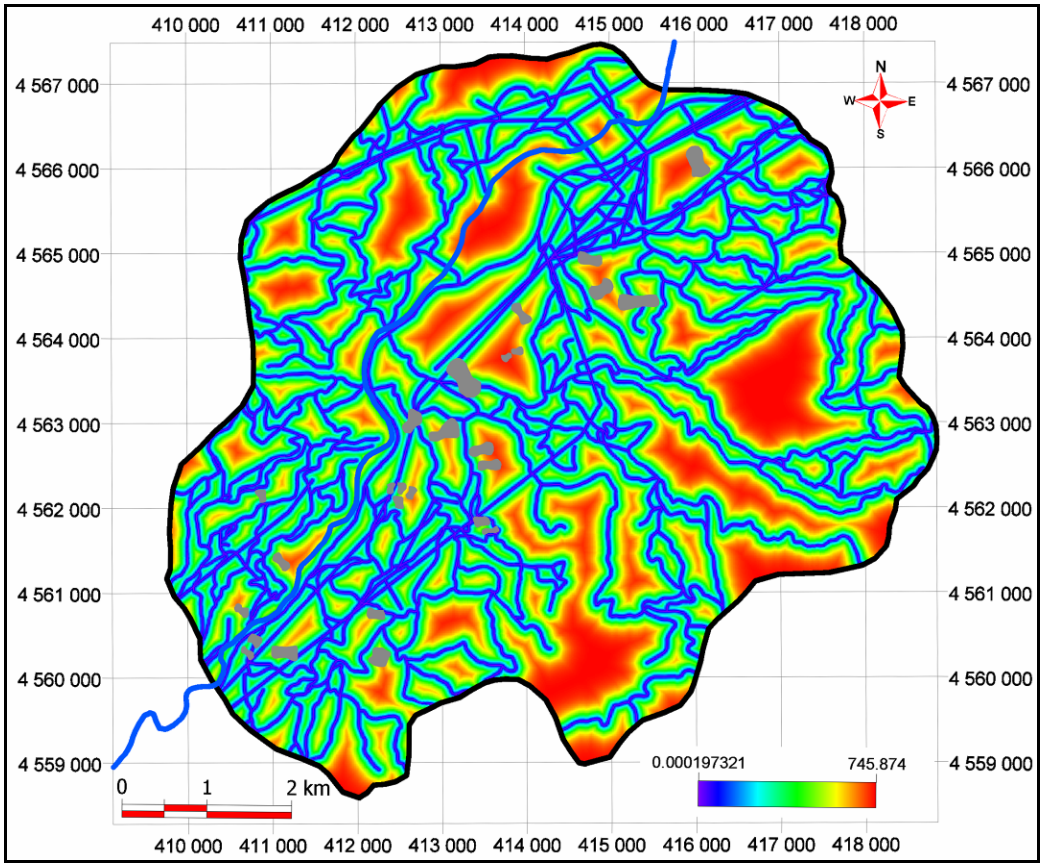

Figure 3.15. Distance to road and power line network map of the study area presented with landslides (gray polygons).

3.1.4. Lithology

The geological map of the study area is compiled from existing geological maps and publications from the literature. The existing maps contain information

inadequacies and mismatches, so they were checked and refined in the field surveys. The compiled map is digitized (Figure 3.16). A database concerning the lithology names and symbols are attached. Five lithologic units are identified in the study area. Their areal distribution is presented in Figure 3.17. Çaycuma Formation has the greatest areal coverage with almost the half of the study area. Majority of the landslides occurred in this formation.

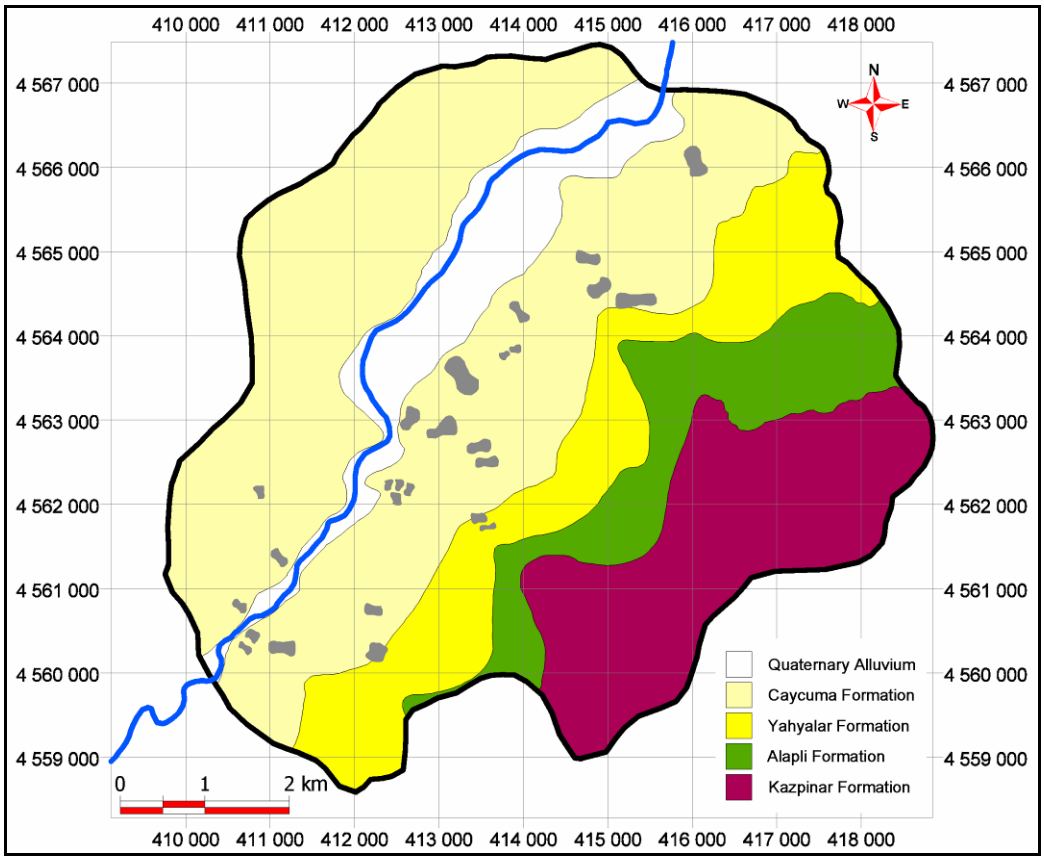

Figure 3.16. Geological map showing the lithologic units in the study area presented with landslides (gray polygons) (modified from Yergök et al., 1987).

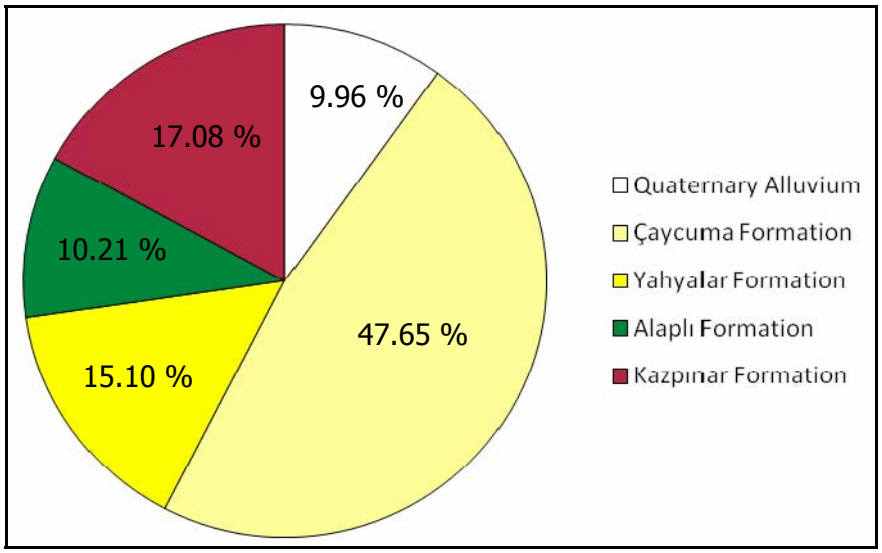

Figure 3.17. Areal distribution of the lithologic units in the study area.

3.2. Production of Databases

3.2.1. Decision Rules for Database Production

After completing the parameter maps, decision rules of landslide occurrences should be created. The new approach called "seed cells" introduced by Süzen and Doyuran (2004a) is followed to create the decision rules in this study. The idea behind the seed cells concept is that the best undisturbed morphological conditions (conditions before landslide occurs) would be extracted from the vicinity of the landslide polygon itself. This is achieved by adding a buffer zone to the crown and flanks of the landslide. In this study three different sets of seed cells are used in order to compare their results in susceptibility mapping:

1. Crowns and flanks
2. Crowns
3. Flanks

The distance of 50 meters is taken for the buffer line. If the distance between the slide boundary and microcatchment divide line is smaller than 50 meters, the microcatchment divide line is used for the buffer zone. If the distance is larger, the 50-meter buffer line is used for seed cell generation (Figure 3.18). Higher values than 50 meters are tested and it is observed that most of the cells falls beyond the microcatchment divide lines.

To create the databases, a point mesh grid of 12.5 meters is laid over the study area. The seed cell polygons are extracted from this grid. The raster values of the parameter maps are transferred to the midpoint nodes of the cells and stored as three different seed cell attribute databases (crowns and flanks, crowns, flanks) for the statistical analysis. Table 3.1 presents the amounts of seed cell nodes extracted for each database.

Table 3.1. The number of seed cell nodes of each database.

Database	# of Seed Cell Nodes
Crowns and Flanks	3931
Crowns	2289
Flanks	1642

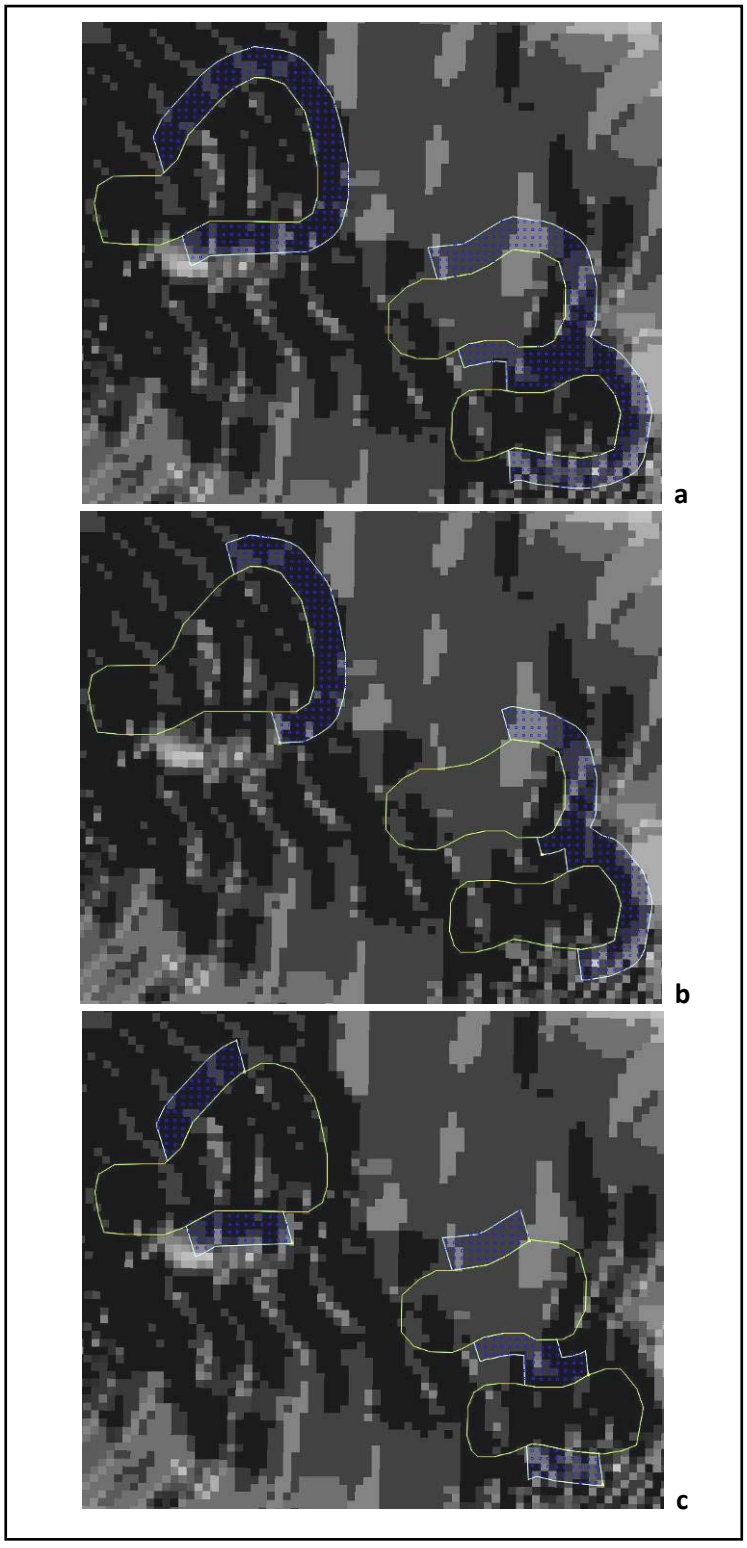

Figure 3.18. Seed cell generation, a. crown and flanks, b. crowns, c. flanks (yellow polygons are landslides, white polygons are seed cell zones).

3.2.2. Seed Cell Databases

Three different databases are created from the parameter maps by using the seed cells of crowns and flanks, only crowns and only flanks. These parameters and their nature and minimum-maximum values are summarized in Table 3.2. The database generation results in 3931 nodes for the crowns and flanks database, 2289 nodes for the crowns database, and 1642 nodes for the flanks database. This section summarizes the statistics and distributions of each attribute of each database.

Table 3.2. The nature and minimum-maximum values of the parameters.

Parameters	Nature	Min-Max Value (Unit)
Elevation	Ratio	65.43 – 1013.22 (m)
Slope	Ratio	0 – 62.964 (deg)
Aspect	Ratio	-1 – 360 (deg)
Profile Curvature	Ratio	-0.0402 – 0.0277 (rad/m)
Plan Curvature	Ratio	-1.7619 – 1.4698 (rad/m)
Distance to Drainage Lines	Ratio	1.123E-10 – 544.677 (m)
Drainage Density	Ratio	19 – 638 (#/km^2)
Distance to Ridges	Ratio	5.604 – 727.719 (m)
Distance to Road & Power Line Network	Ratio	0.0002 – 745.874 (m)
Lithology	Nominal	-

3.2.2.1. Elevation

The elevation values of the study area range from 65 to 1013 meters, but the landslide occurrences are observed in the range of 110 to 392 meters (Table 3.3). This may due to at higher elevations there are more stable rock formations. Majority of the data is distributed between 120 and 230 meters (Figure 3.19).

Table 3.3. Descriptive statistics of the elevation parameter.

STATISTICS	Whole Data	Crowns and Flanks	Crowns	Flanks
Minimum	65.425	110	121.557	110
Maximum	1013.22	392.263	392.263	384.783
Mean	332.817	209.03	220.536	192.988
Standard Deviation	207.296	65.522	67.146	59.608

3.2.2.2. Slope

Landslides are observed on the slopes up to 42 degrees. The steeper slopes of the study area are free of landslides. The flanks data has a slightly narrower range than the others (Table 3.4). Figure 3.20 presents the frequency distributions of the slope parameter of each data set. All data show a normal distribution.

Table 3.4. Descriptive statistics of the slope parameter.

STATISTICS	Whole Data	Crowns and Flanks	Crowns	Flanks
Minimum	0	0.4499	0.450	0.991
Maximum	62.964	41.805	41.805	38.654
Mean	16.483	13.437	13.132	13.862
Standard Deviation	0	0.4499	0.450	0.991

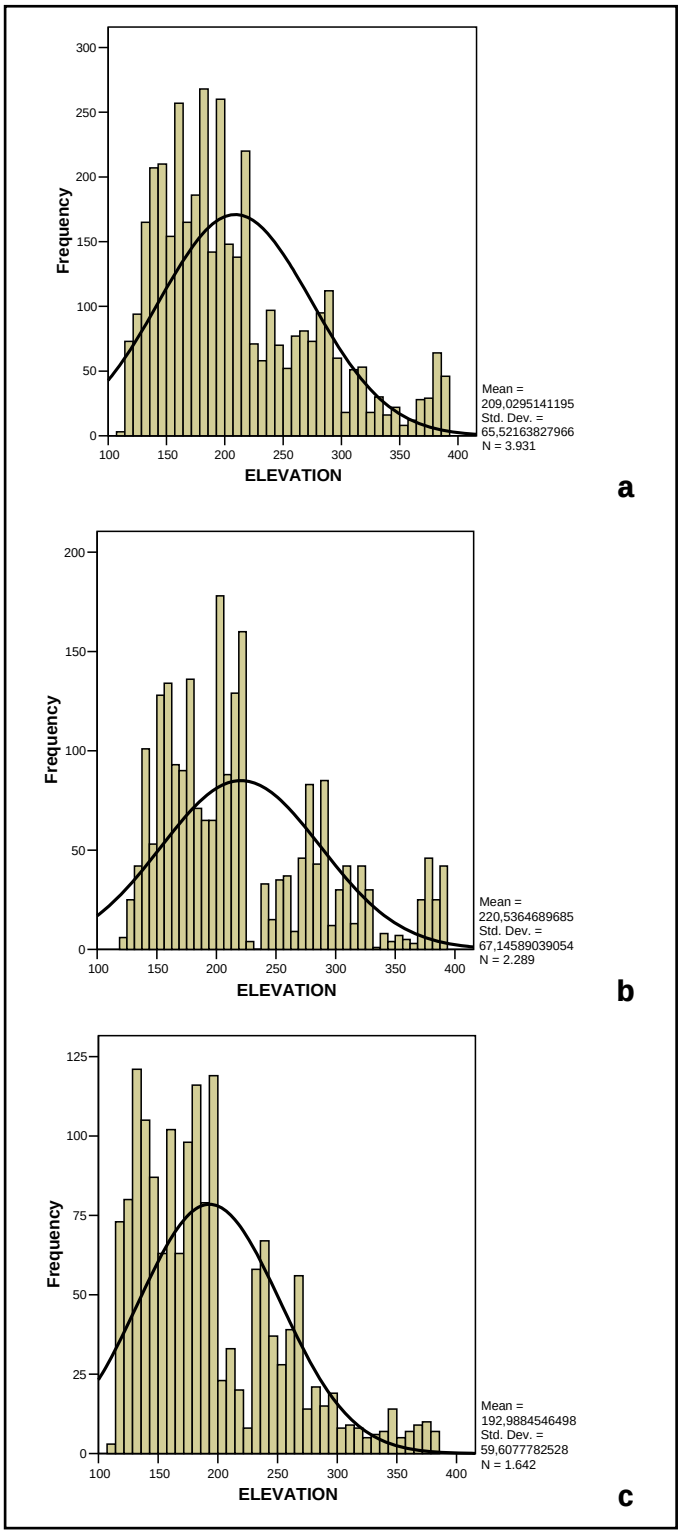

Figure 3.19. Frequency distributions of the elevation parameter, a. crowns and flanks, b. crowns, c. flanks.

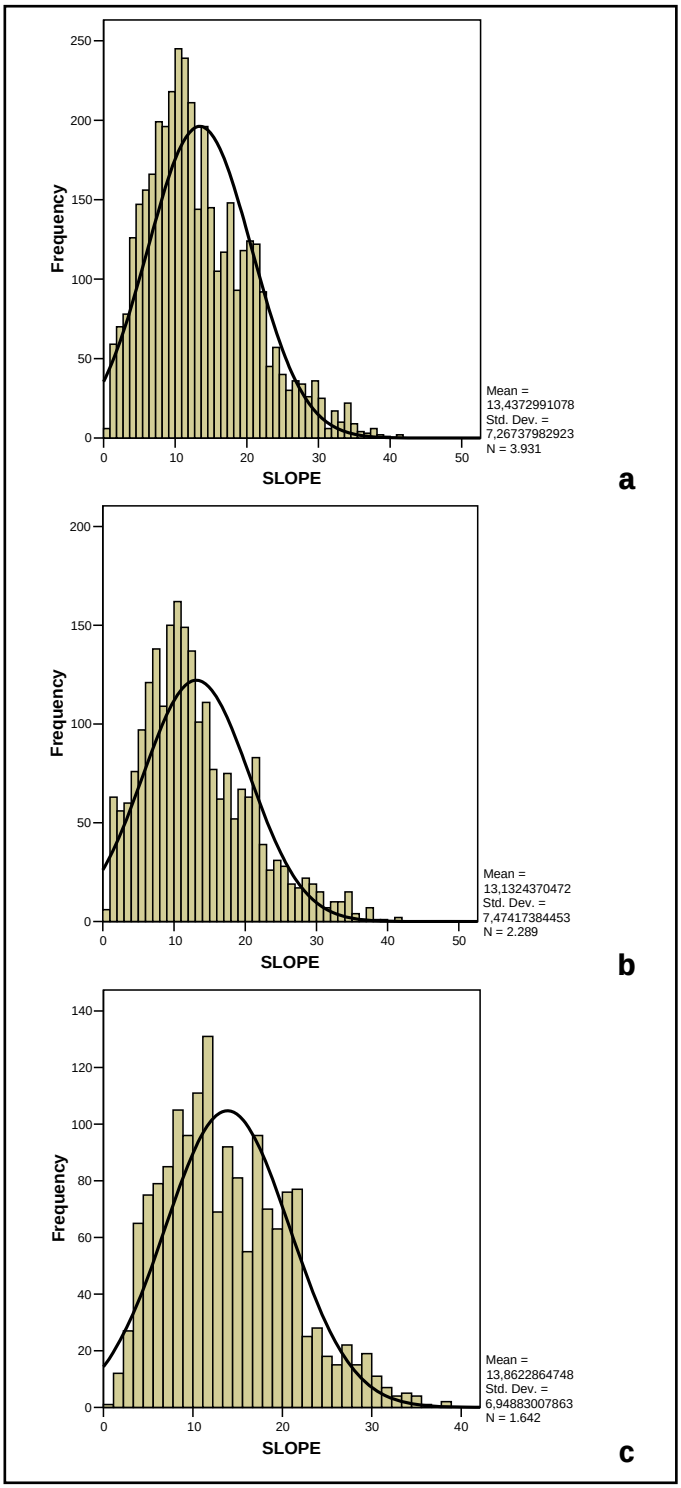

Figure 3.20. Frequency distributions of the slope parameter, a. crowns and flanks, b. crowns, c. flanks.

3.2.2.3. Aspect

The descriptive statistics of the aspect parameter is presented in Table 3.5. The aspect distribution of all databases generally populates between 200 and 360 degrees (Figure 3.21). Thus, the landslides are observed generally on southwest, west and northwest facing slopes.

Table 3.5. Descriptive statistics of the aspect parameter.

STATISTICS	Whole Data	Crowns and Flanks	Crowns	Flanks
Minimum	-1	0	0	0
Maximum	360	360	360	360
Mean	199.848	247.063	250.371	242.451
Standard Deviation	111.555	83.047	79.357	87.749

3.2.2.4. Profile Curvature

The ranges of the seed cell databases are almost the same (Table 3.6), and all data sets are normally distributed (Figure 3.22). Positive values are slightly greater indicating more convex upward surfaces.

Table 3.6. Descriptive statistics of the profile curvature parameter.

STATISTICS	Whole Data	Crowns and Flanks	Crowns	Flanks
Minimum	-0.0402117	-0.00896113	-0.00896113	-0.00811831
Maximum	0.0277101	0.01245040	0.01245040	0.01211208
Mean	-0.0001309	0.00041756	0.00077849	-0.00008558
Standard Deviation	0.0026638	0.00233962	0.00242329	0.00211814

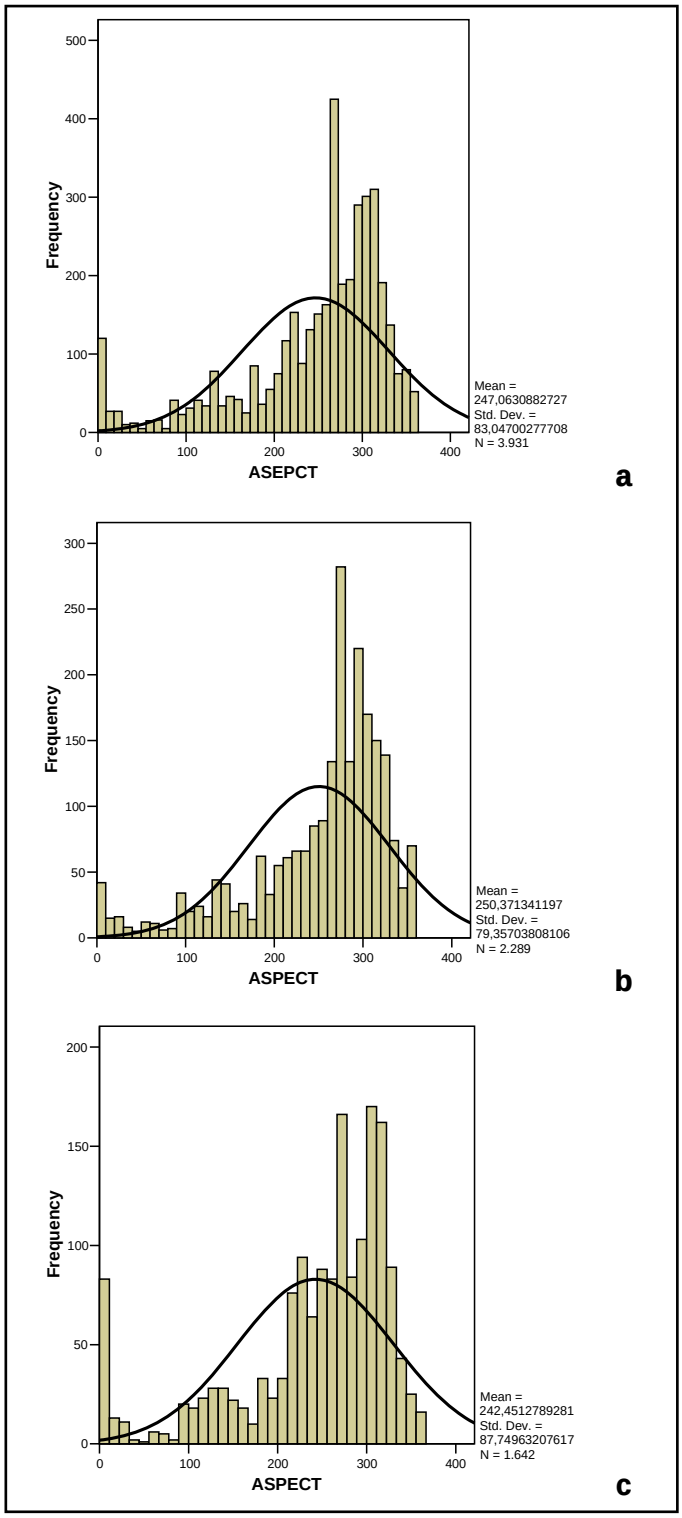

Figure 3.21. Frequency distributions of the aspect parameter, a. crowns and flanks, b. crowns, c. flanks.

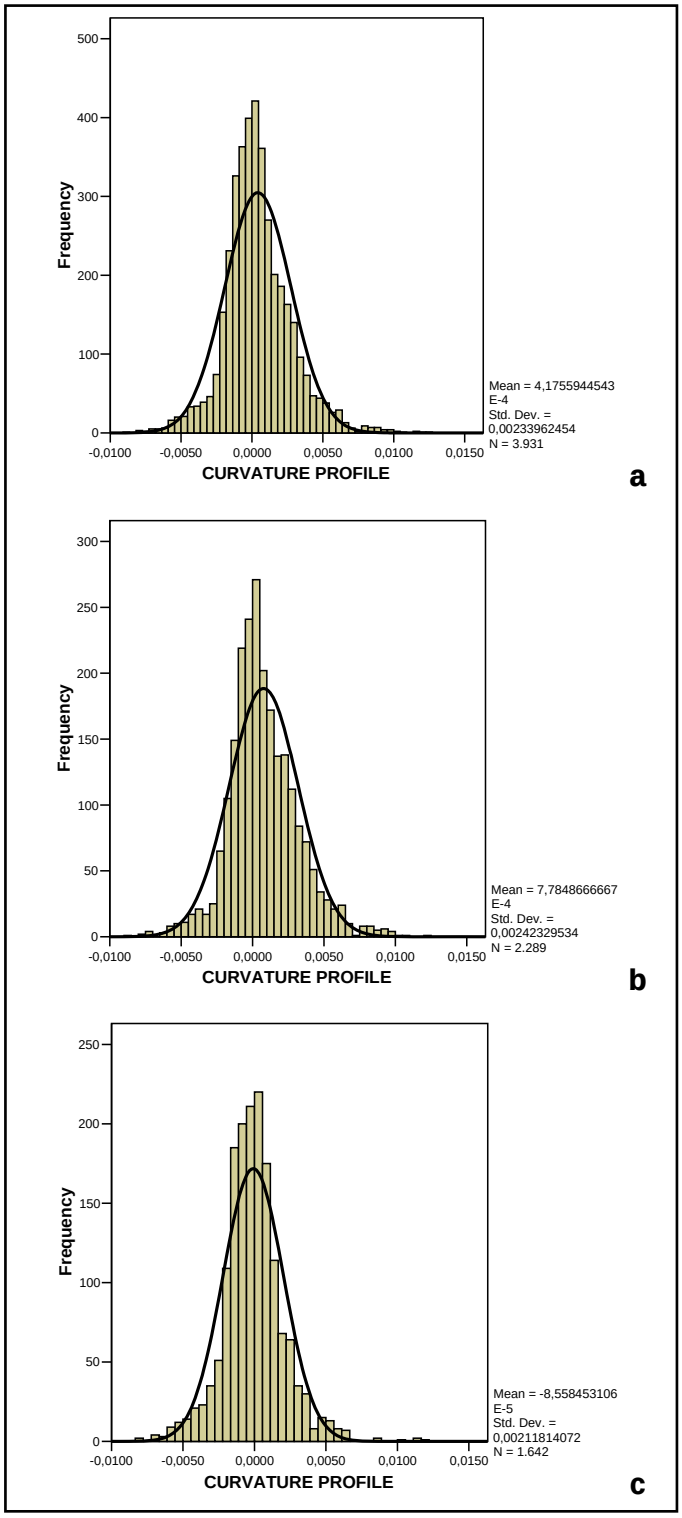

Figure 3.22. Frequency distributions of the profile curvature parameter, a. crowns and flanks, b. crowns, c. flanks.

3.2.2.5. Plan Curvature

The ranges of the crowns and flanks and crowns databases are the same, whereas the flanks database has a narrower range (Table 3.7). All data sets are normally distributed (Figure 3.23). Positive values are slightly greater indicating more convex outward surfaces.

Table 3.7. Descriptive statistics of the plan curvature parameter.

STATISTICS	Whole Data	Crowns and Flanks	Crowns	Flanks
Minimum	-1.7619	-0.23628700	-0.23628700	-0.07972462
Maximum	1.4698	0.30755818	0.30755818	0.05317539
Mean	0.00005	0.00247782	0.00350207	0.00105000
Standard Deviation	0.01791	0.01495275	0.01704703	0.01125961

3.2.2.6. Distance to Drainage Lines

The descriptive statistics of the distance to drainage lines parameter are presented in Table 3.8. The frequency distributions of the data sets indicate the abundance of first order streams in the study area (Figure 3.24).

Table 3.8. Descriptive statistics of the distance to drainage lines parameter.

STATISTICS	Whole Data	Crowns and Flanks	Crowns	Flanks
Minimum	0	0	0	0
Maximum	544.677	268.957	268.957	257.848
Mean	106.967	95.947	104.528	83.986
Standard Deviation	81.928	61.292	62.252	57.860

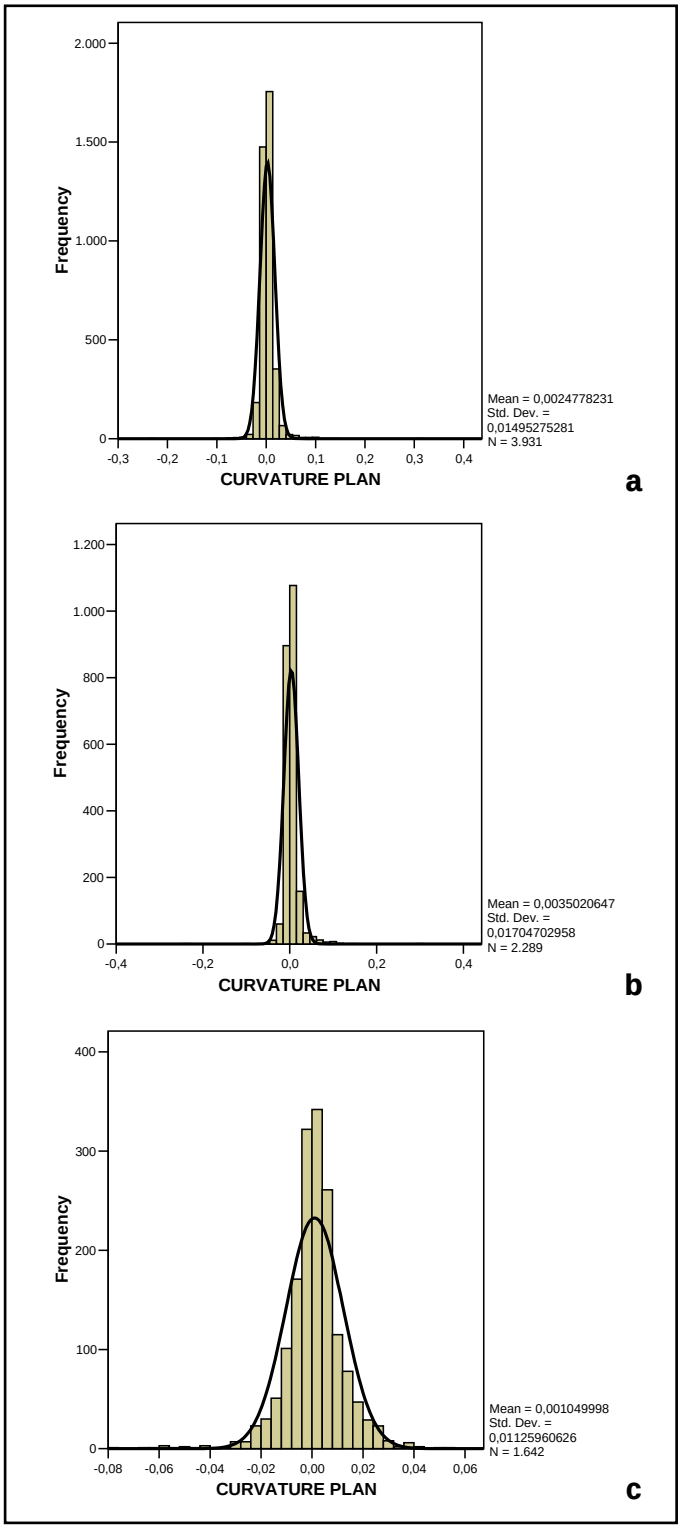

Figure 3.23. Frequency distributions of the plan curvature parameter, a. crowns and flanks, b. crowns, c. flanks.

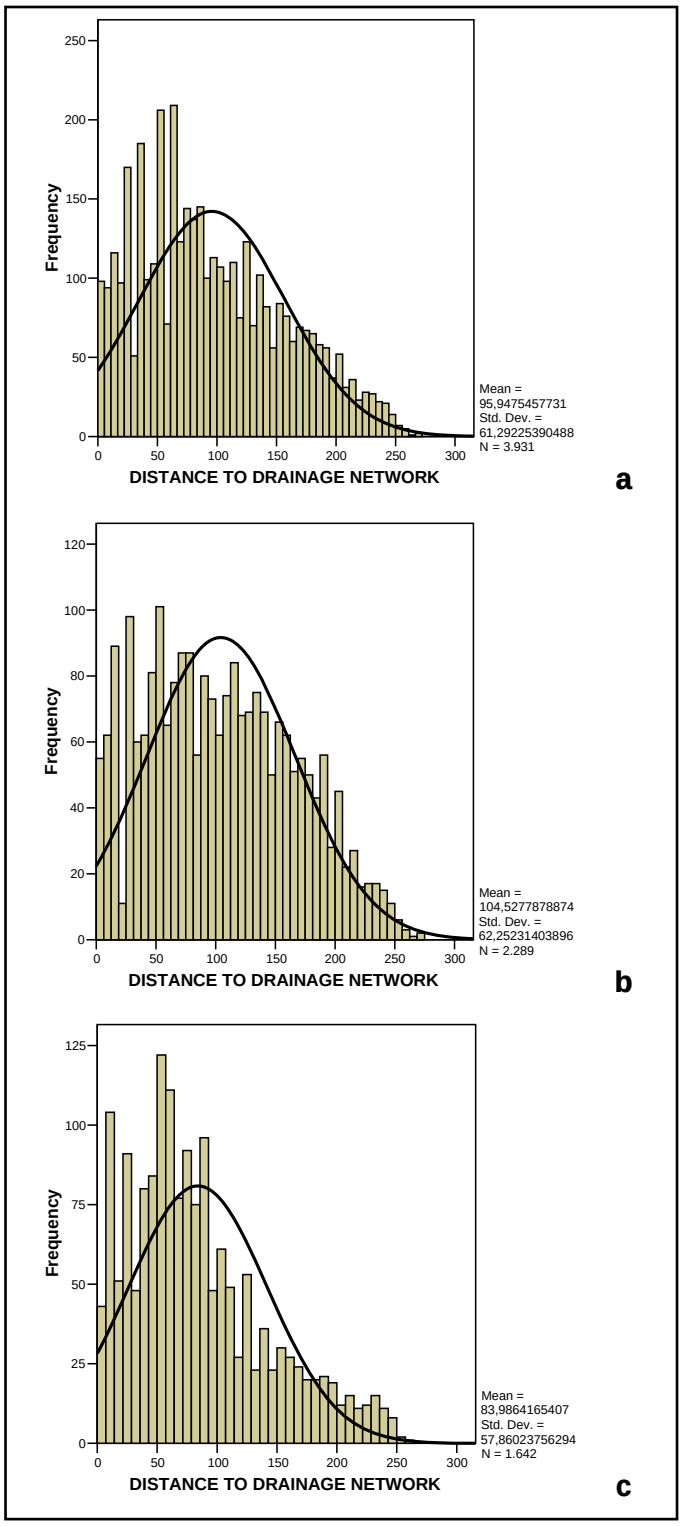

Figure 3.24. Frequency distributions of distance to drainage lines parameter, a. crowns and flanks, b. crowns, c. flanks.

3.2.2.7. Drainage Density

The descriptive statistics of the drainage density parameter are presented in Table 3.9. All databases have nearly the same statistics. The frequency distributions of the data sets are presented in Figure 3.25.

Table 3.9. Descriptive statistics of the drainage density parameter.

STATISTICS	Whole Data	Crowns and Flanks	Crowns	Flanks
Minimum	19	164	164	174
Maximum	638	566	566	537
Mean	293.353	338.125	337.537	338.945
Standard Deviation	98.890	80.666	82.356	78.267

3.2.2.8. Distance to Ridges

The descriptive statistics of the distance to ridges parameter are presented in Table 3.10. All statistics show no significant difference. The distribution of the data sets indicates that landslide abundance is greater near the ridges (Figure 3.26).

Table 3.10. Descriptive statistics of the distance to ridges parameter.

STATISTICS	Whole Data	Crowns and Flanks	Crowns	Flanks
Minimum	5.604	5.722	5.722	6.389
Maximum	727.719	527.810	520.100	527.810
Mean	167.593	193.063	180.383	210.741
Standard Deviation	109.544	123.875	125.207	119.812

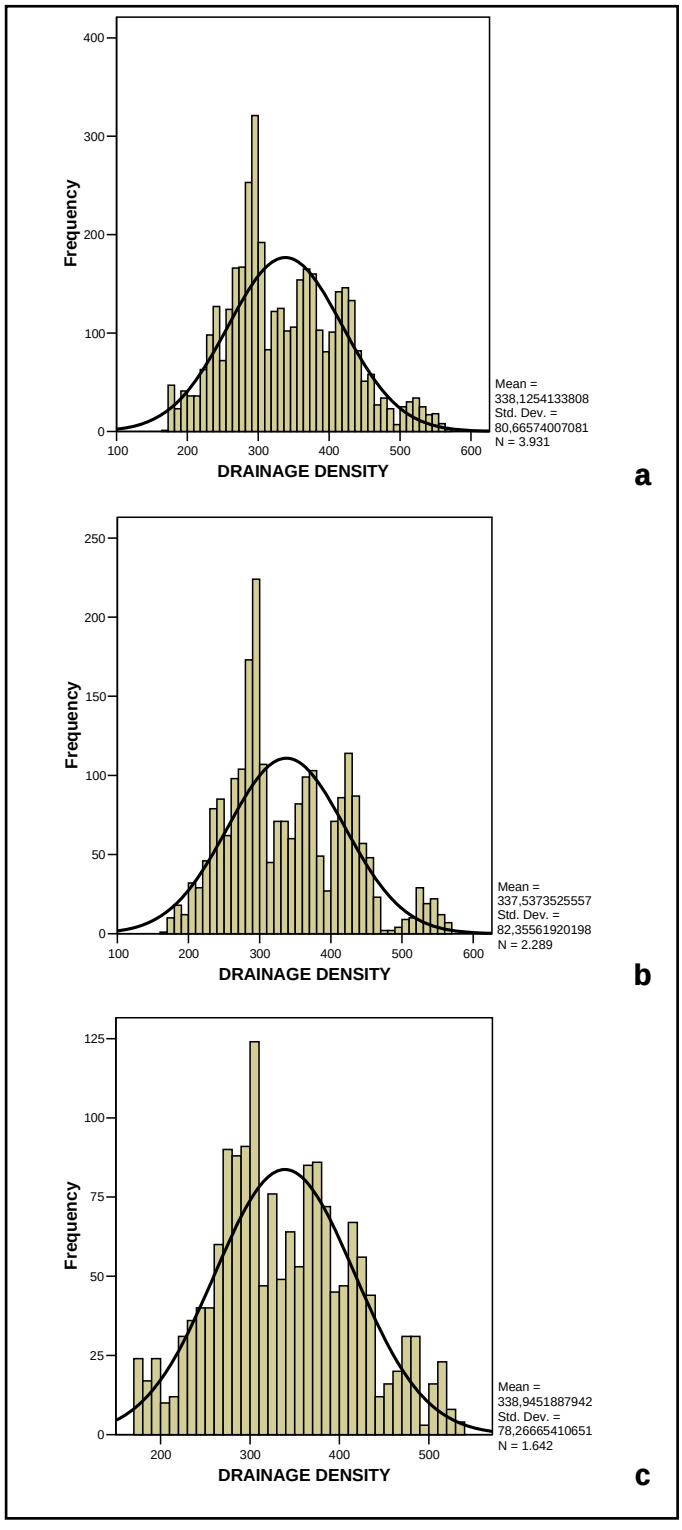

Figure 3.25. Frequency distributions of the drainage density parameter, a. crowns and flanks, b. crowns, c. flanks.

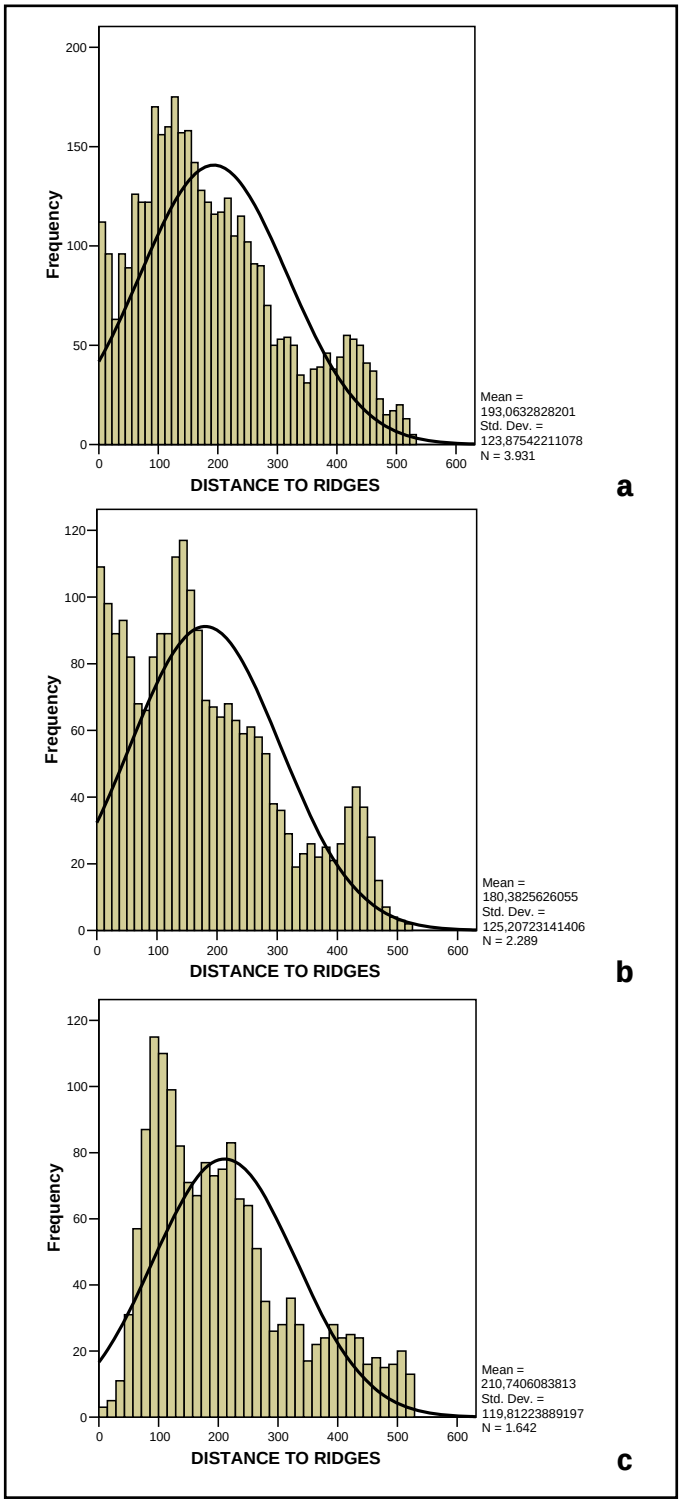

Figure 3.26. Frequency distributions of the distance to ridges parameter, a. crowns and flanks, b. crowns, c. flanks.

3.2.2.9. Distance to Road and Power Line Network

The descriptive statistics of the distance to road and power line network parameter are presented in Table 3.11. All statistics show no significant difference. The distribution of the data sets indicates that landslide abundance increases near the roads and power lines (Figure 3.27).

Table 3.11. Descriptive statistics of the distance to road and power line network.

STATISTICS	Whole Data	Crowns and Flanks	Crowns	Flanks
Minimum	0.0002	0.029	0.046	0.029
Maximum	745.874	383.382	383.382	381.745
Mean	100.268	111.485	102.474	124.046
Standard Deviation	99.353	89.058	90.011	86.181

3.2.2.10. Lithology

There are 5 lithologic units in the study area but landslides exist only in two of them. These are the Çaycuma and Yahyalar formations. Both constitute 63 percent of the study area, where Çaycuma Formation covers almost the half of the area with a percentage of 48. Figure 3.28 presents the areal percentages of seed cells with respect to the lithologic units. In average, approximately 94 percent of the seed cells fall into the Çaycuma Formation for the three different data sets.

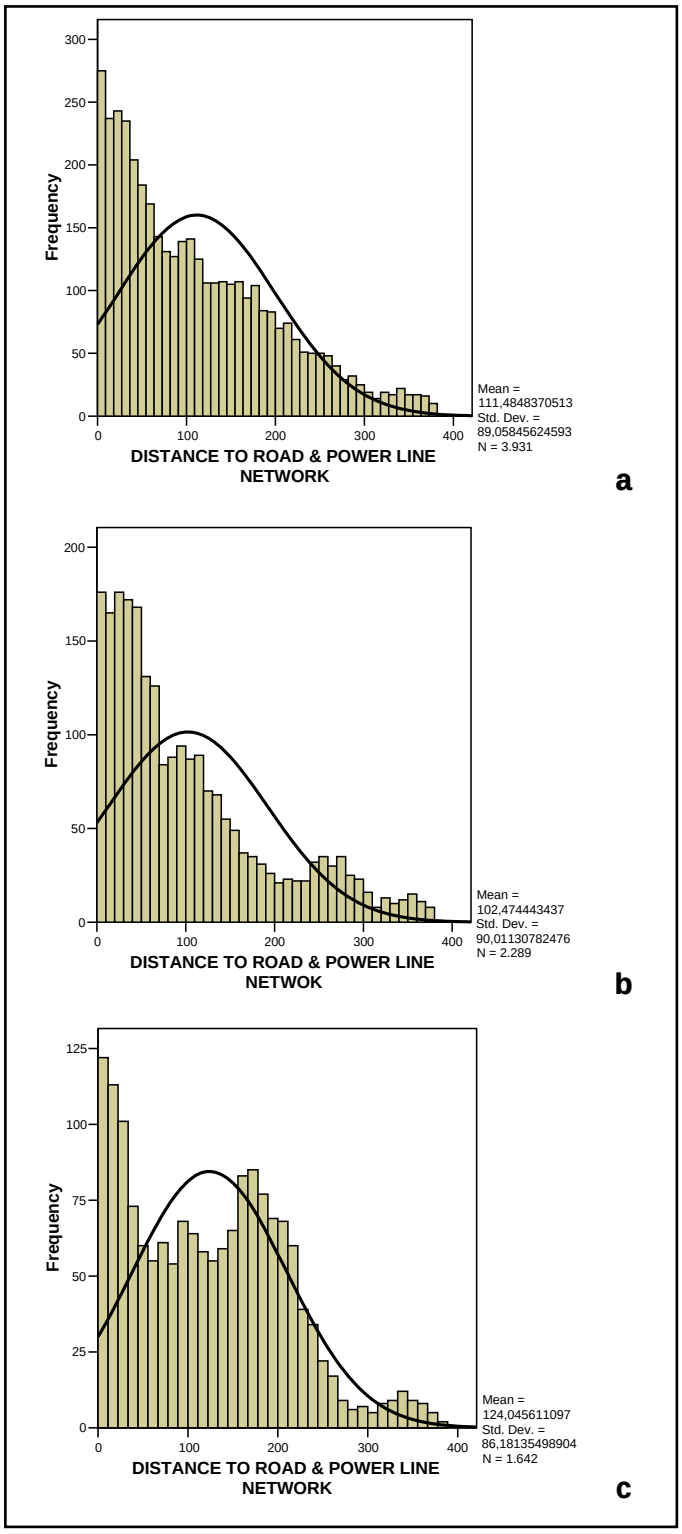

Figure 3.27. Frequency distributions of the distance to road and power line network parameter, a. crowns and flanks, b. crowns, c. flanks.

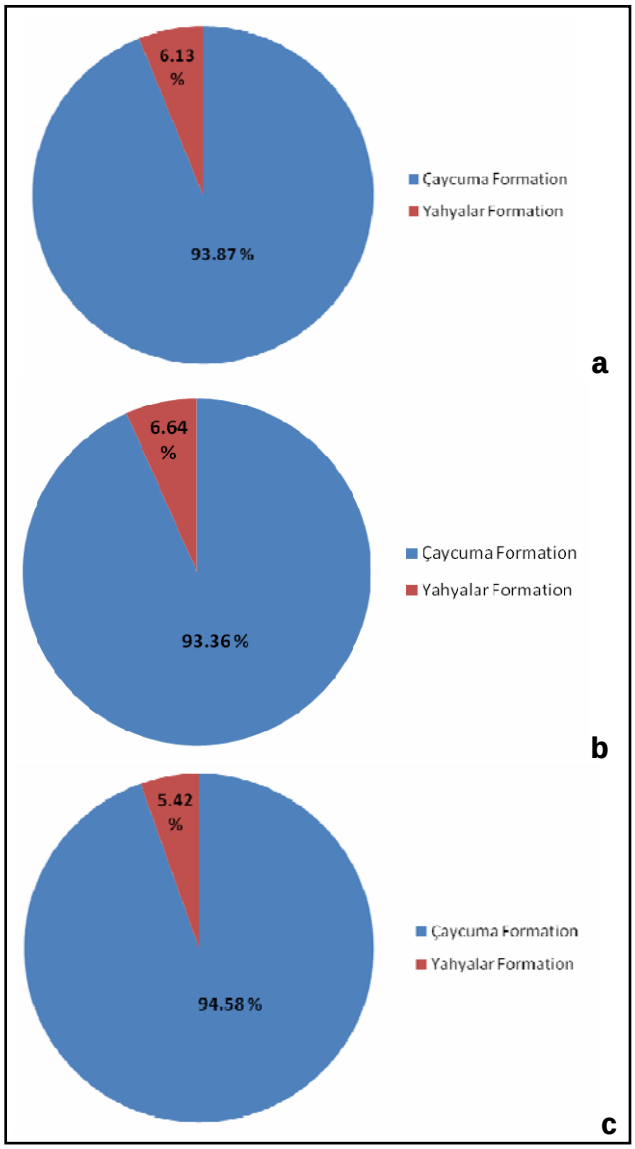

Figure 3.28. Areal percentages of seed cells in corresponding lithologic units, a. crowns and flanks, b. crowns, c. flanks.

CHAPTER 4

LANDSLIDE SUSCEPTIBILITY ANALYSIS

This chapter presents the stages of the landslide susceptibility analysis using GIS. The product maps constructed with the data presented in the previous chapter are introduced at the end of the analysis.

4.1. Data Preparation for the Statistical Analysis

As noted earlier, statistical method is preferred in this study because of its objectivity and data dependency. In this aim, three different databases of seed cells are constructed for the bivariate statistical analysis. For the crowns and flanks database 3931 seed cell nodes, for the only crowns database 2289 seed cell nodes, and for the only flanks database 1642 seed cell nodes are introduced. All seed cell nodes contain data from the 10 parameter maps.

Bivariate statistical methods are used with categorical data sets. They are based on the landslide density or abundance in certain parameter classes. Since the data gathered from the parameter maps is continuous, the problem of conversion the continuous data into categorical data arises. To convert the data, the percentile method proposed by Süzen and Doyuran (2004a) is used. In the percentile method, the continuous data sets are classified into categories based on percentile divisions of seed cells. The percentile of each variable of seed cells are found by utilizing the SPSS software. Then, each parameter map is reclassified according to the percentile limits.

All parameters except the categorical one lithology are analyzed and reclassified for each seed cell database. The results are presented in the following sections.

4.1.1. Reclassification of the Maps by Crowns and Flanks Data

Table 4.1 presents the percentiles for the seed cells of crowns and flanks. The reclassified parameter maps based on the percentiles are presented in Figures 4.1, 4.2, 4.3, 4.4 and 4.5.

Table 4.1. Percentile values of crowns and flanks seed cells of each parameter.

Percentiles	Elevation	Slope	Aspect	Profile Curv.	Plan Curv.	Dist. to Drain.	Drain. Dens.	Dist. to Ridges	Dist. to Road
10	138.96	4.99	123	-0.00200	-0.00963	18.29	192	46.54	13.97
20	152.30	7.17	196	-0.00122	-0.00552	38.16	199	85.65	28.69
30	165.01	8.98	230	-0.00069	-0.00282	53.63	222	112.49	44.24
40	179.86	10.54	257	-0.00022	-0.00067	70.62	301	139.32	65.39
50	195.10	12.07	270	0.00021	0.00146	86.87	317	168.53	92.51
60	208.87	14.15	284	0.00064	0.00361	104.85	336	204.72	118.67
70	224.80	16.81	298	0.00124	0.00596	125.86	346	242.65	152.41
80	268.32	19.68	311	0.00210	0.00889	152.82	355	293.62	188.27
90	303.08	23.01	324	0.00330	0.01491	186.43	363	393.92	242.15

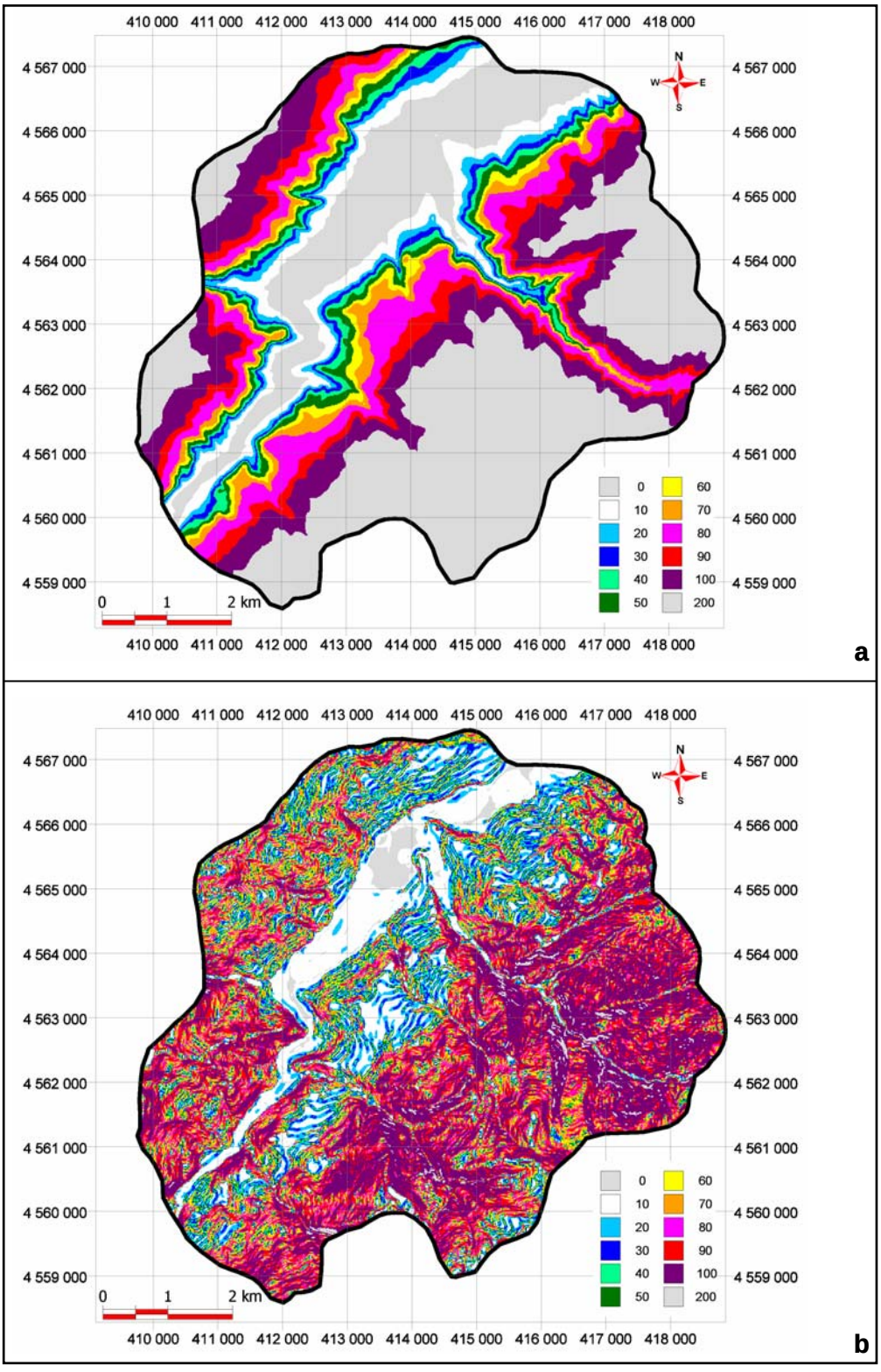

Figure 4.1. Reclassified parameter maps of the study area based on percentiles of the seed cells of crowns and flanks database, a. Elevation, b. Slope.

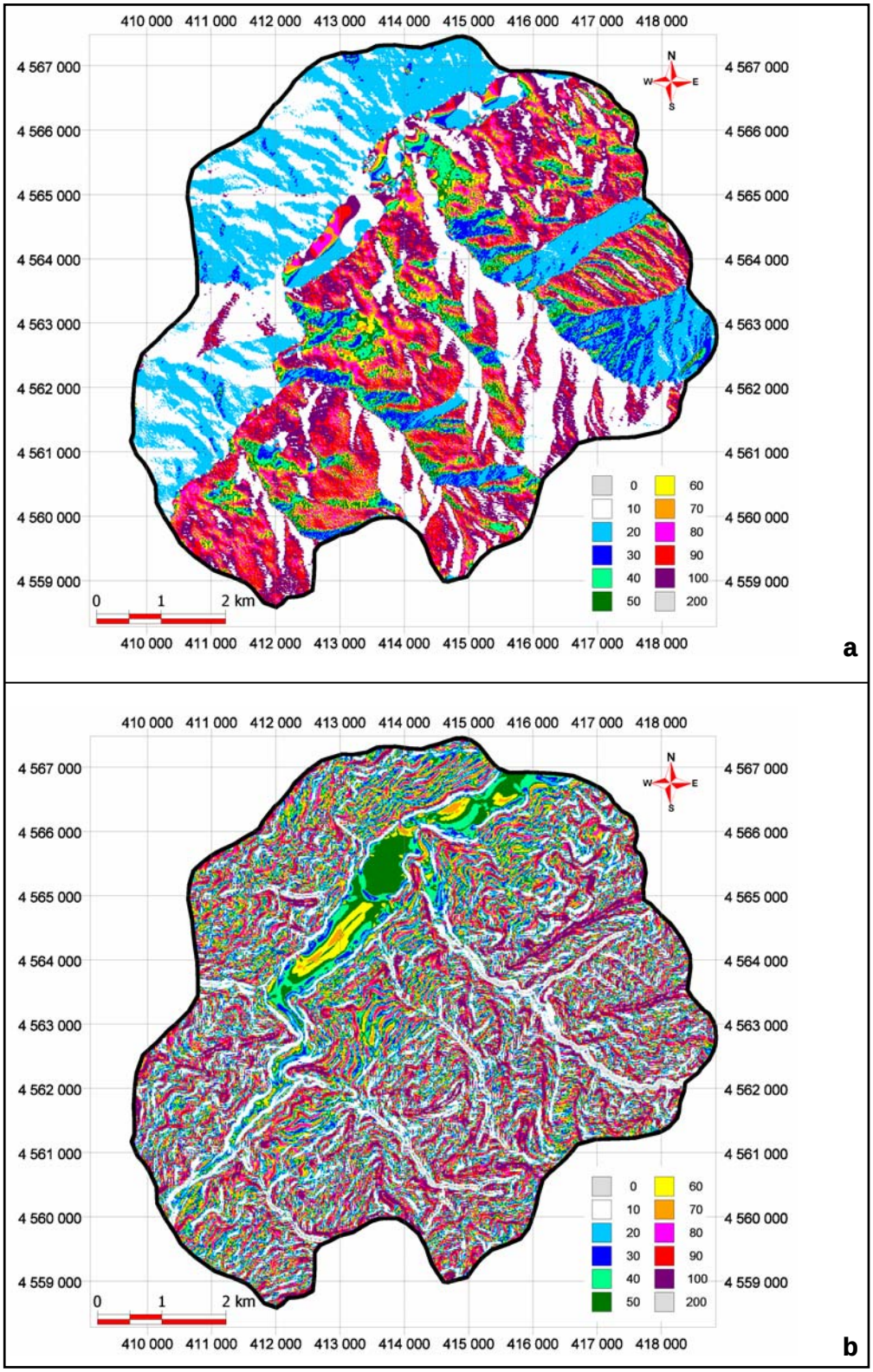

Figure 4.2. Reclassified parameter maps of the study area based on percentiles of the seed cells of crowns and flanks database, a. Aspect, b. Profile curvature.

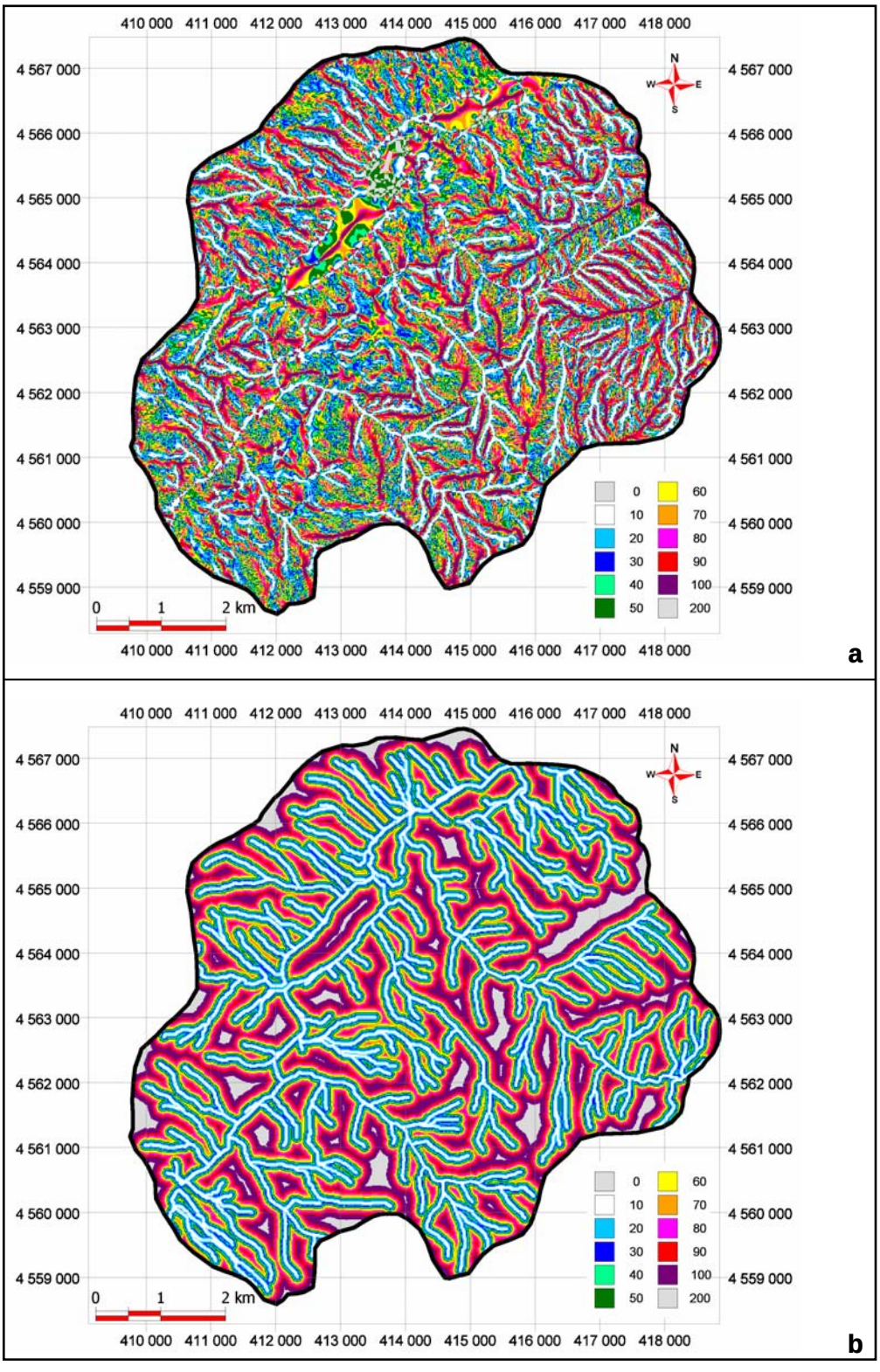

Figure 4.3. Reclassified parameter maps of the study area based on percentiles of the seed cells of crowns and flanks database, a. Plan curvature, b. Distance to drainage lines.

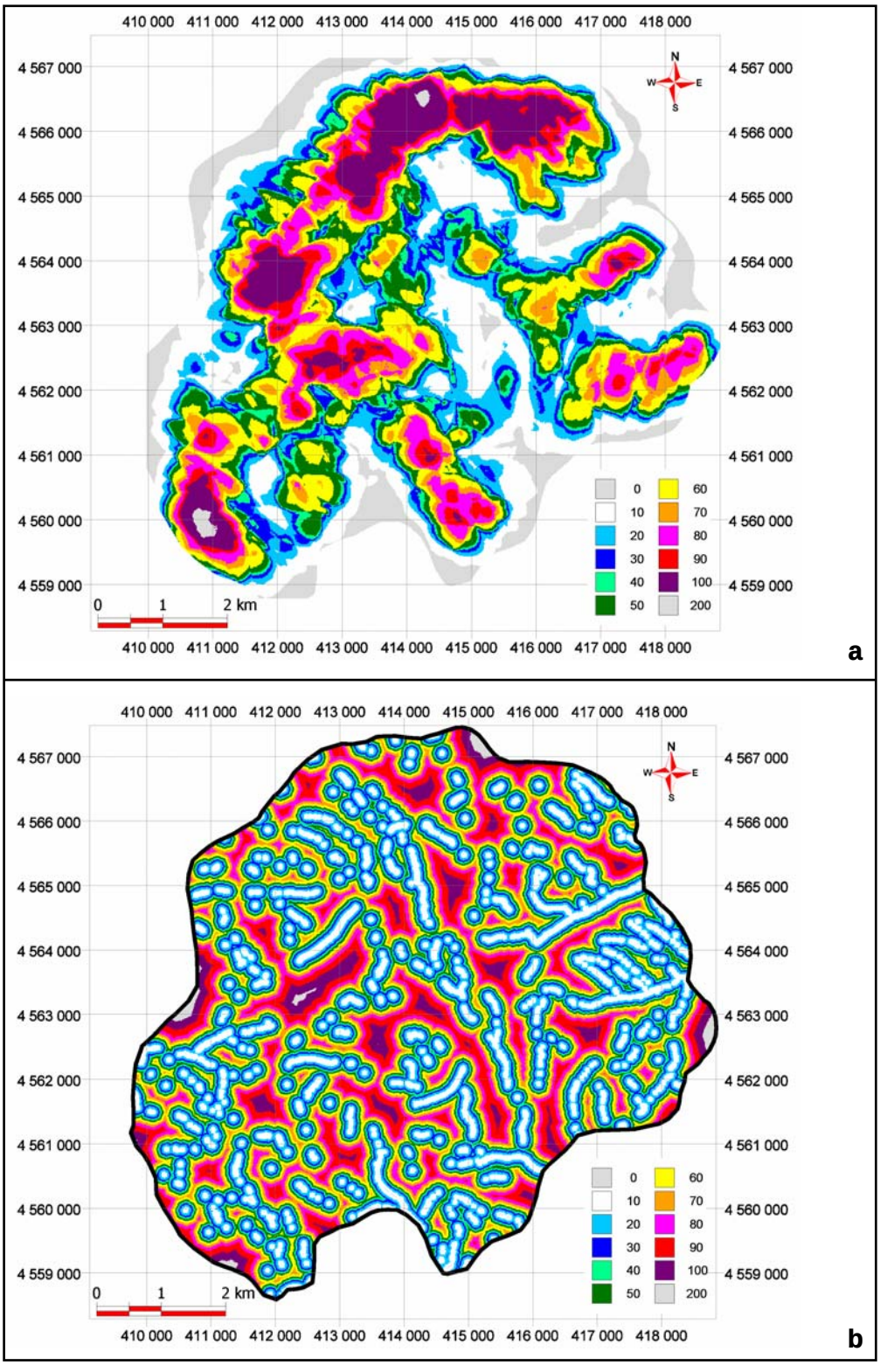

Figure 4.4. Reclassified parameter maps of the study area based on percentiles of the seed cells of crowns and flanks database, a. Drainage density, b. Distance to ridges.

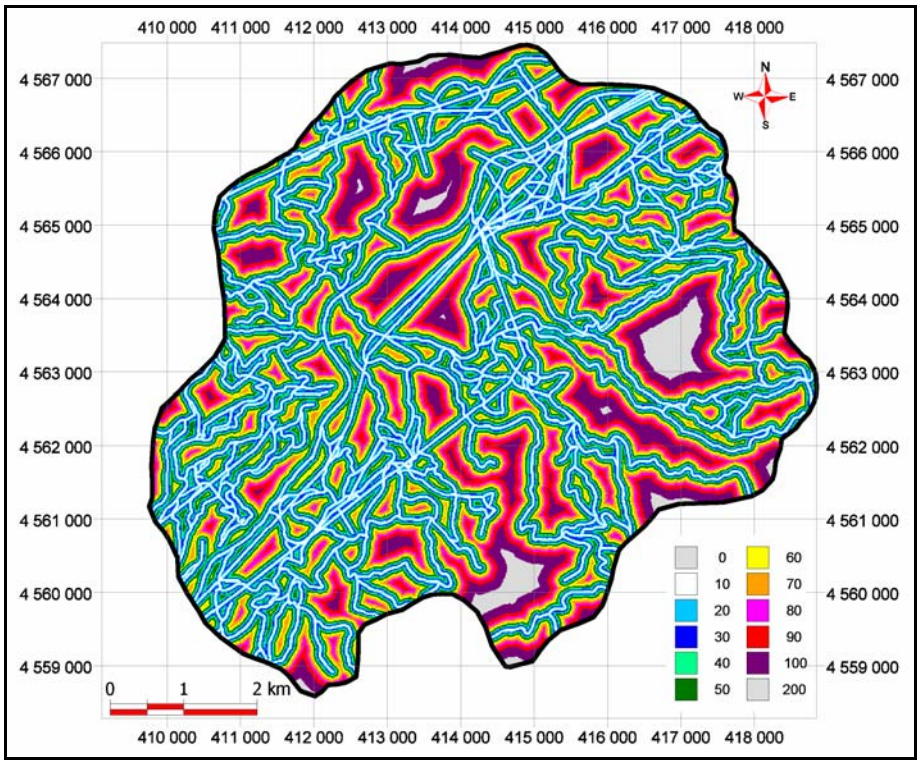

Figure 4.5. Reclassified parameter map of the study area based on percentiles of the seed cells of crowns and flanks database: Distance to road and power line network.

4.1.2. Reclassification of the Maps by Crowns Data

Table 4.2 presents the percentiles for the seed cells of crowns. The reclassified parameter maps based on the percentiles are presented in Figures 4.6, 4.7, 4.8, 4.9 and 4.10.

Table 4.2. Percentile values of crowns seed cells of each parameter.

Percentiles	Elevation	Slope	Aspect	Profile Curv.	Plan Curv.	Dist. to Drain.	Drain. Dens.	Dist. to Ridge	Dist. to Road
10	149.28	4.54	133	-0.00176	-0.00927	25.02	194	26.95	13.83
20	160.00	6.82	200	-0.00095	-0.00558	44.39	206	61.03	26.45
30	176.43	8.69	237	-0.00043	-0.00286	62.53	245	99.96	39.80
40	190.00	10.23	262	-0.00003	-0.00059	79.97	306	130.75	54.52
50	203.18	11.67	270	-0.00046	0.00189	99.90	326	155.79	73.40
60	217.78	13.52	286	-0.00101	0.00425	119.92	341	190.86	99.63
70	243.93	15.89	297	0.00174	0.00653	140.03	346	234.46	126.46
80	282.68	19.43	310	0.00257	0.00978	163.23	354	283.05	168.72
90	317.26	23.46	325	0.00384	0.01598	190.42	362	384.04	253.07

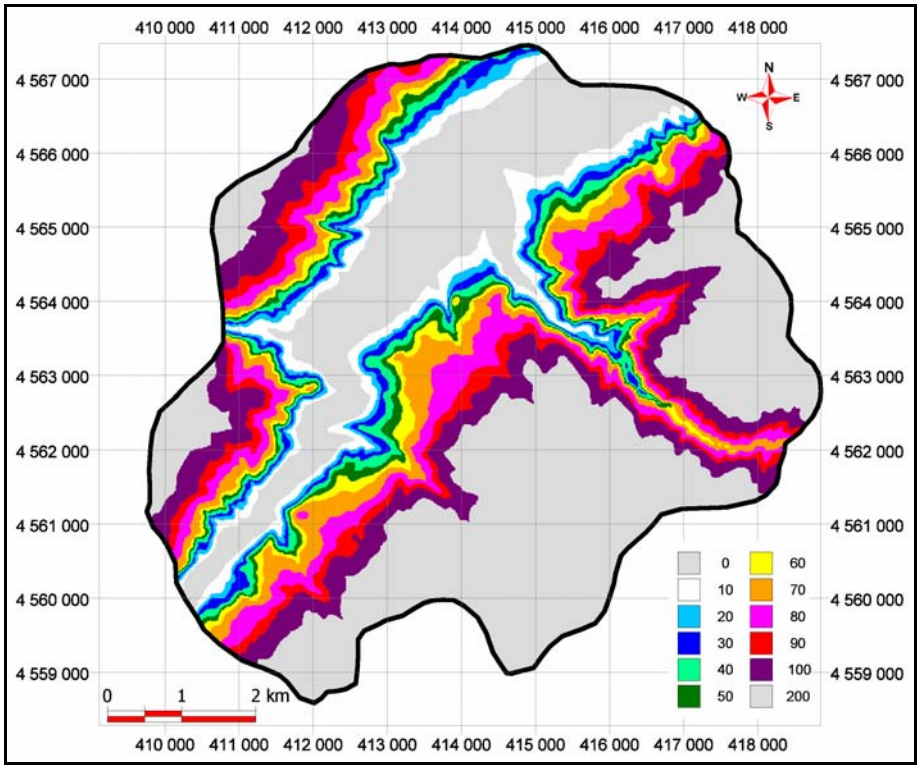

Figure 4.6. Reclassified parameter map of the study area based on percentiles of the seed cells of crowns database: Elevation.

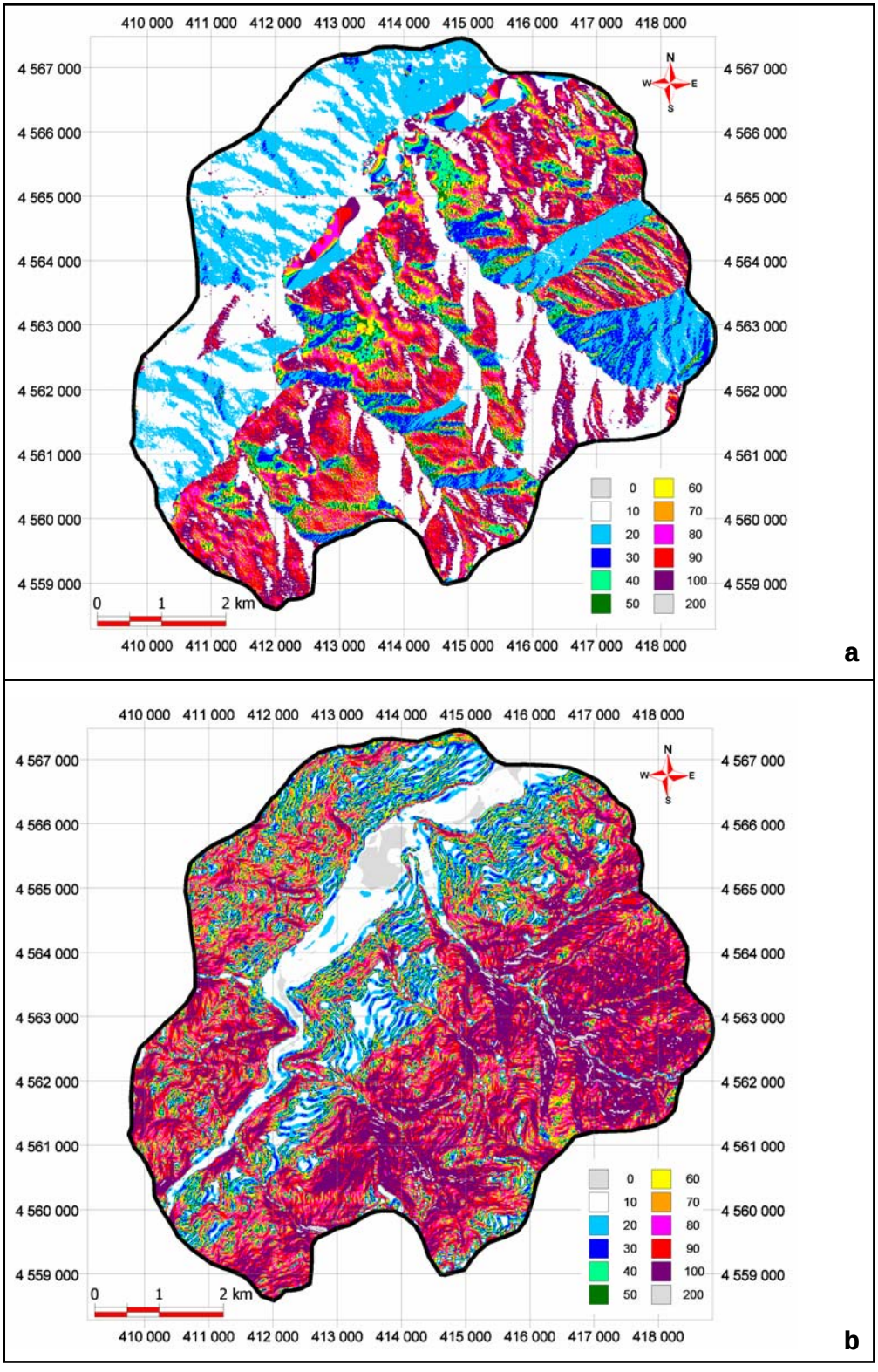

Figure 4.7. Reclassified parameter maps of the study area based on percentiles of the seed cells of crowns database, a. Aspect, b. Slope.

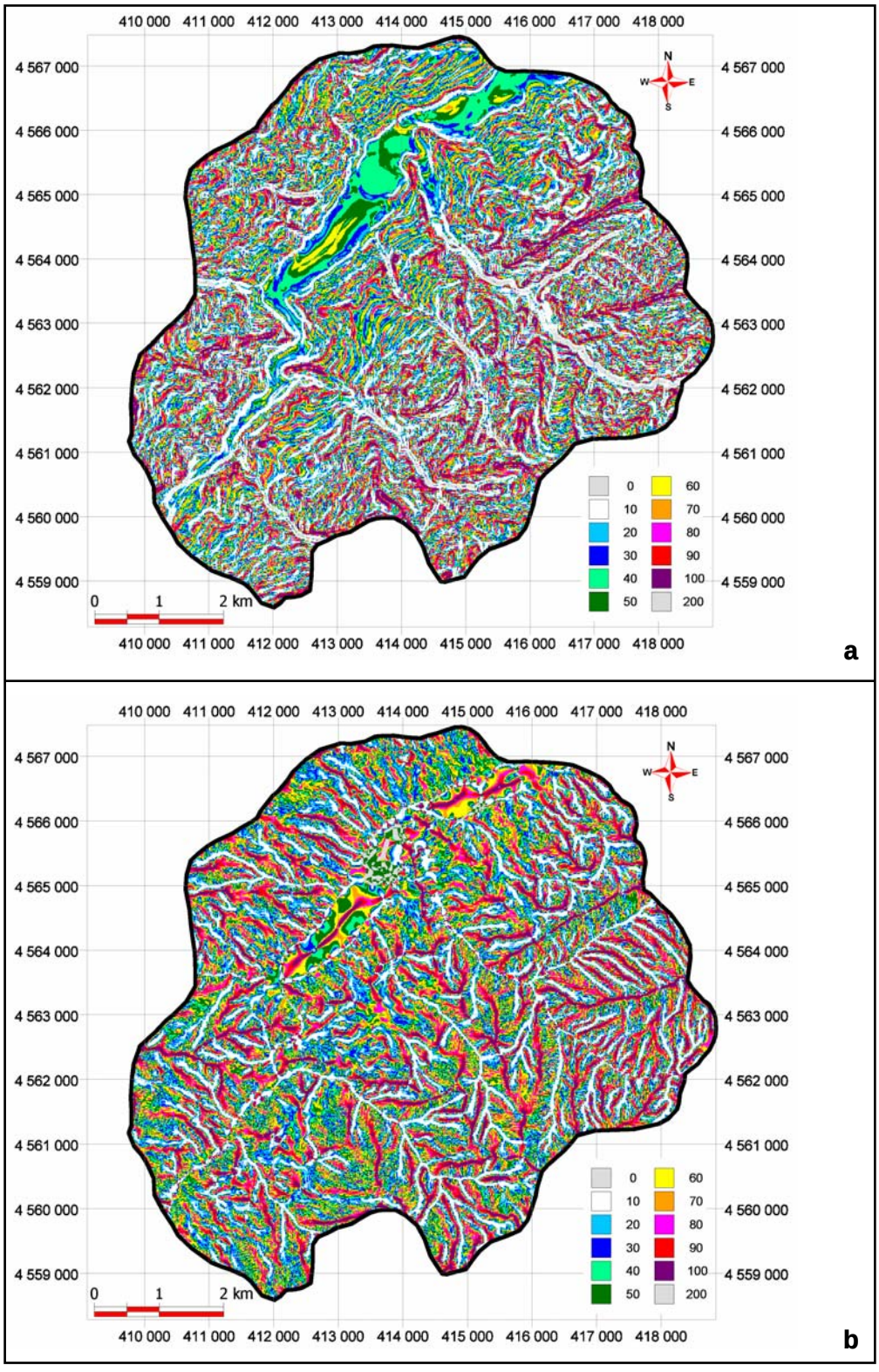

Figure 4.8. Reclassified parameter maps of the study area based on percentiles of the seed cells of crowns database, a. Profile curvature, b. Plan curvature.

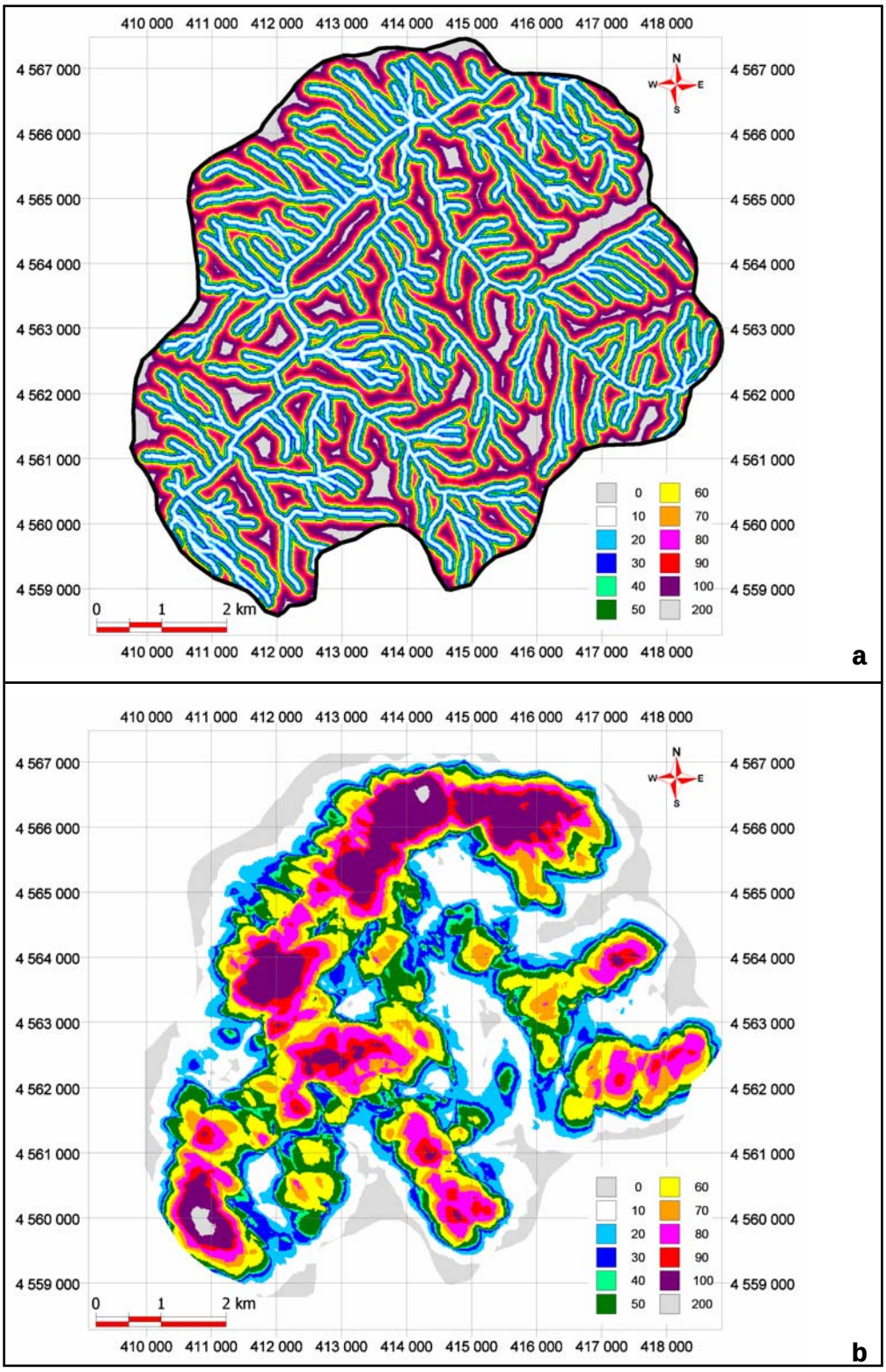

Figure 4.9. Reclassified parameter maps of the study area based on percentiles of the seed cells of crowns database, a. Distance to drainage lines, b. Drainage density.

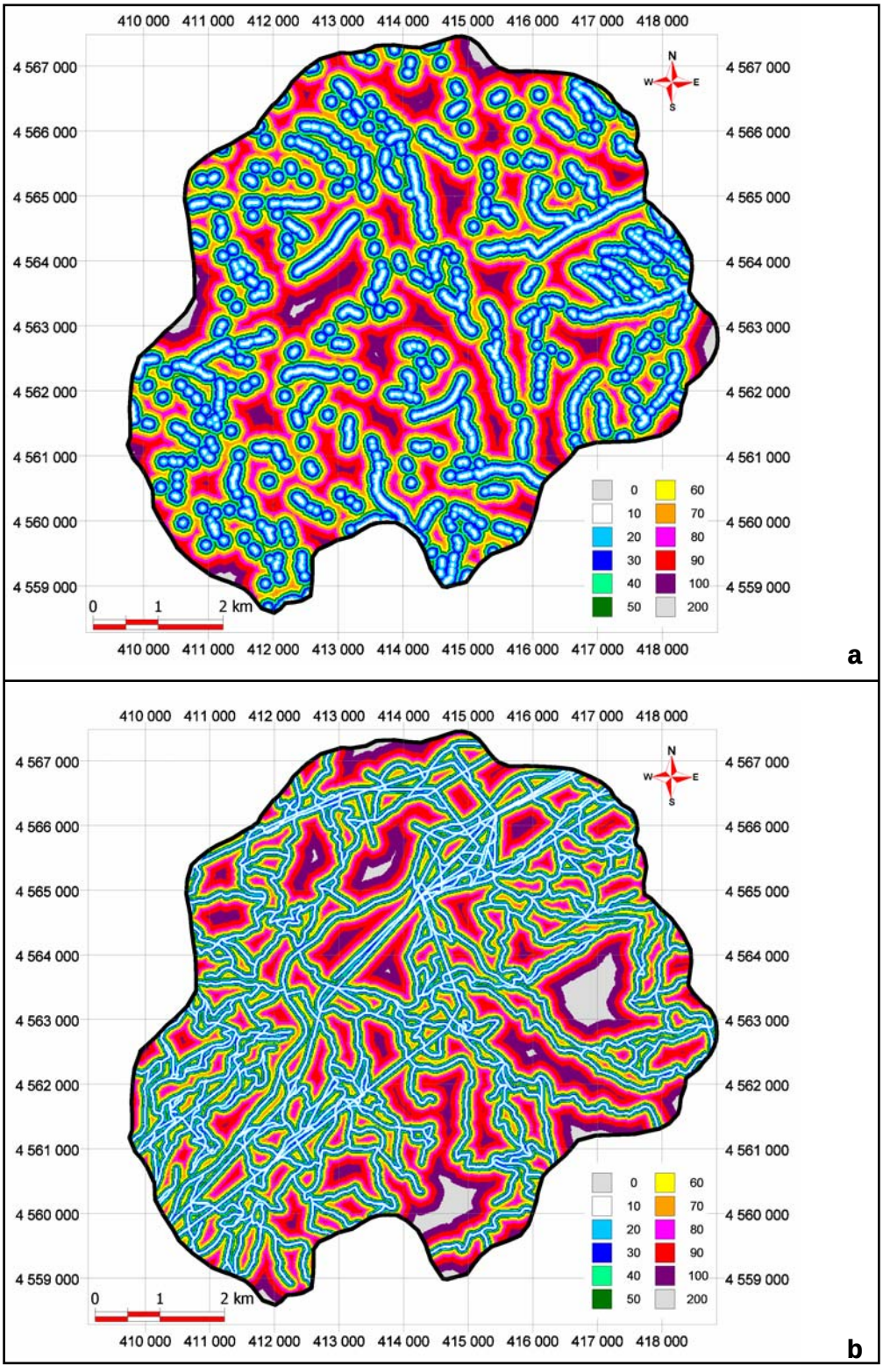

Figure 4.10. Reclassified parameter maps of the study area based on percentiles of the seed cells of crowns database, a. Distance to ridges, b. Distance to road and power line network.

4.1.3. Reclassification of the Maps by Flanks Data

Table 4.3 presents the percentiles for the seed cells of crowns. The reclassified parameter maps based on the percentiles are presented in Figures 4.11, 4.12, 4.13, 4.14 and 4.15.

Table 4.3. Percentile values of flanks seed cells of each parameter.

Percentiles	Elevation	Slope	Aspect	Profile Curv.	Plan Curv.	Dist. to Drain.	Drain. Dens.	Dist. to Ridge	Dist. to Road
10	128.92	5.38	113	-0.00227	-0.01073	17.63	183	81.72	14.43
20	138.52	7.67	190	-0.00149	-0.00542	35.45	195	102.89	32.38
30	153.41	9.37	225	-0.00103	-0.00276	49.66	218	124.89	59.32
40	167.37	11.12	249	-0.00058	-0.00081	61.76	297	154.15	91.46
50	179.86	12.75	269	-0.00016	0.00104	72.70	314	186.67	120.89
60	192.15	14.89	281	0.00028	0.00302	87.03	332	218.49	151.27
70	210.00	17.47	301	0.00071	0.00504	102.53	345	251.89	174.54
80	241.75	20.04	311	0.00128	0.00772	129.56	356	313.35	198.74
90	270.00	22.84	323	0.00239	0.01343	172.56	365	403.99	230.38

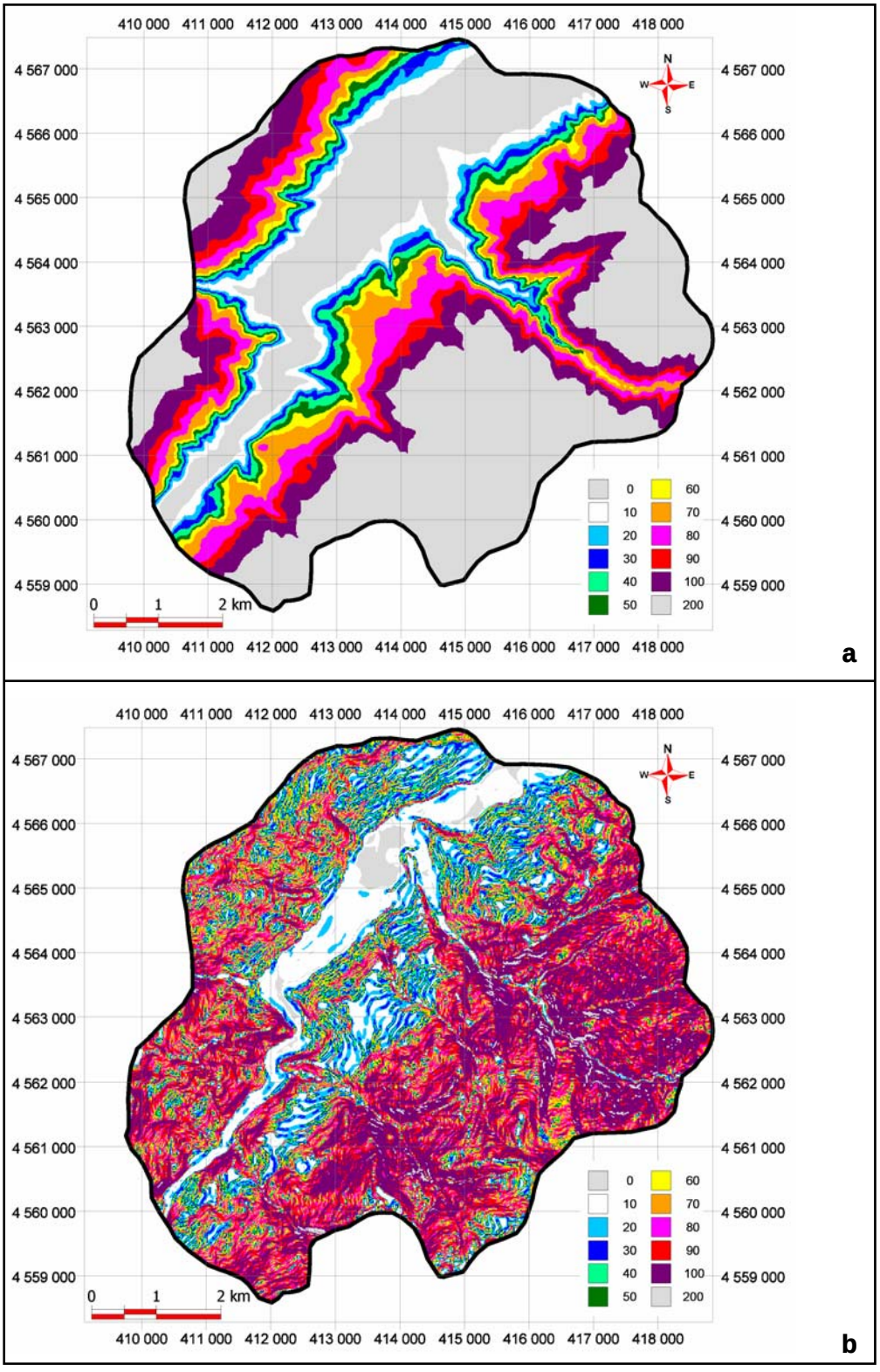

Figure 4.11. Reclassified parameter maps of the study area based on percentiles of the seed cells of flanks database, a. Elevation, b. Slope.

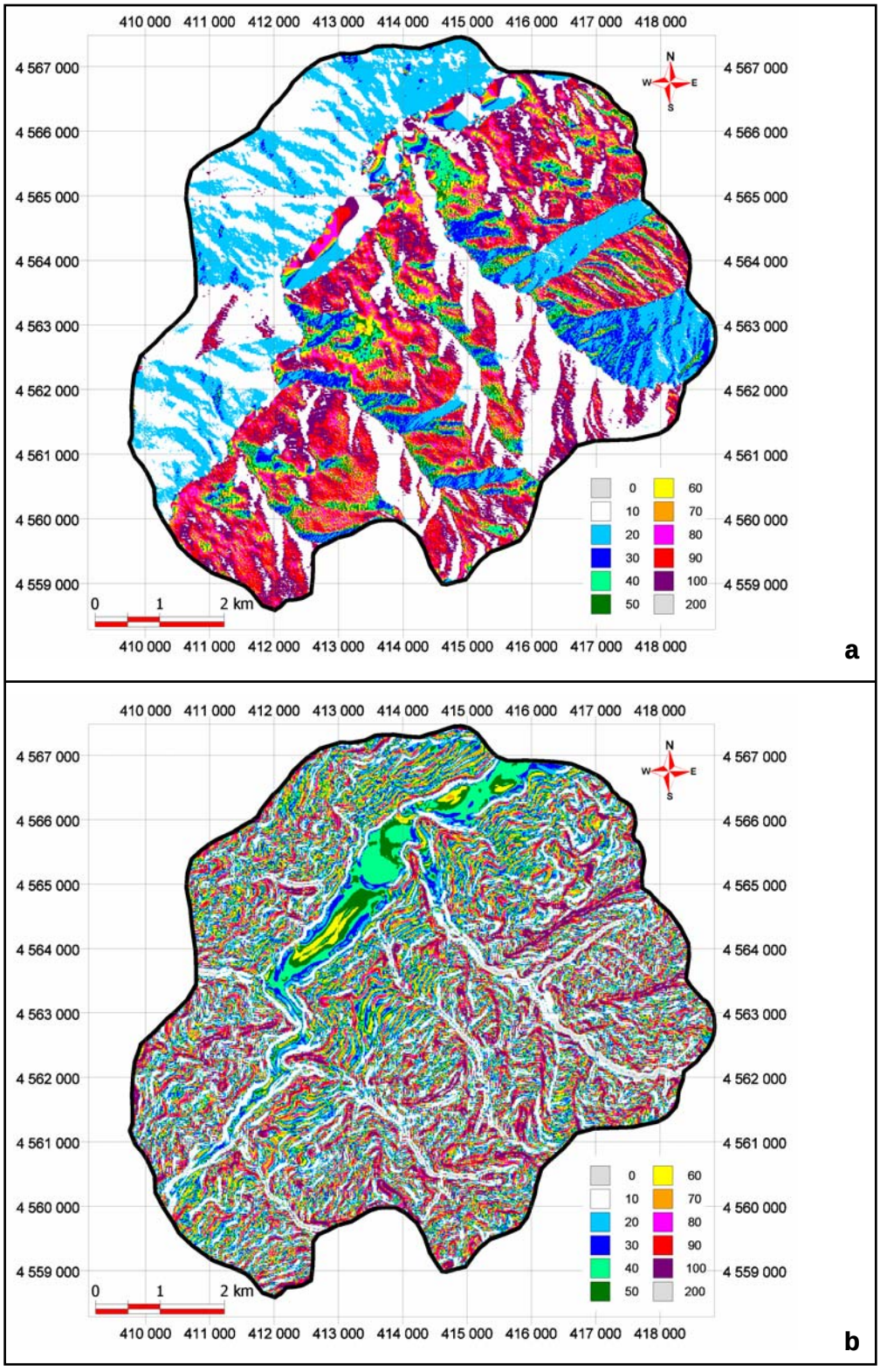

Figure 4.12. Reclassified parameter maps of the study area based on percentiles of the seed cells of flanks database, a. Aspect, b. Profile curvature.

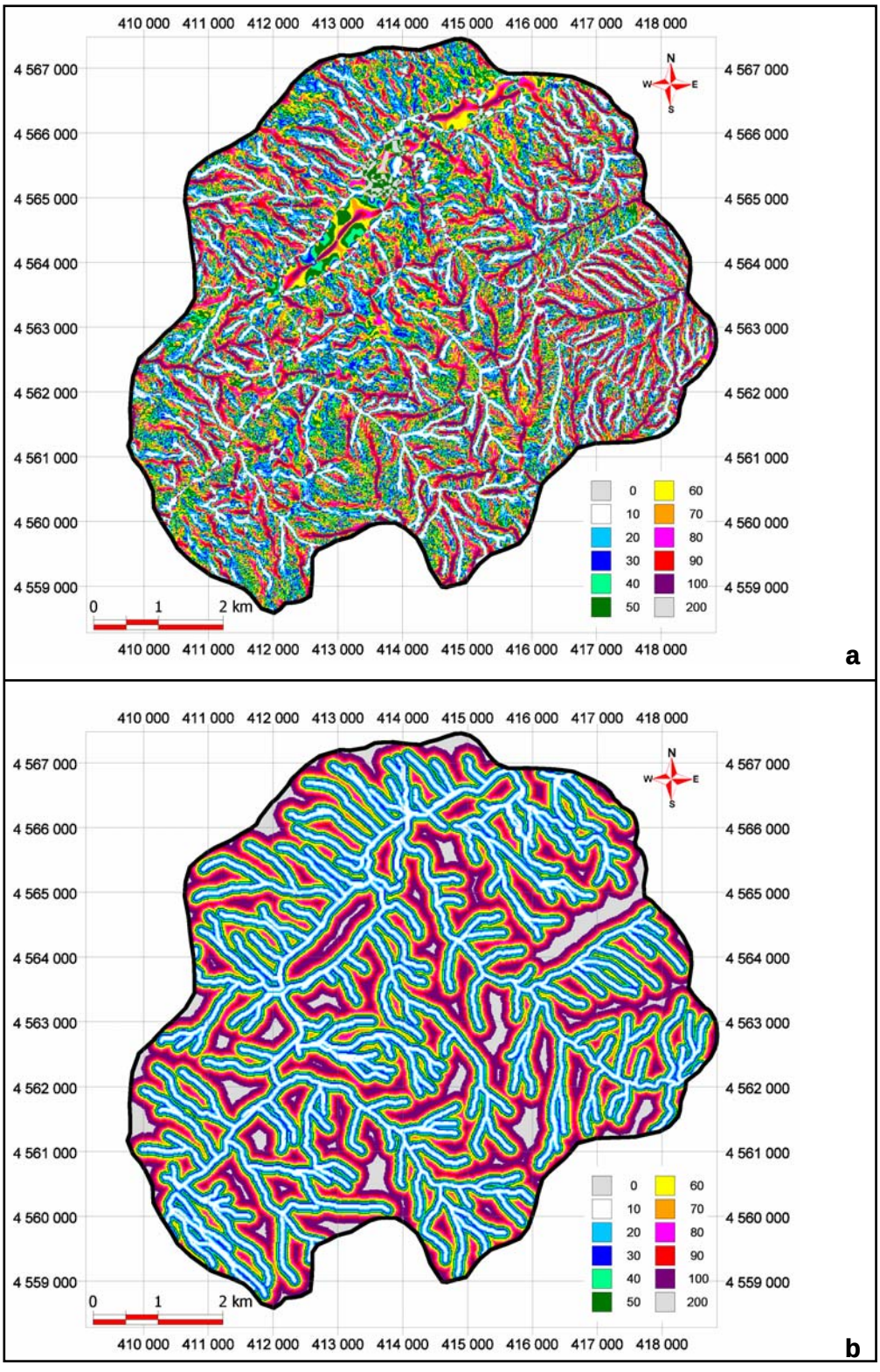

Figure 4.13. Reclassified parameter maps of the study area based on percentiles of the seed cells of flanks database, a. Plan curvature, b. Distance to drainage lines.

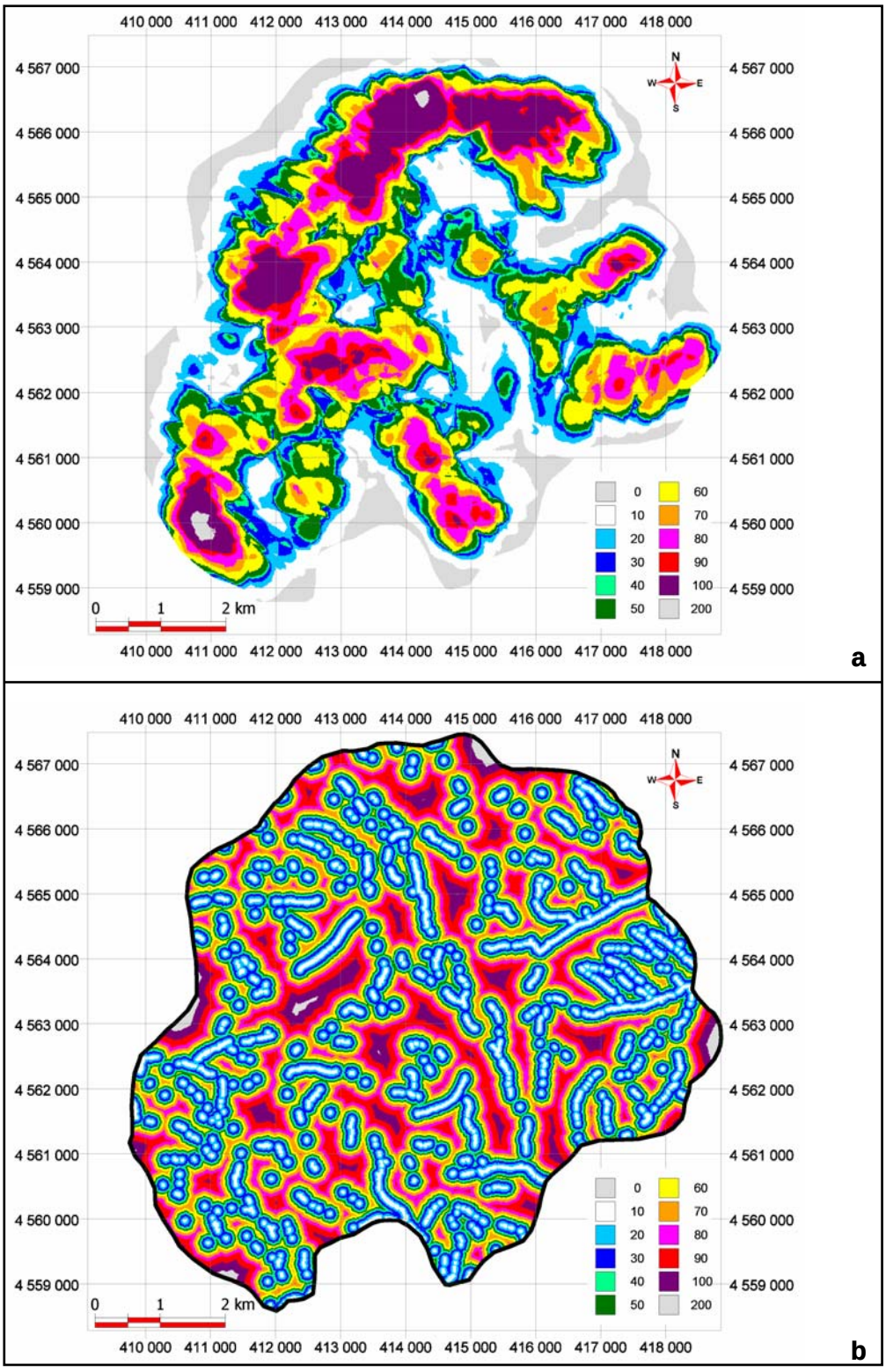

Figure 4.14. Reclassified parameter maps of the study area based on percentiles of the seed cells of flanks database, a. Drainage density, b. Distance to ridges.

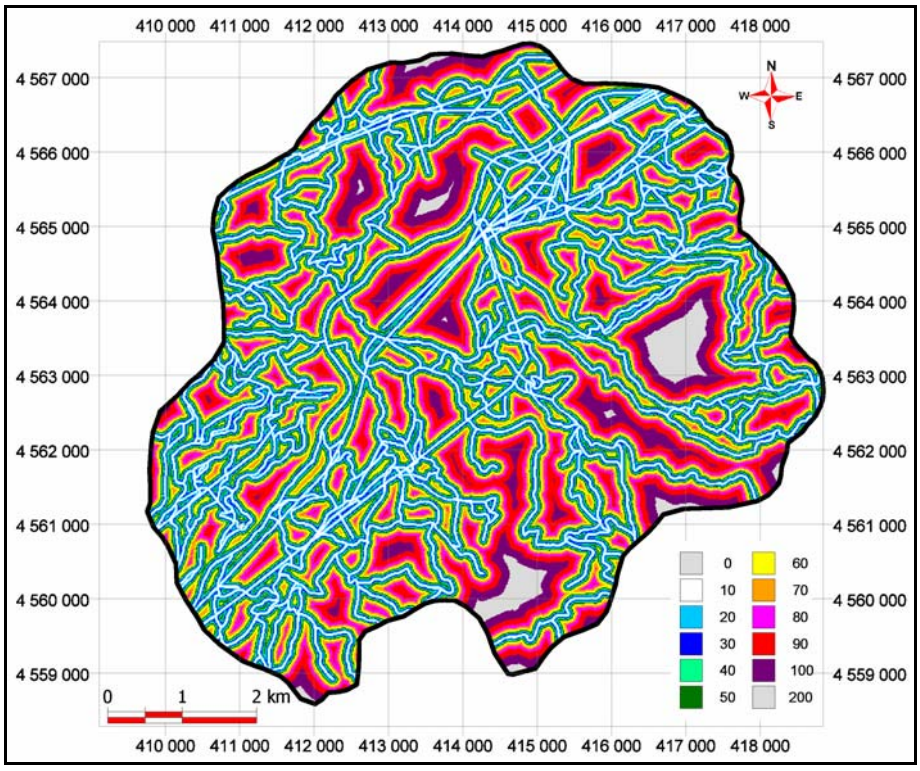

Figure 4.15. Reclassified parameter map of the study area based on percentiles of the seed cells of flanks database: Distance to road and power line network.

4.2. Landslide Susceptibility Analysis

In landslide susceptibility analysis, the occurrence of mass movements is considered as dependent, and parameters are independent variables. Each parameter map (as independent variable) is crossed with landslide distribution map, and weighting values, which demonstrates the relative effect of each parameter or variable to instability, are calculated. Weight value for landslide susceptibility is calculated from the landslide density of each class of each parameter map. The landslide density of each class is calculated from following equation:

$$D_{area} = 1000 \frac{Npix(SX_i)}{Npix(X_i)}$$

where D_{area} is the areal density per mileage, $Npix(SX_i)$ is the number of pixels with mass movements within variable class X_i, and $Npix(X_i)$ is the number of pixels within variable class X_i.

The weight value of each control factor class for landslide is defined as the difference between the landslide density of each class and the average landslide density in the study area. The formula for the weight value is:

$$W_{area} = 1000 \frac{Npix(SX_i)}{Npix(X_i)} - 1000 \frac{\sum Npix(SX_i)}{\sum Npix(X_i)}$$

The calculated weight values are the equal to the degree of susceptibility to landslides of each parameter class. In the presence of a negative weight value, all weights are normalized by adding the absolute value of greatest negative weight to all of the weights of each percentile class. Table 4.4 presents an example for the landslide density and weight calculations of each percentile class of a parameter.

Table 4.4. An example for density and weight values calculation.

Percentiles	Raster Cell Count	% of Seed Cells	# of Seed Cells	Densities (# of Seed Cells/ Raster Cell Count)*1000	Weights	Normalized Weights
10	21413	10	393.1	18.35800682	-2.385618646	10.09126725
20	10717	10	393.1	36.68004106	15.93641559	28.41330149
30	8716	10	393.1	45.10096374	24.35733828	36.83422418
40	9812	9.4	369.514	37.65939666	16.91577119	29.39265709
50	12741	10.6	416.686	32.70434032	11.96071485	24.43760075
60	9590	10	393.1	40.99061522	20.24698976	32.72387566
70	14162	10	393.1	27.7573789	7.013753437	19.49063934
80	31392	10	393.1	12.52229867	-8.22132679	4.25555911
90	23409	10	393.1	16.79268657	-3.950938891	8.525947009
100	47552	10	393.1	8.266739569	-12.4768859	0

Tables 4.5, 4.6 and 4.7 present the calculated weights for each percentile class of each parameter for the three different databases in this study.

Table 4.5. Weight values of all parameter classes of the crowns and flanks database.

Parameter Class	Parameter								
	Elevation	Slope	Aspect	Profile Curv.	Plan Curv.	Dist. to Drain.	Drain. Dens.	Dist. to Ridges	Dist. to Road
10	10.09	5.12	0	0	0	0	0	1.12	0
20	28.41	12.61	1.93	4.78	3.53	1.54	4.99	0	0.79
30	36.83	13.28	18.80	5.87	3.17	5.23	11.10	2.88	1.53
40	29.39	15.71	20.85	4.64	2.87	5.81	16.55	2.98	0.19
50	24.44	15.22	29.69	4.38	1.35	5.95	5.23	2.67	0.11
60	32.72	8.87	20.79	6.43	2.16	4.91	4.71	1.67	3.25
70	19.49	8.69	17.88	5.02	3.39	4.70	13.41	3.55	4.09
80	4.26	6.35	14.46	5.07	4.55	3.79	9.59	3.91	8.56
90	8.53	3.98	6.87	8.14	3.56	4.03	21.20	3.93	9.28
100	0	0	4.66	8.71	7.38	0.51	10.93	26.10	8.12

Lithology	Quaternary Alluvium	Çaycuma Formation	Yahyalar Formation	Alaplı Formation	Kazpınar Formation
	0	17.71	0	0	0

Table 4.6. Weight values of all parameter classes of the crowns database.

Parameter Class	Parameter								
	Elevation	Slope	Aspect	Profile Curv.	Plan Curv.	Dist. to Drain.	Drain. Dens.	Dist. to Ridges	Dist. to Road
10	6.36	3.58	0	0	0	0	0	5.75	0
20	18.25	7.06	1.71	2.31	2.96	0.94	3.24	1.65	1.26
30	14.60	7.39	9.86	3.23	2.05	2.45	6.38	0	1.66
40	13.95	9.23	12.59	2.63	1.56	2.97	12.15	1.10	1.89
50	18.50	9.79	18.86	3.94	0.24	3.03	3.30	2.58	1.24
60	15.87	6.19	13.47	3.30	1.14	3.33	2.24	1.04	0.58
70	4.44	5.09	12.76	3.55	2.89	4.67	6.62	0.97	2.28
80	2.41	2.61	9.01	5.92	2.80	4.66	4.81	2.29	1.58
90	4.96	1.53	3.64	7.51	3.29	5.13	14.92	1.76	1.11
100	0	0	3.03	9.08	5.88	1.30	6.44	12.88	6.24

Lithology	Quaternary Alluvium	Çaycuma Formation	Yahyalar Formation	Alaplı Formation	Kazpınar Formation
	0	10.02	0	0	0

Table 4.7. Weight values of all parameter classes of flanks database.

Parameter Class	Parameter								
	Elevation	Slope	Aspect	Profile Curv.	Plan Curv.	Dist. to Drain.	Drain. Dens.	Dist. to Ridges	Dist. to Road
10	8.89	2.07	0	0	0.03	0.94	0	0	0.86
20	18.62	4.64	0.42	2.27	0	1.69	1.92	3.76	0.61
30	13.29	5.83	8.45	3.31	0.73	2.69	3.74	3.65	0
40	14.77	5.57	9.32	2.54	1.12	4.52	5.86	2.32	0.31
50	16.77	5.45	11.49	1.81	0.57	4.26	2.36	2.29	1.79
60	12.18	3.56	8.54	1.16	0.59	4.19	2.40	3.10	3.32
70	8.99	3.93	5.91	2.39	1.20	3.12	6.44	4.00	7.66
80	3.83	3.12	29.87	1.89	1.08	1.29	4.73	2.71	10.12
90	5.47	2.22	1.60	0.81	0.15	0.33	7.50	4.53	10.24
100	0	0	1.62	0.38	1.59	0	4.81	14.99	3.39

Lithology	Quaternary Alluvium	Çaycuma Formation	Yahyalar Formation	Alaplı Formation	Kazpınar Formation
	0	7.69	0	0	0

4.3. Production of Landslide Susceptibility Maps

After calculation of the weights, the weights are assigned to the parameter classes of parameter maps. In order to standardize all parameter maps, they are all resampled by using the DEM as a reference raster. As a result, all extents and centers of the pixels of the parameter maps are fixed. The resampling process provides the avoidance of errors during the production of the susceptibility maps.

After resampling, all 10 parameter maps are spatially summed up to create the susceptibility map. The resultant map is then reclassified into 4 susceptibility classes (very low, low, high, very high) using the susceptibility map distribution parameters. The mean value of the susceptibility map is taken as the pivot point, and classes are assigned to the + and – one standard deviations of the distribution.

The distribution of the susceptibility map of crowns and flanks data set results in a mean value of 45.72 and a standard deviation of 21.95. The resultant susceptibility map classified according to these values is presented in Figure 4.16. Table 4.8 presents the ranges and the area covered of the susceptibility classes, and the percentage of seed cells in each susceptibility class. According to these results, 44.77 % of the study area is classified as high and very high susceptibility. 93.39 % of the seed cells are in the high and very high susceptibility classes. On the other hand, 55.23 % of the study area is classified as low and very low susceptibility. 6.61 % of the seed cells are encountered in these classes.

The distribution of the susceptibility map of crowns data set results in a mean value of 27.60 and a standard deviation of 12.65. The resultant susceptibility map classified according to these values is presented in Figure 4.17. Table 4.9 presents the ranges and the area covered of the susceptibility classes, and the percentage of seed cells in each susceptibility class. According to these results, 46.47 % of the study area is classified as high and very high susceptibility. 94.71 % of the seed cells are in the high and very high susceptibility classes.

On the other hand, 53.53 % of the study area is classified as low and very low susceptibility. 5.29 % of the seed cells are encountered in these classes.

The distribution of the susceptibility map of crowns data set results in a mean value of 21.21 and a standard deviation of 11.05. The resultant susceptibility map classified according to these values is presented in Figure 4.18. Table 4.10 presents the ranges and the area covered of the susceptibility classes, and the percentage of seed cells in each susceptibility class. According to these results, 44.18 % of the study area is classified as high and very high susceptibility. 94.15 % of the seed cells are in the high and very high susceptibility classes. On the other hand, 55.82 % of the study area is classified as low and very low susceptibility. 5.85 % of the seed cells are encountered in these classes.

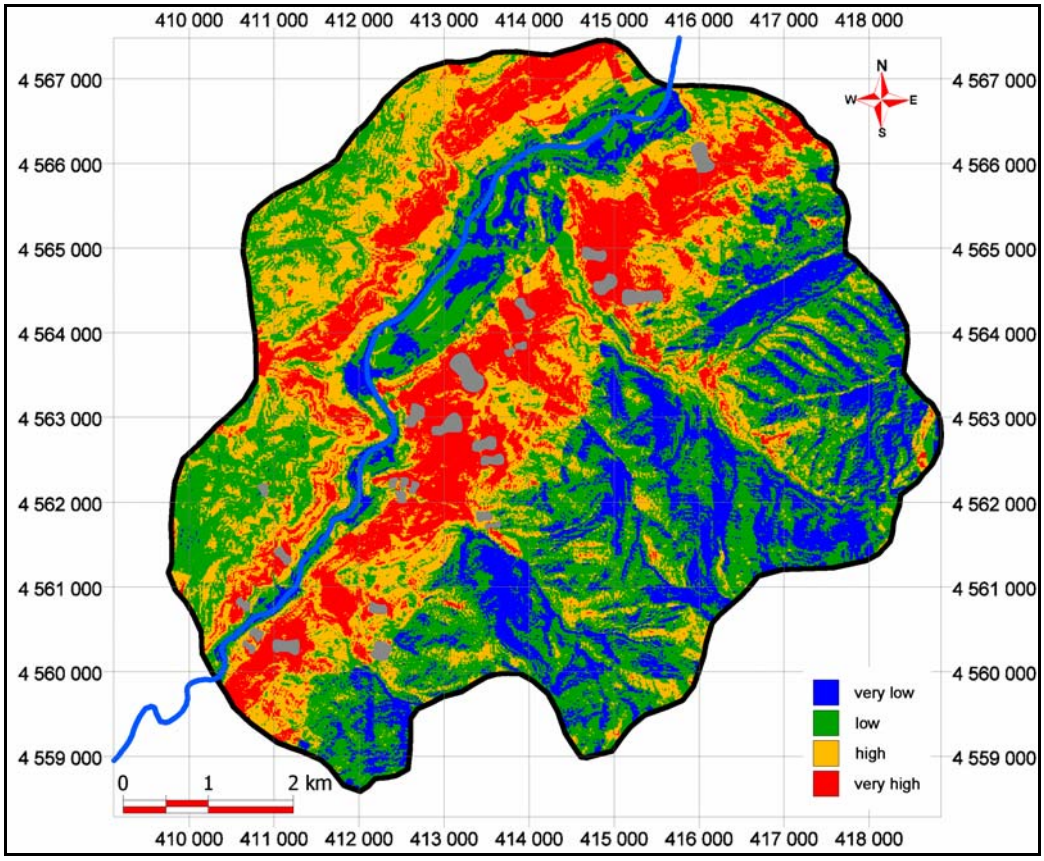

Figure 4.16. Landslide susceptibility map of the study area produced from the seed cells of crowns and flanks presented with landslides (gray polygons).

Table 4.8. The range and areal coverage of the susceptibility classes in the map produced from crowns and flanks database.

Susceptibility Class	Range	Area Covered (%)	Seed Cells (%)
Very low	0 – 23.76	17.22	0.10
Low	23.76 – 45.72	38.01	6.51
High	45.72 – 67.67	26.78	18.29
Very high	67.67 – 137.40	17.99	75.10

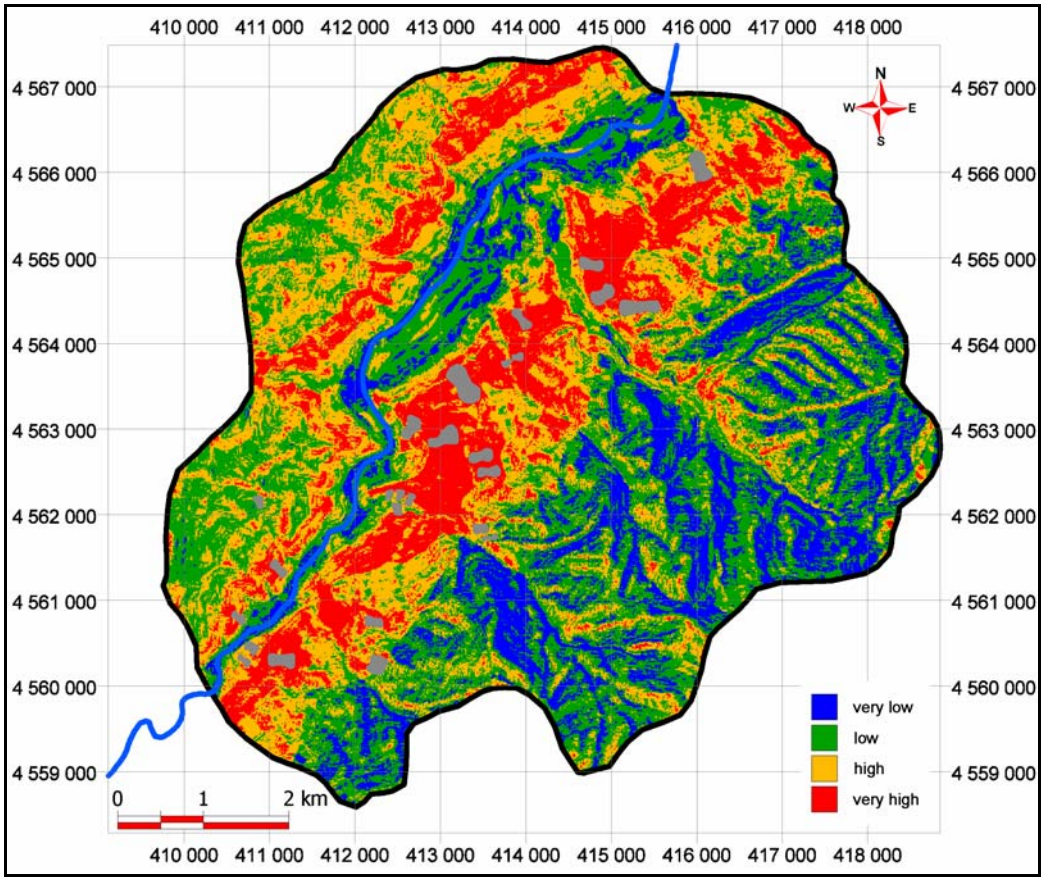

Figure 4.17. Landslide susceptibility map of the study area produced from the seed cells of crowns presented with landslides (gray polygons).

Table 4.9. The range and areal coverage of the susceptibility classes in the map produced from crowns database.

Susceptibility Class	Range	Area Covered (%)	Seed Cells (%)
Very low	0 – 14.94	16.25	0.09
Low	14.94 – 27.60	37.28	5.20
High	27.60 – 40.25	29.37	19.09
Very high	40.25 – 80.02	17.10	75.62

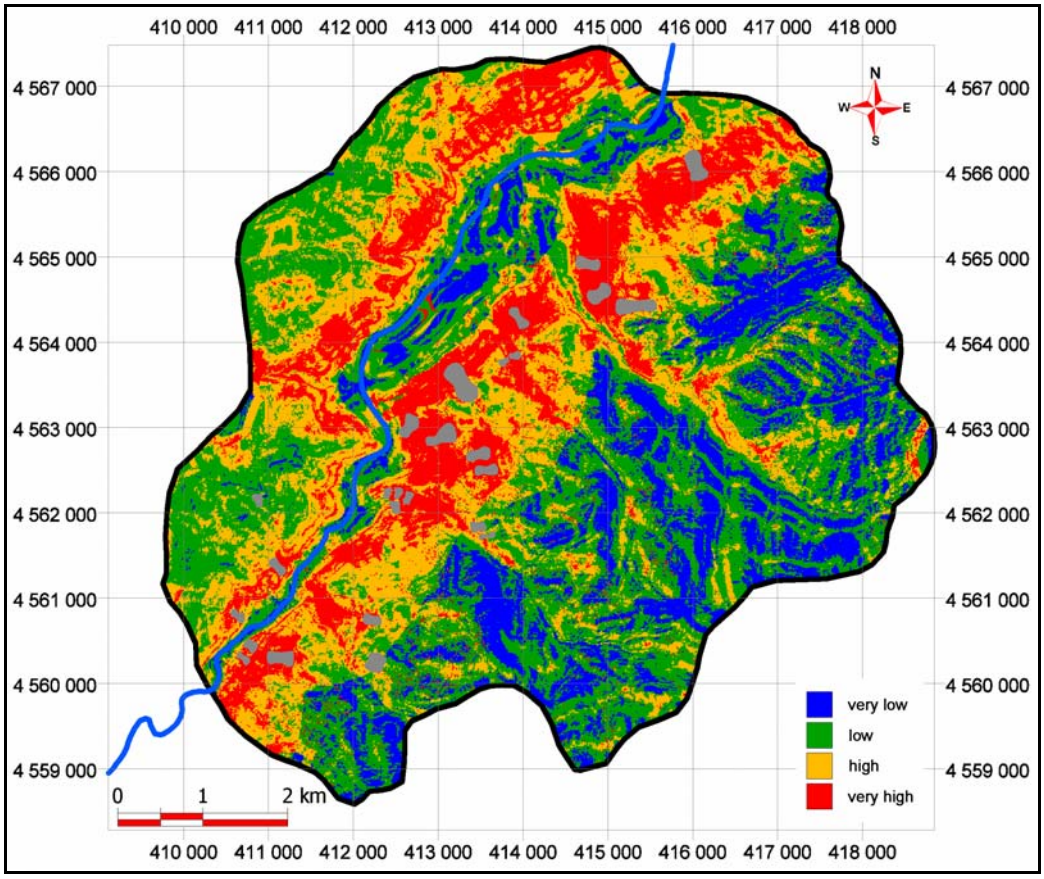

Figure 4.18. Landslide susceptibility map of the study area produced from the seed cells of flanks presented with landslides (gray polygons).

Table 4.10. The range and areal coverage of the susceptibility classes in the map produced from crowns database.

Susceptibility Class	Range	Area Covered (%)	Seed Cells (%)
Very low	0 – 10.16	16.58	0.30
Low	10.16 – 21.21	39.24	5.54
High	21.21 – 32.27	26.94	20.40
Very high	32.27 – 89.56	17.24	73.75

4.4. Comparison of the Susceptibility Maps

Three different susceptibility maps are produced from the seed cell databases. These maps are compared by examining the areas of susceptibility classes and the corresponding densities of landslides. An ideal susceptibility map has minimum areas for high susceptibility classes, while covering most of the landslides present in the areas. The areal coverage of the classes and the landslide densities of the resultant maps show that all three seed cell databases produce acceptable results, since majority of the seed cells fall in high and very high susceptibility classes. However, the shapes and areas of the susceptibility classes of the three maps are differing. Therefore, the maps have to be analyzed in order to find the most accurate and successful resulting data set of the seed cells.

In order to compare the results of the three seed cell databases, Seed Cell Area Index (SCAI) of the susceptibility classes of the maps is calculated (Table 4.11). SCAI is simply the density of landslides among the classes, and is calculated by dividing the susceptibility class area percent values by the landslide seed cell percent values. The logic behind SCAI lies in the correct classification of seed cells within a very conservative areal extent. As a result, it was desired that the high and very high susceptibility classes should have very small SCAI values and low and very low susceptibility classes to have higher SCAI values (Süzen and Doyuran, 2004b).

Table 4.11. The densities of landslides among susceptibility classes of the three data sets.

Data Set	Susceptibility Class	Area Covered (%)	Seed Cell (%)	SCAI
Crowns and Flanks	Very Low	17.22	0.10	172.2000
	Low	38.01	6.51	5.8387
	High	26.78	18.29	1.4642
	Very High	17.99	75.10	0.2395
Crowns	Very Low	16.25	0.09	180.5556
	Low	37.28	5.20	7.1692
	High	29.37	19.09	1.5385
	Very High	17.10	75.62	0.2261
Flanks	Very Low	16.58	0.30	55.2667
	Low	39.24	5.54	7.0830
	High	26.94	20.40	1.3206
	Very High	17.24	73.75	0.2338

When the SCAI values of the three seed cell data sets are compared, it is seen that the crowns database has the most desirable SCAI values in the very low, low and very high susceptibility classes. For the high susceptibility class, the SCAI values are very close to each other, but flanks database has the best result. When the crowns and flanks data sets are compared in terms of the high susceptibility class, it is found that the crowns database produces a 2.43 % greater areal extent than the flanks database with only 1.31 % decreases in the landslide seed cells, which could be accepted. As a result of the SCAI analysis, the most accurate and successful map of the study area is produced by the seed cells of crowns.

CHAPTER 5

DISCUSSION

In this chapter, the procedures used in this study are examined while lightening the possible errors with their reasons. The significance and success of the results are evaluated to better understand the contribution of different parameters to the occurrence of landslides.

This landslide susceptibility assessment study was conducted by utilizing Geographical Information Systems (GIS). The use of GIS was very essential, since it facilitates the data production, manipulation and analysis stages of landslide susceptibility mapping procedures.

The landslide susceptibility assessment of the Devrek area was carried out by using 10 different parameters of the study area. These are lithology, elevation, slope, aspect, profile curvature, plan curvature, distance to drainage lines, drainage density, distance to ridges, and distance to road and power line network. All these parameters are accepted as landslide contributing factors and widely used in landslide susceptibility assessment studies in the literature. Although earthquakes and precipitation are important landslide triggering factors, they are not taken into account in this study. Since the study area is very small, the effect of seismicity and precipitation is expected to be uniform over the whole study area. Another important parameter in landslide susceptibility assessment is the land cover. However, land cover could not be used in this study because of data availability problems.

By taking the aim of the study, available data and the size of the study area into account, the working scale of the landslide susceptibility assessment was chosen as 1:25000, which is referred as medium-scaled (IAEG, 1976). At large

scales, different factors such as water table depth and soil thickness will be used. These data are difficult to obtain for relatively bigger areas.

The landslide susceptibility assessment was carried out by using bivariate statistical method. Besides the scale of the work, statistical method was chosen because of its objectivity and data dependency. However, some procedures in bivariate statistical method are still subjective. Questions arise in the classification of parameter classes and the division of the final susceptibility map into susceptibility classes. To overcome the problem in the classification of parameter classes, percentile method (Süzen and Doyuran, 2004a) was applied. By using the percentile method, the parameters were directly classified according to the data itself. On the other hand, the final susceptibility map was divided into susceptibility classes by using the susceptibility map distribution. As a result, the objectivity and data dependency of the study were secured.

As noted in the previous chapter, the analyses of the three data sets resulted in acceptable susceptibility maps since majority of the seed cells falls in high and very high susceptibility classes in each data set. All three maps are also quite identical. All the weight values calculated are consistent and reflect no significant extremes which could lead to inconsistencies in the production of susceptibility maps. If the weight values of each parameter class of every attribute are sorted from the highest to the lowest value, elevation, lithology, slope, aspect and drainage density are found to be the highest contributing factors of landslide occurrence in the study area in all data sets.

The analysis carried out with the crowns and flanks data set indicates that the slopes in the Çaycuma Formation with angles from 5 to 17 degrees having altitude values of 139 to 225 meters, and facing to southwest, west and northwest are identified as unstable. Drainage density affects the instability where the drainage density values are from 270 to 300 and from 357 to 566 per square kilometers. Distance to ridges is the least contributing factor since landslides occurred mostly in the lower parts of hills. In the case of crowns data set, landslide susceptibility accumulates on the slopes of Çaycuma Formation with angles from 5 to 16 degrees, which are facing to southwest, west and

northwest at elevations from 150 to 218 meters. Drainage density values range between 268 to 296 and 417 to 566 per square kilometers. Distance to road and power line network parameter has the least effect on the landslide occurrences in the analysis of crowns data set. The results of the flanks data set are also similar. Instabilities are on the slopes of the Çaycuma Formation with angles from 5 to 13 degrees at elevations of 110 to 210 meters, facing to southwest, west and northwest. Drainage density values are from 273 to 307 and from 360 to 537 per square kilometers. Plan curvature parameter has the least effect on the slope instabilities in the case of flanks data set.

All three susceptibility maps are consistent with the field observations. However, there are no landslides observed in the west of the Devrek Stream where landslide susceptibility is classified as high and very high. These parts of the study area are densely populated and covered by many roads, particularly the northwest sections. The morphology of the area had changed throughout the years in these sections. Therefore, ancient landslides may have been missed to identify during the field investigations. Another possibility is to refine the susceptibility maps by introducing bedding related parameters of the lithological units. The sliding direction of majority of the landslides is in the dip direction of bedding planes. Therefore, the generation of landslides may be structurally controlled in the study area.

In all susceptibility maps, the alluvial deposits of the Devrek Stream are classified as low and very low susceptible. These parts of the area are flat and there is no possibility of landslide occurrence. However, these parts of the study area were included in the analyses by the computer software. All parameter maps created from the Digital Elevation Model (DEM) of the study area are continuous maps. Therefore, all pixels of all parameters in these parts get values computed by the algorithms used in the computer software. So, every part of the study area is considered in the analysis whether the pixel values reflect the real world situations or not.

CHAPTER 6

CONCLUSIONS AND RECOMMENDATIONS

The conclusions and recommendations derived form this study are the followings:

1. A total of 26 landslides were identified in the study area. All of them are classified as slides. They are generally shallow and observed in the Çaycuma Formation on gentle slopes.

2. Three susceptibility maps of the study area were produced by using three different data sets of seed cells. The data sets were created by using the seed cells of crowns and flanks, only crowns, and only flanks. All data sets produced identical and acceptable results. In all data sets, elevation, lithology, slope, aspect and drainage density were found as the most effective parameters on landslide occurrence of the study area.

3. Based on the comparison of the susceptibility maps by using the Seed Cell Area Index (SCAI), the map produced from the crowns data set was found as the most accurate and successful landslide susceptibility map of the study area. Seed cells reflect the conditions before landslide occurs and used as decision rules generators for landslide occurrences. Since a landslide starts to be formed at the crown part, choosing only crowns for seed cells might be enough according to the results of this study.

4. The susceptibility maps should be refined by introducing new parameters since no landslides have been observed in some high and very high classified areas. Especially, land cover and bedding related

(orientation, strike/dip amounts) parameters may overcome this problem.

5. The analysis applied is data dependent and objective. The complexity of this analysis is moderate and it could easily be implemented by non-expert users. The susceptibility map can be reproduced by introducing more parameters under different conditions.

6. This landslide susceptibility assessment study of the Devrek region may serve as useful information for land use planning. The areas of site-specific studies can be identified and prioritized for detailed geotechnical investigations.

REFERENCES

Abdolmasov, B. and Obradovic, I., 1997, Evaluation of geological parameters for landslide hazard mapping. Proc. Int. Symp. Eng. Geol.&Env., 23-27 June 1997, Athens, Greece, P.G. Marinos, G.C. Koukis, G.C. Tsiambaos and G.C. Stournaras (eds.), Balkema, 471-476.

Abella, E. and van Westen, C.J., 2007, Qualitative landslide susceptibility assessment by multicriteria analysis: A case study from San Antonio del Sur, Guantánamo, Cuba. Geomorphology (unpublished).

AİGM DAD, 2007, Afet İşleri Genel Müdürlüğü Deprem Araştırma Dairesi. http://www.deprem.gov.tr/linkhart.htm

Aleotti, P. and Chowdhury, R., 1999, Landslide hazard assessment: summary review and new perspectives. Bull Eng Geol Env, 58, 21-44.

Atkinson, P., Jiskoot, H., Massari, R. and Murray, T., 1998, Generalized linear modelling in geomorphology. Earth Surf.ProcessLandforms, 23, 1185-1195.

Ayalew, L. and Yamagishi, H., 2005, The application of GIS-based logistic regression for landslide susceptibility mapping in the Kakuda-Yahiko Mountains, Central Japon. Geomorphology, 65(1-2), 15-31.

Ayanew, T. and Barbieri, G., 2005, Inventory of landslides and susceptibility mapping in the Dessie area, northern Ethiopia. Engineering Geology, 77(1-2), 1-15.

Baeza, B. and Corominas, J., 2001, Assessment of shallow landslide susceptibility by means of multivariate statistical techniques. Earth Surface Processes and Landforms, 26, 1251-1263.

Barredo, J., Benavides, A., Hervas, J. and van Westen, C.J., 2000, Comparing heuristic landslide hazard assessment techniques using GIS in the Tirajana basin, Gran Canaria Island, Spain. JAG, 2, 9-23.

Bughi S., Aleotti P., Bruschi R., Andrei G., Milani G., and Scarpelli G., 1996, Slow movements of slopes interferring with pipelines: modelling vs monitoring. In: Proc 15th Int Conf OMAE, Firenze, June 1996

BÜ KRDAE, 2007, Boğaziçi Üniversitesi Kandilli Rasathanesi Deprem Araştırma Enstitüsü. http://www.koeri.boun.edu.tr/sismo/default.htm

Capolongo, D., Refice, A. and Mankelow, J., 2002, Evaluating earthquake-triggered landslide hazard at the basin scale through GIS in the Upper Sele River Valley. Surveys in Geophysics, 23, 595-625.

Carrara A., 1983, Multivariate methods for landslide hazard evaluation. Mathematical Geol, 15, 403–426.

Carrara, A., 1988, Landslide hazard mapping by statistical methods: A "Black Box" approach. In Workshop on Natural Disaster in European Medditerranean Countries, Perugia, Italy, Consiglio Nazionale delle Ricerche, Perugia, pp. 205-224.

Çevik, E. and Topal, T., 2003, GIS-based landslide susceptibility mapping for a problematic segment of the natural gas pipeline, Hendek (Turkey). Environmental Geology, 44, 949-962.

Chi, K.H., Park, N.W. and Chung, C.J., 2002, Fuzzy logic integration for landslide hazard mapping using spatial data from Boeun, Korea. Symposium on Geospatial Theory, Processing and Application,145-151.

Dai, F.C. and Lee, C.F., 2001, Terrain-based mapping of landslide susceptibility using a georaphical information system: a case study. Can. Geotech. J., 38, 911-923.

Dai, F.C. and Lee, C.F., 2003, A spatiotemporal probabilistic modeling of storm-induced shallow landsliding using aerial photographs and logistic regression. Earth Surface Processes and Landforms, 28, 527-545.

Dai, F.C., Lee, C.F. and Xu, Z.W., 2001, Assessment of landslide susceptibility on the natural terrain of Lantau island, Hong Kong. Environmental Geology, 40,3, 381-391.

Davis, T.J. and Keller, C.P., 1997, Modelling uncertainty in natural resource analysis using fuzzy sets and Monte Carlo simulation, slope stability prediction. Int. J. Geog. Inf. Sci., 11 (5), 409-434.

DMİ, 2007, Devlet Meteoroloji İşleri Genel Müdürlüğü. http://www.meteoroloji.gov.tr/2006/arastirma/arastirma.aspx.

Ercanoğlu, M., 2003, Bulanık mantık ve istatistiksel yöntemlerle heyelan duyarlılık haritalarının üretilmesi: Batı Karadeniz Bölgesi (Kumluca Güneyi-Yenice Kuzeyi). H.Ü. Fen Bilimleri Enstitüsü, Jeoloji Mühendisliği Bölümü Doktora Tezi, Ankara, 203 s. (yayımlanmamış).

Ercanoğlu, M., 2005a, Landslide mapping techniques and assessments: general aspects and trends. Intermountain GIS User's Conference, Pocatello, Idaho, USA, 18-22 April 2005, p.23.

Ercanoğlu, M., 2005b, Landslide susceptibility assessment of SE Bartın (West Black Sea Region, Turkey) by artificial neural networks. Natural Hazards and Earth System Science, 5, 979-992.

Ercanoğlu, M. and Gökçeoğlu, C., 2002, Assessment of landslide susceptibility for a landslide-prone area (north of Yenice, NW Turkey) by fuzzy approach. Env. Geol., 41, 720-730.

Ercanoğlu, M. and Gökçeoğlu, C., 2004, Use of fuzzy relations to produce landslide suzceptibility map of a landslide prone area (West Black Sea Region, Turkey). Engineering Geology, 229-250.

Ercanoğlu, M., Temiz, N. ve Kaşmer, O., 2006, Heyelan duyarlılık haritalarının üretilmesinde bulanık mantık ve yapay sinir ağlarının kullanımının araştırılması. TÜBİTAK YDABAG, Proje No: 103Y126, 186 s.

Fall, M., Azzam, R. and Noubactep, C., 2006, A multi-method approach to study the stability of natural slopes and landslide susceptibility mapping. Engineering Geology, 82, 241-263.

Gomez, H. and Kavzaoğlu, T., 2005, Assessment of shallow landslide susceptibility using artificial neural Networks in Jabonosa River Basin, Venezuela. Engineering Geology, 78, 11-27.

Gorsevski, P.V., Gessler, P.E. and Jankowski, P., 2003, Integrating a fuzzy k-means classification and a Bayesian approach for spatial prediction of landslide hazard. Journal of Geographical Systems, 5, 223-251.

Gökçeoğlu, C. and Aksoy, H., 1996, Landslide susceptibility mapping of the slopes in the residual soils of the Mengen region (Turkey) by deterministic stability analyses and image processing techniques. Eng. Geol., 44, 147-161.

Guinau, M., Pallas, R. and Vilaplana, J.M., 2005, A feasible methodology for landslide susceptibility assessment in developing countries: A case-study of NW Nicaragua after Hurricane Mitch. Engineering Geology, 80, 316-327.

Guzzetti, F., Carrara, A., Cardinalli, M., and Reichenbach, P., 1999, Landslide hazard evaluation: A review of current techniques and their application In a multi-case study, central Italy. Geomorphology, 31, 181-216.

IAEG, 1976, International Association of Engineering Geology. Engineering geological maps: A guide to their preparation, UNESCO Press, Paris, 79pp.

Lin, M. and Tung, C., 2003, A GIS-based potential analysis of the landslides induced by the Chi-Chi earthquake. Engineering Geology, 71, 63-77.

Lee, S. and Min, K., 2001, Statistical analysis of landslide susceptibility at Yongin, Korea. Environmental Geology, 40, 1095-1113.

Lee, S., Choi, J. and Min, K., 2002, Landslide susceptibility analysis and verification using the Bayesian probability model. Environmental Geology, 43, 120-131.

Lee, S., Ryu, J.H., Min, K. and Won, J.S, 2003a, Lanslide susceptibility analysis using GIS and artificial neural network. Earth Surface Processes and Landforms, 1361-1376

Lee, S., Chwae, U. and Min, K., 2003b, Landslide susceptibility mapping by correlation between topography and geological structure: the Janghung area, Korea. Geomorphology, 44, 223-245.

Lee, S., Ryu, J.H., Won, J.S. and Park, H.J., 2004, Determination and application of the weights for landslide susceptibility mapping using an artificial neural network. Engineering Geology, 71, 289-302.

Leroi, E., 1996, Landslide hazard – Risk maps at different scales: objectives, tools and developments. Proc VII Int Symp Landslides, 1, 35-52.

Mejia-Navarro, M. and Wohl, E.E., 1994, Geological hazard and risk evaluation using GIS: methodology and model applied to Medellin, Colombia. Bull. Assoc. Eng. Geol., XXXI (4), 459-481.

MicroImages, 2007, Terrain curvature.
http://www.microimages.com/documentation/cplates/70CurvScript.pdf

Montgomery, D.R., Sullivan, K. and Greenberg, H.M., 1998, Regional test of a model for shallow landsliding. Hyro.Proc., 12, 943-955.

MTA, 2007, Maden Tetkik ve Arama Genel Müdürlüğü. Türkiye Diri Fay Haritası.
http://www.mta.gov.tr/mta_web/dirifay.asp

Nefeslioğlu, H., Duman, T. and Durmaz, S., 2007, Landslide susceptibility mapping for a part of tectonic Kelkit Valley (Eastern Black Sea region of Turkey). Geomorphology (unpublished).

Neuhauser, B. and Terhorst, B., 2007, Landslide susceptibility assessment using "weights-of-evidence" applied to a study area at the Jurassic escarpment (SW-Germany). Geomorphology, 86, 12-24.

Remondo, J., Gonzalez-Diez, A., Teran, J.R.D.D. and Cendrero, A., 2003, Landslide susceptibility models utilising spatial data analysis techniques. A case study from the Lower Deba Valley, Guipuzcoa (Spain). Natural Hazards, 1-13.

Sabto, M., 1991, Probabilistic modeling applied to landslides in Central Colombia using GIS procedures. Unpublished Msc thesis, ITC, Enschede, Netherlands, 26 p.

Santacana, N., Baeza, B., Corominas, J., De Paz, A. and Marturia, J., 2003, A GIS-based multivariate statistical analysis for shallow landslide susceptibility mapping in La Pobla de Lillet area (Eastern Pyrenees, Spain). Natural Hazards, 30, 281-295.

Sakellariou, M.G. and Ferentinou, M.D., 2001, GIS-based estimation of slope stability. Natural Hazards Review, 2, 12-21.

Soeters, R. and van Westen, C.J., 1996, Slope instability recognition analysis and zonation, In Landslides: Investigation and Mitigation (Turner, K.T, and Schuster, R.L. eds). Transportation Research Board National Research Council, Special Report no: 247, Washington D.C., pp 129-177.

SSGM, 2007, Sivil Savunma Genel Müdürlüğü.
http://www.ssgm.gov.tr/afetler/heyelan.asp.

Süzen, M.L., 2002, Data driven landslide hazard assessment using geographical information systems and remote sensing. Ph.D. Thesis, Middle East Technical University, Turkey, pp 196.

Süzen, M.L. and Doyuran, V., 2004a, Data driven bivariate landslide susceptibility assessment using geographical information systems: a method and application to Asarsuyu catchment, Turkey. Engineering Geology, 71, 303-321.

Süzen, M.L. and Doyuran, V., 2004b, A comparison of the GIS based landslide susceptibility assessment methods Multivariate versus bivariate. Environmental Geology, 45, 665-679.

Tangestani, M.H., 2003, Landslide susceptibility mapping using the fuzzy gamma operation in GIS, Kakan catchment area, Iran. Map India Conference, 157-164.

Thiery, Y., Malet, J.-P., Sterlacchini, S., Puissant, A. and Maquaire, O., 2007, Landslide susceptibility assessment by bivariate methods at large scales: Application to a complex mountainous environment. Geomorphology (unpublished).

TNT Mips, 2000, TNT Mips Manual: Processes.

Van Westen, C.J., 1993, Application of geographic information systems to landslide hazard zonation. ITC Publication no: 15. International Institute for Aerospace and Earth Resources Survey, Enschede, The Netherlands, 245 pp.

Van Westen C.J., 1997, Statistical landslide hazard analysis. ILWIS 2.1 for Windows application guide. ITC Publication, Enschede, pp 73–84

Van Westen, C.J., Soeters, R. and Sijmons, K., 2000, Digital geomorphological landslide hazard mapping of the Alpago area, Italy. JAG, 2, 51-60.

Varnes, V., 1978, Slope movement types and processes, Landslides Analysis and Control: Natiopnal Academy of Sciences Transportation Research Board Special Report 176, p. 12-33.

Wachal, D.J. and Hudak, P.F., 2000, Mapping landslide susceptibility in Travis County, Texas, U.S.A. Geo Journal, 51, 245-253.

Yalçın, A., 2007, GIS-based landslide susceptibility mapping using analytical hierarchy process and bivariate statistics in Ardesen (Turkey): Comparisons of results and confirmations. Catena (unpublished).

Yergök, A.F., Akman, Ü., İplikçi, E., Karabalık, N., Keskin, İ., Mengi, H., Umut, M., Armağan, F., Erdoğan, K., Kaymakçı, H. and Çetinkaya, A., 1987, Batı Karadeniz bölgesinin jeolojisi, MTA Rapor No: 8273 (unpublished).

Yeşilnacar, E. ve Topal, T., 2005, Landslide susceptibility mapping: A comparison of logistic regression and neural Networks methods in a medium scale study, Hendek region (Turkey). Eng. Geol, 79, 251-266.

Yin, K.L., and Yan, T.Z., 1988, Statistical prediction model for slope instability of metamorphosed rocks. In Proc., Fifth International Symposium in Landslides (C.Bonnard ed), Lausanne, A.A. Balkema, Rotterdam, Netherlands, Vol.2, 1269-1272.